SOLID-STATE STABILITY OF ANTIBODY-DRUG CONJUGATES

by

Eunbi Cho

A Dissertation

Submitted to the Faculty of Purdue University

In Partial Fulfillment of the Requirements for the degree of

Doctor of Philosophy

Department of Industrial and Physical Pharmacy

West Lafayette, Indiana

August 2021

THE PURDUE UNIVERSITY GRADUATE SCHOOL
STATEMENT OF COMMITTEE APPROVAL

Dr. Elizabeth M. Topp, Chair

College of Pharmacy

Dr. Alina Alexeenko

School of Aeronautics and Astronautics

Dr. Gregory T. Knipp

College of Pharmacy

Dr. Gregory A. Sacha

Baxter BioPharma Solutions

Approved by:

Dr. Rodolfo Pinal

Soli Deo Gloria. (Psalm 40:5)

ACKNOWLEDGMENTS

I would like to first thank my academic advisor, Dr. Elizabeth M. Topp for being an excellent mentor. The academic discussions with her helped me to approach the study with various perspectives and to grow as an independent scientist. Her encouragement allowed me to persist through the past seven years. I also express the sincere appreciation to my committee members, Dr. Gregory T. Knipp, Dr. Alina Alexeenko, and Dr. Gregory A. Sacha for their huge supports and advice. They allowed me to pursue the research with excitement and joy. I would also like to thank my previous and current lab members for cooperation during the study.

I would like to thank the colleagues from Baxter BioPharma Solutions, Dr. Steven L. Nail, Dr. Gregory A. Sacha, Dr. Jayasree M. Srinivasan, Brendan M. Mayhugh, and Jacquelyn Karty. Dr. Nail has been a great mentor and has supported me with his in-depth scientific insights. The encouragement and academic inputs from Dr. Sacha and Dr. Srinivasan also allowed me to move forward with confidence. I thank all the Baxter colleagues, especially Angie Kruszynski, for the warm welcomes and the times spent during the internship and the business trips. I also thank Baxter BioPharma Solutions for their financial supports.

I would like to express the deepest appreciation to my family for the continuous prayers and supports. The prayers from my parents allowed me to stand firm in the midst of all the hardships during the study. I thank my siblings, Kevin and Grace, for being so supportive and being faithful. Without my family, I would not be able to stand where I am now.

Special thanks to Mary Ellen Hurt for the continuous support throughout my Ph.D life. I would also like to thank my previous and current church members for the endless prayers and cares. I would also like to thank Dr. Jeff Schumm and Kim Schumm for their love and support.

TABLE OF CONTENTS

LIST OF TABLES

Appendix A. Tables

Appendix B. Tables

Appendix C. Tables

LIST OF FIGURES

Appendix A. Figures

Appendix B. Figures

Appendix C. Figures

LIST OF ABBREVIATIONS

ABC	ATP-binding cassette
AcBut	4-(4'-acetylphenoxy) butanoic acid
ADC	antibody-drug conjugate
AJS ESI	Agilent Jet Stream Electrospray Ionization
ANOVA	analysis of variance
bFGF	basic fibroblast growth factor
BR96-DOX	BR96-doxorubicin
CM	capacitance manometer
CNTF	ciliary neurotropic factor
DAR	drug-to-antibody ratio
D_{max}	maximum level of deuterium incorporation
DMF	dimethylformamide
DSC	differential scanning calorimetry
ESI-QTOF	electrospray ionization coupled quadrupole time-of-flight
Fab	fragment antigen-binding
FT-IR	Fourier-transform infrared spectroscopy
GDH	glutamate dehydrogenase
HC	heavy chain
HDX	hydrogen/deuterium exchange
HMW	high molecular weight
HPLC	high performance liquid chromatography
HSA	human serum albumin
iEC	ion exchange chromatography
IgG	immunoglobulin G
IL-1ra	interleukin-1 receptor antagonist
KF	Karl Fischer coulometry
LC	light chain
LDH	lactate dehydrogenase
mAb	monoclonal antibody

MC	maleimidocaproyl
MCC	maleimidomethyl cyclohexane-1-carboxylate
MDH	malate dehydrogenase
MDR	multidrug resistant
MS	mass spectrometry
MTD	maximum tolerated dose
MWCO	molecular weight cut-off
NHS	N-hydroxy succinimide
NIR	near-infrared spectroscopy
PABC	para-amino benzyl alcohol
PBD	pyrrolobenzodiazepine
PFK	phosphofructokinase
P-gp	P-glycoprotein
POE	poly(oxyethylene)
PPE	personal protective equipment
PS	polysorbates
QTOF-LC/MS	liquid chromatography coupled quadrupole time-of-flight mass spectrometry
RH	relative humidity
RT	room temperature
SEC	size-exclusion chromatography
SMCC	succinimidyl 4-(N-maleimidomethyl) cyclohexane-1-carboxylate
SPDB	N-Succinimidyl-4-(2-pyridyldithio) butanoate
SPP	N-succinimidyl-4-(2-pyridyldithio) pentanoate
ssHDX-MS	solid-state hydrogen/deuterium exchange coupled with mass spectrometry
T	toxin
TCEP	tris-(2-carboxyethyl)-phosphine
T-DM1	trastuzumab emtansine
T_g	glass transition temperature
TNFbp	tumor necrosis factor binding protein
UV	ultraviolet
XRPD	x-ray powder diffraction

ABSTRACT

Antibody-drug conjugates (ADCs) combine the cytotoxicity of traditional chemotherapy with the site-specificity of antibodies by conjugating payloads to antibodies with immunoaffinity. However, the conjugation alters the physicochemical properties of antibodies, increasing the risks of various types of degradation. The effects of common risk factors such as pH, temperature, and light on the stability of ADCs differ from their effects on monoclonal antibodies (mAb) due to these altered physicochemical properties.

To date, ADC researchers have developed linkers with improved *in vivo* stability, and begun to understand the deconjugation mechanisms *in vivo*. In contrast, the *in vitro* stability of ADCs has not gained comparable attention. All nine of the U.S. FDA approved ADCs are lyophilized to minimize the potential for degradation. However, there are few studies on the solid-state stability of ADCs. To evaluate lyophilized solids, pharmaceutical development relies heavily on accelerated stability studies, which take months to determine the best formulation. Characterization methods that are often used orthogonally with accelerated studies include Fourier-transform infrared spectroscopy (FT-IR), Raman spectroscopy, near-infrared spectroscopy (NIR), differential scanning calorimetry (DSC), and x-ray powder diffraction (XRPD). Results from these methods are often poorly correlated with stability, however. Thus, stability evaluation of solid-state ADC products, and other recombinant protein drugs, is often a bottleneck in their development.

To provide knowledge on how to improve the *in vitro* stability of lyophilized ADC formulations, the solid-state stability of ADC formulations with varying risk factors was studied in this dissertation project. The first study investigated interactions between an ADC and excipients in terms of solid-state stability enhancement. The second study investigated the process-driven instability of ADCs during lyophilization using various concentrations of ADCs. The first two studies incorporate a new method called solid-state hydrogen/deuterium exchange coupled with mass spectrometry (ssHDX-MS) as an analytical predictor of solid-state stability. The last study investigated the effects of pH on the stability of labile hydrazones, as a model for common linker chemistry used in ADCs.

CHAPTER 1. INTRODUCTION

In recent decades, antibody-drug conjugates (ADCs) have been studied extensively as a next generation of antibody-based therapy, and more than 80 ADCs are currently in clinical trials.[1-2] ADCs have been introduced to resolve issues with toxicity and selectivity of traditional chemotherapy. In ADCs, cytotoxic payloads are attached to an antibody to ensure drug delivery to tumor sites with a higher safety margin. The conjugation of payloads to antibody is achieved using linkers that typically react with lysine and cysteine residues on the antibodies.[3] In the past, oncology aspects and *in vivo* stability of ADCs have been addressed.[1,4-8] The synthesis, conjugation, and analytical challenges of ADCs also have been investigated to a similar extent.[9-13] However, the *in vitro* stability of ADCs during formulation and storage has not received as much attention as the former topics.

In this chapter, 1) the stability issues associated with the linker system of ADCs during formulation and storage and 2) the benefits of lyophilization for ADC stability are addressed. Furthermore, a new analytical method to evaluate solid-state stability of ADC is introduced.

1.1 Stability concerns in ADC components

ADCs are mainly composed of three parts: antibody, linker, and payload (**Figure 1.1**). Each component exhibits distinct physicochemical properties, and the way that risk factors affect the stability of each component also differs.

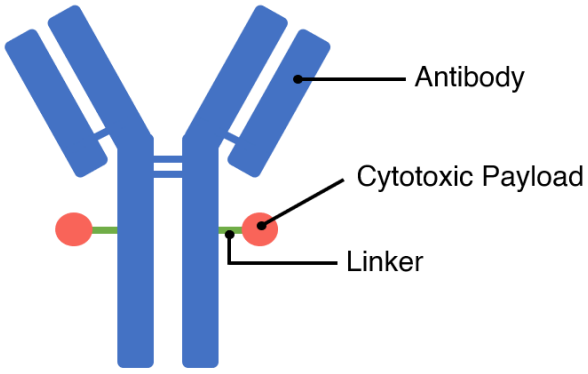

Figure 1.1. Components of ADC.

1.1.1 Antibody component

Due to the size and complexity of the antibody molecule, various studies have been performed to yield antibody formulations with better stability.[14-19] Knowledge of antibody *in vitro* and *in vivo* behavior has developed to allow the use of antibodies as carriers for chemotherapeutic agents. Since the antibody plays an important role in the selectivity of ADCs, the antibody component must retain its high immunoaffinity toward the target antigen after conjugation. Xie *et al*. found that the biodistribution of ADCs is affected by the antibody component rather than the linker or payload component.[20] To avoid undesired immune reactions, currently ADCs are conjugated to fully humanized or human sequenced immunoglobulin G (IgG). IgG1, IgG4, and IgG2 isotypes are usually used, and different isotypes exhibit various effector functions that may be beneficial depending on the purpose and target of the ADCs.[21-22] Although all the commercially available ADCs are conjugated to intact antibodies, fragmented antibodies that have binding affinity to Fc-gamma receptor or neonatal Fc receptor are under evaluation for use in ADC development.[23-24] Recombinant fragmented antibodies with higher affinity and higher tissue penetration abilities are expected to provide advantages by narrowing the biodistribution of ADCs.[7] Yet, binding affinity over the antigens does not guarantee high efficacy because high affinity only confers rapid internalization. In addition to binding affinity, many factors affect the efficacy of ADCs such as bystander effect, deconjugation of payloads, and plasma clearance.[4,25] Unfortunately, the clearance of fragmented antibodies is much faster than that of intact IgG isotypes.[26] Therefore, intact antibody molecules are often preferred due to their longer half-life in plasma that enables prolonged dosing intervals and therapeutic effects.[21]

Current conjugation methods utilize the primary amine and sulfhydryl group at lysine and cysteine residues, respectively, on the antibody **(Figure 1.2**). Most current conjugation mechanisms yield ADCs with different drug-to-antibody ratios (DAR) having various charge variants. For example, IgG1 has more than thirty modifiable Lys residues that may randomly conjugate with the linker-drug moiety. A DAR of eight has been reported as the maximum for Lys-conjugated ADCs. On the other hand, there are only four interchain disulfide bridges in IgG1. The theoretical maximum conjugation is eight for Cys-conjugated ADCs. However, both Lys-conjugated and Cys-conjugated ADCs face issues with undesirable heterogeneity, which makes scale-up and manufacturing challenging.[3] Heterogeneity affects the antigen-binding properties of the antibody moiety and alters the potency, solubility, and pharmacokinetics of the ADC. To

minimize changes in antibody binding and function, antibodies are engineered to selectively conjugate with a DAR of 1-2.[27] ThioMab, for example, contains engineered cysteine residues introduced into the sequence of a traditional antibody to limit the sites and number of reactive free thiol groups. Engineered ADCs and ADCs with site-specific conjugation have reduced batch-to-batch heterogeneity.[28-29]

The factors affecting the stability of the antibody component are similar to those for conventional antibodies: temperature, pH, light, ionic strength, and surface exposure. Yet, the hydrophobic drug payload alters the physicochemical properties of antibodies to a great extent, complicating the characterization of ADCs.[30] Typical conjugation payloads often lead to an increased risk of aggregation and fragmentation. An understanding of both the antibody and the payload is required to formulate stable ADC products.[21,31]

1.1.2 Linker component

ADC linkers can be categorized into two main types: cleavable linkers, and non-cleavable linkers (**Figure 1.2**). Cleavable linkers are sensitive to proteases or pH, or to the environment at the target site (**Figure 1.2b-e**). ADCs with non-cleavable linkers undergo lysosomal degradation at the target site to deconjugate payloads from the parent antibodies (**Figure 1.2a**). Even though cleavable linkers have a higher risk of premature cleavage than non-cleavable linkers, cleavable linkers are widely utilized for several reasons. Cleavable linkers are used when payloads do not have a functional group that can be substituted to the non-cleavable linkers or when substitution may alter potency. Cleavable linkers may be used to yield faster activation.[32] Some of the currently marketed ADCs use a combination of cleavable and non-cleavable linkers to achieve the desired release profile at the target site. Often, non-cleavable linkers such as maleimidocaproyl (MC) or maleimidomethyl cyclohexane-1-carboxylate (MCC) are used to conjugate antibodies, and cleavable linkers are used either to connect other linkers or to conjugate payloads.[3,6,33] Self-immolative linkers such as para-amino benzyl alcohol (PABC) are often used to allow release of unmodified payloads (**Figure 1.2c**).[3-4,35]

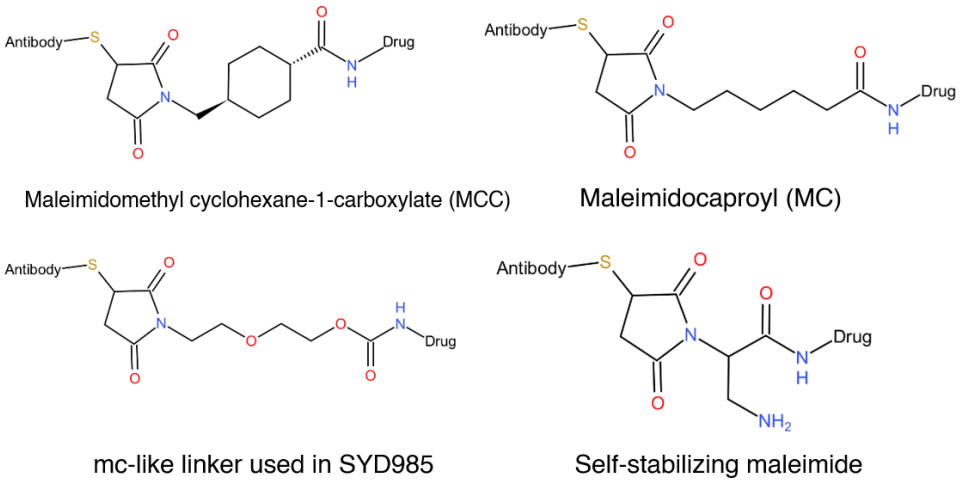

a. Linkers utilized in Cys-conjugated ADCs

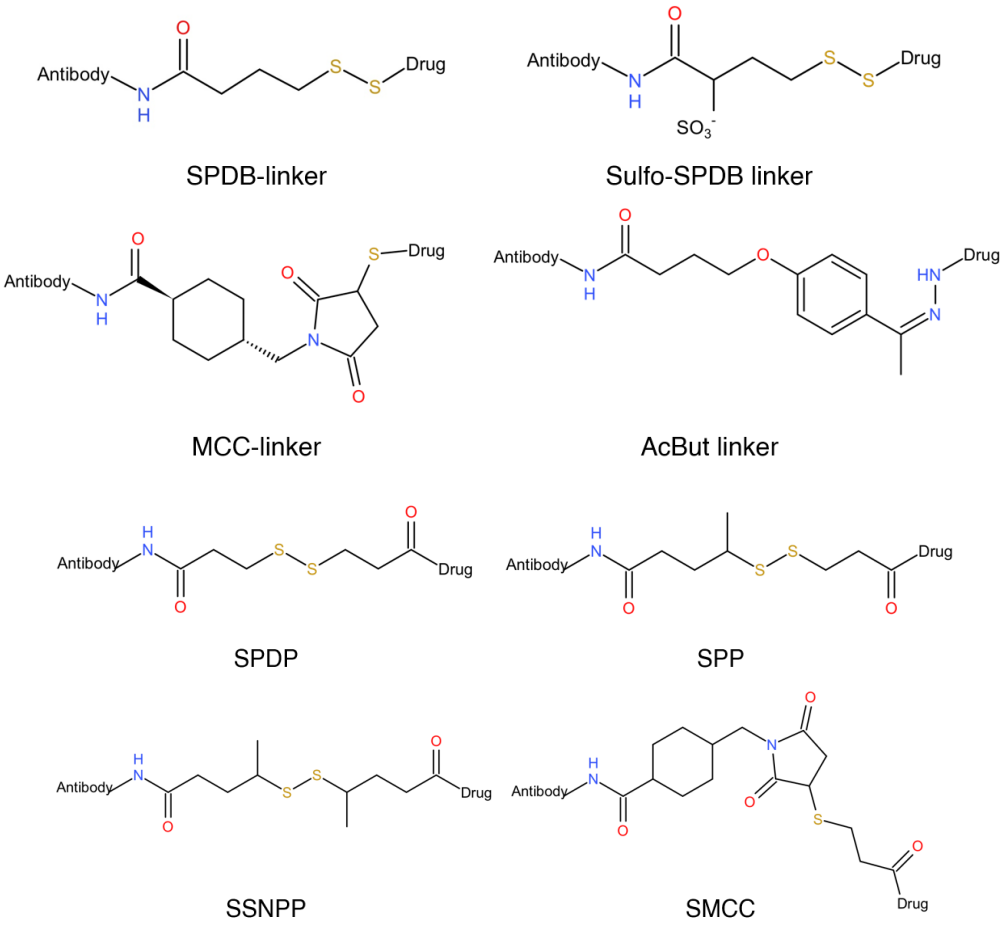

b. Linkers utilized in Lys-conjugated ADCs

Figure 1.2. Types of various linkers and the structures. Adapted from: a,b(top),d;[3] b(bottom);[34] e.[4]

Figure 1.2 continued

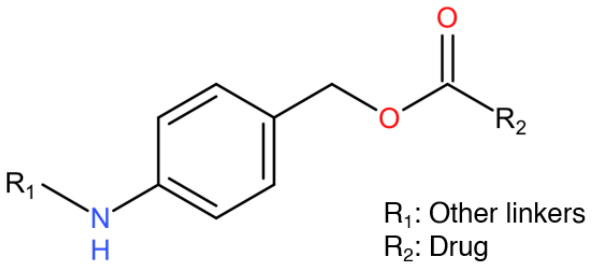

Para-amino benzyl alcohol (PABC)

c. Self-immolative spacer

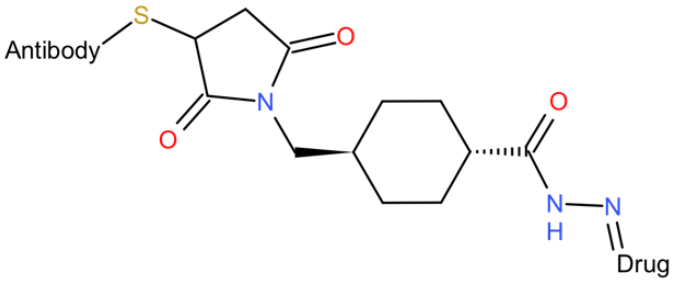

mcc-hydrazide linker

d. pH-sensitive linker

[Protease-sensitive Linkers]

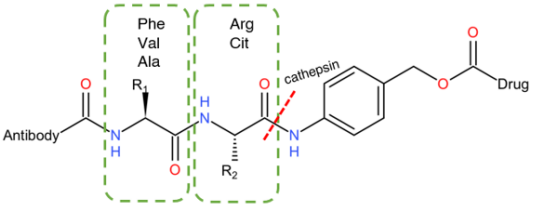

Dipeptide linker

[Phosphatase-sensitive Linkers]

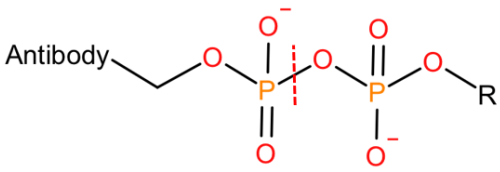

Pyrophosphate-containing linker

[Glycosidase-sensitive Linkers]

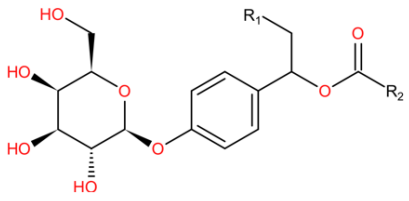

Beta-galactoside-containing linker

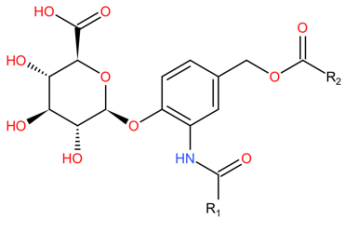

Beta-glucuronic acid-containing linker

e. Enzyme-sensitive linkers

The selection of linker affects both the antigen binding and the thermal stability of ADCs.[8,21] The length of the linker also determines plasma stability. Furthermore, the choice of linker defines DAR, drug load distribution, and the stability of the linkage. In Cys-conjugated ADCs, shorter linkers may reduce the risk of reduction, whereas linkers protruding from the antibody can be more prone to reduction.[36] However, in plasma, robust chemical stability of the linker is not always correlated with high tolerability. In maytansinoid-conjugated ADCs, clinical data showed an inverse relationship between chemical stability and maximum tolerated dose (MTD) among three linkers tested: SPP, SPDB, and SMCC (**Figure 1.2b**).[37] However, during storage, both the chemical and physical stability of the linker are crucial in assuring product quality, safety, and efficacy.[38] The stability of the linker system is addressed below in greater detail.

1.1.3 Payload component

Auristatin-containing motifs, pyrrolobenzodiazepine (PBD), duocarmycin, SN-38 (a topoisomerase I inhibitor), doxorubicin, maytansinoid, and calicheamicin are the cytotoxins that have been widely used for ADC development. The payloads of ADCs mainly target 1) tubulin so that the tumor cell mitotic cycle is hindered or 2) DNA of the tumor cells.[39] The payloads are typically 700-750 Da and have a log P value around 4.[31] Payloads must be conjugated to the linker without affecting their potency. Metabolites of deconjugated payloads that behave as a prodrug may be considered as candidate payloads for ADC development.[23] Metabolite toxicity should be investigated prior to development since ADC toxicity is attributed to the intrinsic toxicity of the payloads more than to the linker-dependent distribution of the ADCs.[37,40] A detailed review on the toxicity of payloads is provided in Beck *et al*.[6]

Hydrophobic payloads affect overall ADC stability to a great extent. They affect the physicochemical properties of the ADC molecules depending on DAR values.[30] If the DAR is too low, the ADC molecule may not have the desired overall potency, whereas, if the DAR is too high, the ADC molecule may be more susceptible to physical degradation. In Cys-conjugated ADCs, despite no change in overall protein conformation, the conformational energy of unfolding is reduced relative to the native mAb, so that more hydrophobic local surface is exposed to the solvent. The hydrophobicity of payloads may induce aggregate formation.[23,31] Similarly, formulation to improve the solubility of hydrophobic payloads may instead cause instability of ADCs. The potential risks of excipients for ADC stability are further discussed below.

1.2 Factors impacting stability of linker system

ADC molecules experience a higher risk of instability than the parent mAb due to the introduction of the linker system. There are numerous factors that influence the stability of ADCs, and they are somewhat interconnected. ADC molecules face different types of risks depending on conjugation sites and/or linker type. Many reviews have introduced the various types of linkers and their conjugation/release mechanisms.[3-4,6,10,29,32] Most of the reviews focus on the *in vivo* stability of ADCs. Herein, factors that may endanger the linker system before *in vivo* administration are mainly addressed. It should be noted that the payloads themselves may have susceptibilities to the factors described below and are not discussed here.

1.2.1 pH

The development of ADCs with pH-labile linkers requires special attention to maintaining appropriate pH for both *in vivo* stability and *in vitro* stability. For example, the hydrazone linker is pH-sensitive and cleaves in the acidic pH environment near cancer cells. Hydrazone is known to hydrolyze into ketone and hydrazide moieties around pH 5 (**Figure 1.3**).[3,41] However, the hydrazone linker has a risk of premature release of payloads *in vivo*. In 2010, the hydrazone-based ADC Mylotarg® was withdrawn temporarily due to a discrepancy between plasma stability and buffer stability.[42] Data suggest that it was quite challenging for the molecule to strictly discriminate between pH 5 and 7.4.[4] Like the hydrazone linker, the PABC-peptide-MC linker, also known as CL2A, is a pH-sensitive and was used to connect the SN-38 payload.[7]

In addition to pH-sensitive hydrazone linkers, various linkers utilize ester or amide linkages to conjugate the antibody and the linker, or the linker and the payload (**Figure 1.2a-c, e**). Since an ester linkage is weaker than an amide linkage, many clinically available ADCs use Lys residues to conjugate antibodies.[7,43] In Cys-conjugated ADCs, the functional group that connects payloads to the linker is an amide group. MC-derivative linkers and self-stabilizing maleimide are examples (**Figure 1.2a**).

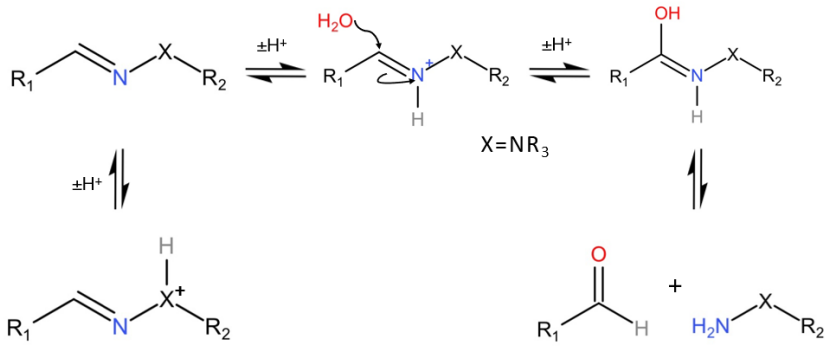

Figure 1.3. Putative mechanism of hydrazone hydrolysis. Adapted from ref. 41.

Even though most pH-sensitive linkers are acid-labile, increasing pH may not stabilize the ADC formulation. As pH increases, the rates of Asn deamidation and succinimide hydrolysis increase, whereas at low pH, Asp may undergo isomerization. Thus, a slightly acidic pH is recommended to avoid such chemical degradation.[44] Mohamed *et al*. evaluated the stability of trastuzumab and trastuzumab emtansine (T-DM1) under various pH conditions. The results showed that the parent mAb was more stable than the conjugated ADCs at pH 4, 6, 8, and 10. Extremes in pH led to conformational changes, especially in the Fc domain, and further induced aggregation. Moreover, T-DM1 showed greater degradation under all pH conditions upon incubation at 37 °C for 4 weeks. T-DM1 showed more than 40% degradation at pH values other than pH 6. The results suggest that conjugation with the linker system increases susceptibility to extreme pH conditions.[45-46]

1.2.2 Reducing agents

As shown in the **Figure 1.2a-b**, most linkers contain disulfide or thioether linkages that are susceptible to nucleophilic attack from sulfhydryl groups, inducing a reversible dissociation reaction (**Figure 1.4**).[44] A common reducing agent present in the plasma is human serum albumin (HSA). Cross-reactivity with albumin dissociates the disulfide bond and results in increasing off-target toxicity. Even outside the plasma, disulfide-based linkers may react with excipients or buffers with thiol groups. Yet, susceptibility to reduction differs with the site of conjugation; conjugation at a solvent-accessible sulfhydryl group is more prone to reduction.[44,47]

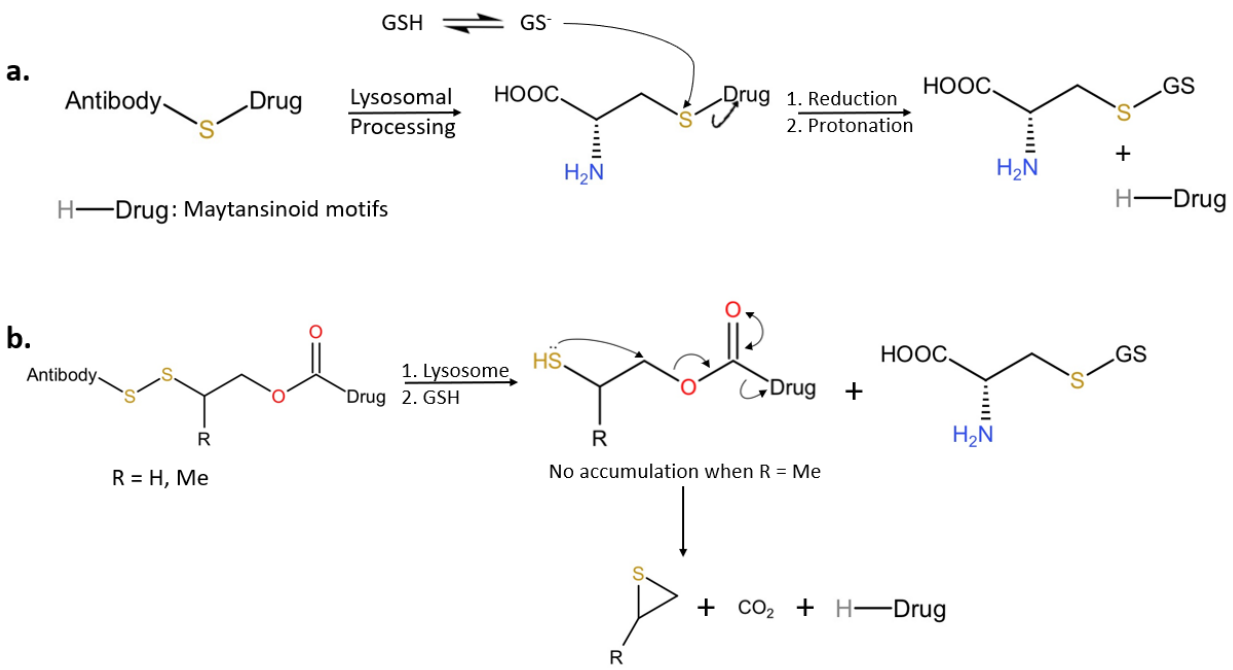

Figure 1.4. De-conjugation mechanisms of a. thioether and b. disulfide-based linkers. Adapted from ref. 4.

Most Cys-conjugated ADCs utilize succinimide to connect the antibody to the linker (**Figure 1.2a**). MC, MCC, and self-stabilizing maleimide are examples. In the absence of a reducing agent, the thioether linkage is relatively stable, whereas, in the presence of reducing agent, it may undergo reversible dissociation (**Figure 1.4a**). Thus, Baldwin *et al*. studied the rate of the retro-Michael reaction under reducing conditions. While observing the reaction cycle, the hydrolysis of succinimide into the open ring form was found to positively affect the stability of the thio-succinimide linker (**Figure 1.5**). Formation of the open ring stabilized the thio-succinimide linker and reduced the retro-Michael reaction, even in the presence of a Michael donor such as HSA.[48] Fortunately, succinimide hydrolysis is faster than the retro-Michael reaction, especially at high pH.[49] Studies on "self-hydrolyzing maleimide" linkers are under development.[50]

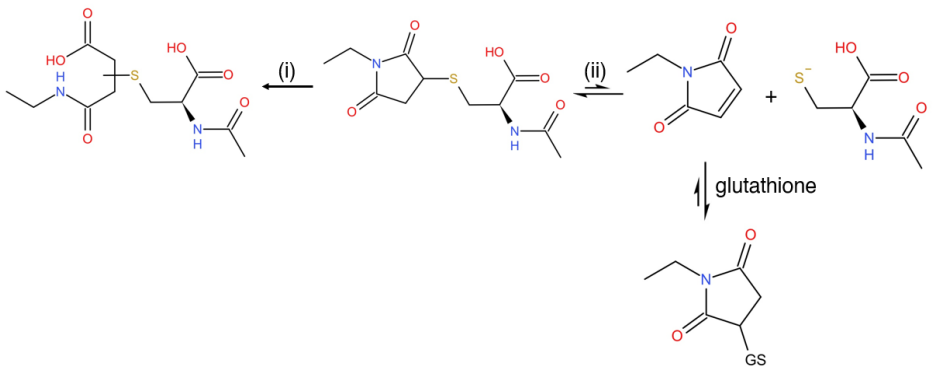

Figure 1.5. Thio-succinimide linker degradation pathway (i) hydrolysis of succinimide to form open ring formation (ii) retro-Michael reaction in the presence of thiol compounds. Adapted from ref. 44.

Shen *et al*. further studied the effect of local charge and solvent accessibility on the stability of the succinimide linker using an antibody conjugated at three different sites: light chain (LC), heavy chain (HC), and Fc domain. They reported that, as the most positively charged species, LC conjugation showed the best stability by attracting hydroxide ions around the moiety and accelerating hydrolysis of succinimide, which minimizes the cleavage of the thio-succinimide linker by slowing the retro-Michael reaction. Conversely, the Fc domain showed the worst stability due to its high solvent accessibility. Therefore, controlling conjugation sites and pH environment may reduce the risk of cleavage of the thioether linkage.[49,51]

1.2.3 Temperature

Molecular mobility increases with increasing temperature, and increased temperature may accelerate the rates of various degradation pathways. During conjugation of Cys-linked ADCs, reduction of antibodies is typically carried out at 37 °C using tris-(2-carboxyethyl)-phosphine (TCEP). At this temperature, antibodies may undergo undesired chemical degradation reactions such as hydrolysis, deamidation, and isomerization, and may form aggregates. Thermal degradation of IgG, for example, is initiated by unfolding, followed by irreversible aggregation.[52] Mohamed *et al*. attributed the thermal degradation of ADCs to a decreased activation energy, increased hydrophobic interaction, increased protein diffusion, and increased molecular collisions.[45] Beckley *et al*. reported higher sensitivity to heat in Cys-conjugated ADCs with high DAR compared to unconjugated and low DAR species. When stored at 40 °C for 8 weeks, ADCs with DAR 6 formed more than 27% of high molecular weight (HMW) species while DAR 2 and

3.5 species formed 2-5% of HMW species. Beckley *et al*. also suggested that conjugation of payloads near the C_H2 domain may cause increased thermal sensitivity of the tertiary structure of ADCs, decreasing the melting temperature of the protein.[53] Increased thermal susceptibility was also observed for a Lys-conjugated ADC with denatured C_H2 domains.[54]

Changes in temperature affect not only ADCs but also the surrounding environment. For example, buffer pH is affected by temperature variations. At high temperature, base-type buffers such as Tris and histidine buffers generate less hydroxide ion than acid-type buffers such as acetate buffer. Since the hydroxide concentration affects chemical degradation reactions such as deamidation of Asn, isomerization of Asp, and hydrolysis of succinimide, buffer selection may influence ADC stability under heat-stress.[44] Increased temperature may induce amino acid isomerization in the hinge region of the antibody and may lead to aggregation.[55] Conversely, at freezing temperature, the pH of the buffer may be shifted due to crystallization of buffer components. According to Sundaramurthi *et al*., crystallizing excipients such as glycine and mannitol may induce buffer crystallization even at low buffer concentration, whereas amorphous excipients such as sucrose and trehalose may completely inhibit buffer crystallization. In addition, the degree of pH shift differed with the initial pH and the buffer concentrations.[56-58]

1.2.4 Light

Light is an important stability risk factor for most biologics, including ADCs.[59] Especially in mAb[60-61] and ADCs,[62] some amino acids such as Trp, Tyr, Phe, His, and Cys are known to undergo photo-oxidation. The absorption of ultraviolet (UV) light often generates not only excited state species but also radicals by photo-ionization.[63] Factors such as pH, ionic strength, and hydrophobicity in the region near the chromophore can affect protein conformation, thereby affecting light absorption and the degree of photo-degradation.[59,63]

Figure 1.6 shows the photolytic degradation pathways of tryptophan. Other light-sensitive amino acids have similar photolytic pathways. Trp has the highest molar absorption coefficient among other light-sensitive amino acids, thus the presence of Trp in the sequence may have a greater effect on photo-degradation than other amino acids. As shown in **Figure 1.6**, initial photolysis begins with the generation of triplet state amino acids. Excited triplet state amino acids with chromophores further react with oxygen, forming peroxy radicals that degrade proteins.[59,63] Many clinically available ADCs such as Mylotarg® and Besponsa® are light-sensitive and require

special primary packaging to prevent photo-degradation.[31] Cockrell *et al*. studied photo-degradation of a Lys-conjugated ADC with DAR of 1-2. In the study, the parent mAb and the linker alone were not susceptible to photo-degradation, whereas the conjugated ADC showed photo-induced aggregation. Cockrell *et al*. also incubated the mAb and the linker without conjugation and found no aggregated species.

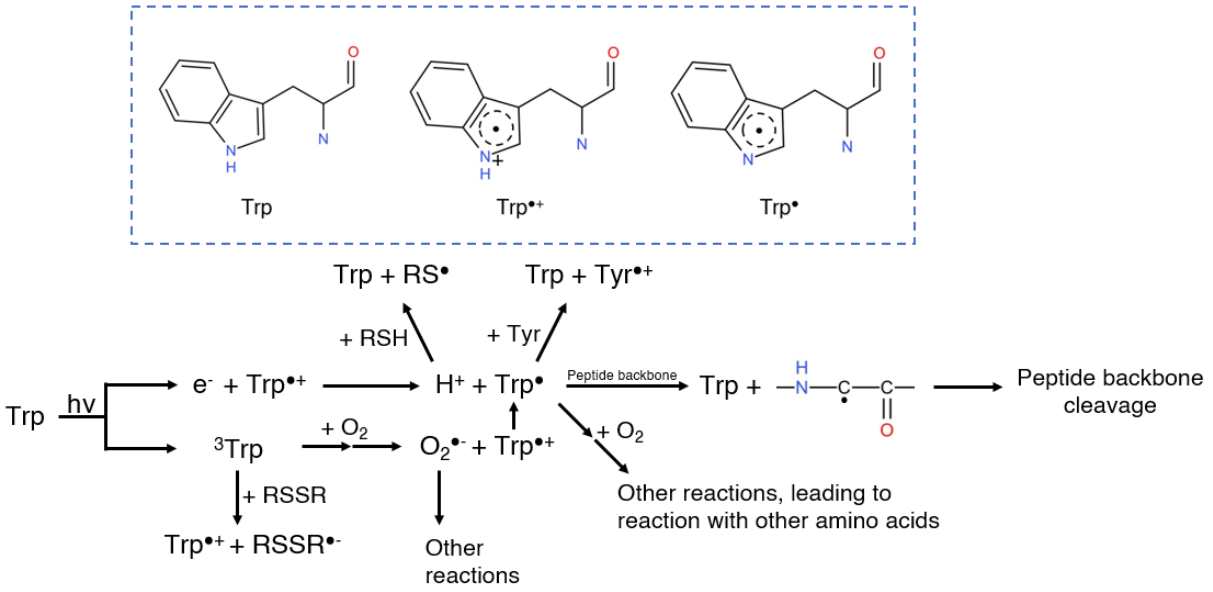

Figure 1.6. Structure of Trp and common pathways of Trp-activated photolysis. Adapted from ref. 59.

This result suggests that conjugation alters the photosensitivity of ADCs by introducing photo-sensitive functional groups. When analyzed using MS/MS, the sequence containing Trp, Phe, Cys, Met, His, and Tyr residues was found to be highly susceptible to photo-degradation.[62] Furthermore, Steinmann *et al*. investigated the susceptibility of disulfide linkages to photo-degradation. The results suggest that ADCs conjugated with disulfide-based linkers may also be prone to photo-induced degradation.[64]

1.2.5 Excipients

Excipients are typically included in ADC formulations to improve the physical and chemical stability. The excipients are expected to be inert, but some can negatively affect the stability of the formulation. Some buffering agents, such as histidine buffer, contain primary

amines that may be sources of cross-reactivity with NHS-based linkers.[65] Adem *et al*. observed a high degree of aggregation in auristatin E-ADCs formulated with high ionic strength buffer. In the study, both an NaCl-containing buffer and an arginine-HCl-containing buffer showed increased aggregate formation, although the NaCl-containing buffer showed higher aggregate levels. Regardless of antibody isotype, ADCs with high DAR underwent aggregation to a greater extent. Adem *et al*. suggested that reduced electrostatic repulsion between single molecules in high ionic strength buffer may have induced the aggregation.[66] Shifts in pH induced by changing buffer composition caused aggregate formation in ADCs.[67] During conjugation of ADCs, organic solvents are used to resolve solubility issues with hydrophobic payloads and linkers. For Mylotarg®, around 20% of dimethylformamide (DMF) was used as a co-solvent; exacerbated aggregation was a result.[55,68]

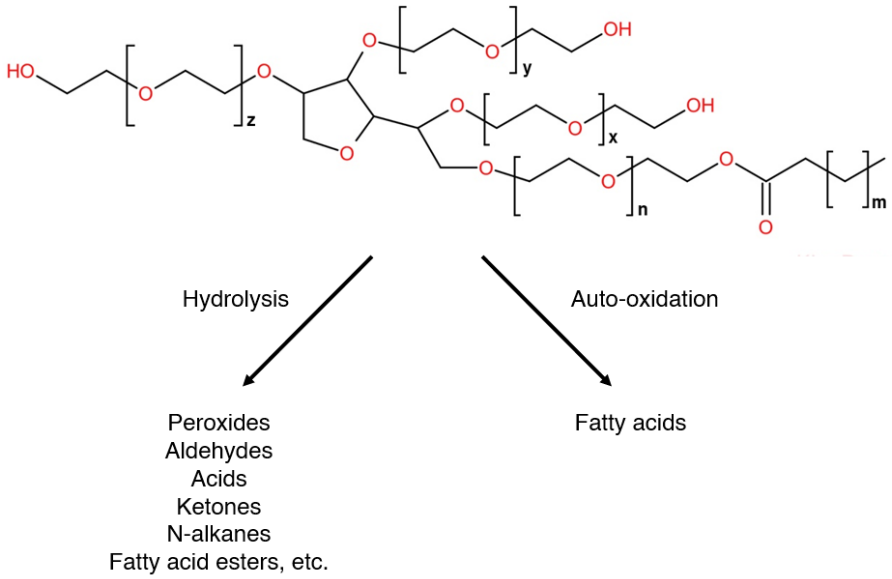

Figure 1.7. Main Scheme of polysorbate degradation. Adapted from ref. 69.

Polysorbates (PS), which play a role in minimizing interfacial stress, are susceptible to ambient oxygen and light. Under light exposure, the peroxide content in PS solutions increases and induces degradation of PS, generating more than 30 species of degradants (**Figure 1.7**).[69] Since commercially available PS are a mixture of chemically diverse poly(oxyethylene) (POE) species, the presence of residual peroxides in PS raises another stability concern. The molecular heterogeneity of PS contributes to a build-up of peroxide that can lead to auto-oxidation and

hydrolysis of PS molecules.[70] As a result, degraded PS has a reduced ability to protect the formulation from interfacial stress. In addition, accumulation of peroxide degradants may also cause instability of ADCs.[69]

1.2.6 In-vivo components

As mentioned above, HSA is a major cause of payload loss in Cys-conjugated ADCs during circulation. Most current ADCs utilize enzyme-labile linkers that are sensitive to cathepsin B, serine hydrolase, glycosidase, or phosphatase (**Figure 1.2e**). However, unwanted encounter with these enzymes at non-target sites may increase the toxicity of ADCs.[4] Hydrophobic ADCs, especially their payloads, are good substrates for multidrug resistant (MDR) transporters such as ATP-binding cassette (ABC) transporters. Loganzo *et al*. suggested that efflux by the MDR transporter is one of the resistance mechanisms of ADCs. According to the clinical and preclinical data, a number of ADCs have experienced reduced efficacy due to the MDR transporter. Thus, it is likely that an ADC with high DAR has a higher clearance due to interaction with MDR transporters. In addition, the expression of MDR transporters such as P-glycoprotein (P-gp) on the target cell may increase as ADC treatment progresses.[3,71-72] To minimize resistance, hydrophilic linkers such as glucosidase-labile linker and phosphatase-labile linker are under development.[4,73]

1.3 Effect of Lyophilization on Stability

Lyophilization, also known as freeze-drying, is a widely used method to improve the stability of both biopharmaceuticals and small molecule drugs. Lyophilization removes water molecules from the product without using high temperature,[74] producing a solid powder. The lyophilization process *per se* may harm proteins in the absence of cryo-protectants or excipients,[75-76] and various studies have been conducted to stabilize protein formulations during lyophilization.[77-78] There are two primary hypotheses regarding the mechanisms of protein stabilization in the solid-state. The "water replacement hypothesis" states that excipients, especially sugars, substitute for the thermodynamic role of water molecules to maintain native-like secondary structures of proteins in the solid state. In this hypothesis, excipients form hydrogen bonds with proteins to minimize structural change upon dehydration. The "vitrification hypothesis" states that a glassy lyoprotectant matrix may slow degradation processes by slowing molecular mobility. Since the

two hypotheses are not mutually exclusive, it is difficult to definitively test and support either of the hypotheses.[76,78] Nevertheless, it has been demonstrated that a sugar-protein matrix may reduce conformational instability of proteins upon lyophilization.[79-80]

All U.S FDA approved ADCs are manufactured in lyophilized form to protect the formulation from hydrolysis and from the other risk factors described above.[31] Typically, a solution dosage form is preferred due to its simplicity and low manufacturing cost compared to lyophilized forms. However, solution dosage forms expose the protein to various risk factors, especially during shipping and storage. For example, during shipping, the product may be subjected to agitation, temperature variations, and freeze/thawing. Long-term storage exposes solution-state pharmaceutical products to greater risk of chemical and physical degradation.[74-75]

Solution dosage forms of proteins are prone to chemical degradation reactions such as deamidation and oxidation, and to physical degradation processes such as aggregation and precipitation.[74] Excipients in protein formulations may create a thermodynamically unfavorable state as the chemical potentials of both excipients and proteins increase. In particular, the hydrophobic components of ADC molecules create entropically unfavorable states while in contact with water. Thus, ADCs are at higher risk of aggregation in an aqueous environment, and to product loss due to adsorption to surfaces. Furthermore, solution dosage forms often are not suitable for long-term storage. For long-term storage purposes, solution dosage forms are often frozen until the time of administration. During freezing, proteins are excluded from the ice phase, creating an ice/freeze-concentrate interface. Proteins are under risk of denaturation at this interface. Although the issue with the ice/freeze-concentrate interface also applies for lyophilization, the duration of exposure to the interface is longer for frozen solutions in long-term storage.[81-82] In addition, Kerwin *et al*. noted that lyophilized or solid suspension forms of proteins usually do not have a precaution on light exposure, suggesting lower susceptibility to photodegradation in solids compared to solutions.[59]

ADCs are at greater risk if formulated in solution due to the risk factors associated with the linker system.[83] There are numerous degradation pathways that ADCs may undergo during storage and shipping. Lyophilization may lower the degradation rates by lowering mobility of molecules. Limiting the mobility may reduce the rate of aggregation in ADCs formulations. Removal of water from the product may reduce the risks of hydrolysis and oxidation near the linkers.[74] Furthermore, lyophilized solids will be less susceptible to temperature variations. It is widely accepted that

lyophilized solids are sensitive to temperatures above their glass transition temperature. Yet, glass transition temperatures for ADCs are generally higher than typical storage temperatures.[53-54,75] Lyophilized ADCs may withstand long-term storage better than solution-state ADCs. However, some concerns still remain regarding increased surface area that may contribute to protein instability. Valliere-Douglass *et al*. reported covalent modification of ADCs with buffers and excipients when heat-stressed at 50 °C. The heat-stressed covalent modification has also been observed in parent mAbs, suggesting that the conjugation chemistry of ADCs is not a cause of the modification. It is also not known whether such modifications affect the biological activity of the ADCs.[85] Nevertheless, protection of the linker-based system from potential degradation and aggregation is crucial since it substantially affects the efficacy and therapeutic window of the ADCs. As noted above, unexpected or premature cleavage of the payload may result in increased toxicity and reduced efficacy.[31,38]

Although all U.S. FDA approved ADC products are manufactured in lyophilized form, there is little published literature that addresses the solid-state stability of lyophilized ADCs.[83-89] Barbour *et al*. studied the solid-state stability of BR96-doxorubicin after lyophilization. Compared to the intrinsic instability of BR96-doxorubicin in solution, lyophilized BR96-doxorubicin with excipients such as lactose and sucrose showed improved long-term stability. On the other hand, other studies have not provided deep understanding of the *in vitro* stability of lyophilized ADCs.[83] Clavaud *et al*. focuses on method validation of near-infrared spectroscopy and its ability to determine moisture content within ADC molecules, rather than stability evaluation of ADCs.[86] Conversely, Jaime *et al*. reported preservation of biological activity of ADCs even after lyophilization. In the study, a lyophilized formulation with 0.40 M trehalose showed the greatest retention of immunological activity among the formulations tested.[87] However, the focus of this study was the *in-vivo* activity of ADCs and not the *in vitro* stability. A similar study was conducted using a mouse monoclonal antibody and showed retention of bioactivity even after lyophilization.[89] Apart from these reports, the number of studies that address the *in vitro* stability and solid-state stability of ADCs is limited.

1.4 Solid-state hydrogen-deuterium exchange (ssHDX-MS)

In this study, solid-state hydrogen/deuterium exchange coupled with mass spectrometry (ssHDX-MS) is used as a short-term predictor of solid-state stability in ADC formulations. Herein,

the fundamentals of hydrogen/deuterium exchange (HDX) and the implications of using HDX to evaluate solids are addressed.

HDX is a high-resolution analytical method that probes the conformation and dynamics of proteins. HDX has also been widely used to study ligand binding,[90-92] protein aggregation,[93-94] and stability during formulation development.[95-96] As shown in **Figure 1.8**, in HDX, a protein is exposed to deuterium oxide (D_2O) to allow hydrogens to be exchanged with deuterons. The location of the exchange-labile hydrogens affects the rate of exchange and their detectability. Hydrogens on the side chains of amino acids readily undergo exchange, but are also subject to rapid reverse reaction ("back exchange"), so that deuteration at these sites is not usually detected. In contrast, hydrogens attached to aliphatic carbon atoms exchange very slowly, if at all, in the time course of a typical experiment. Unlike the former two categories, amide hydrogens in the protein backbone undergo deuterium exchange with a measurable rate. Since the rate of exchange on the amide hydrogens depends on temperature and pH (**Figure 1.9**), the reaction can be quenched by lowering temperature and pH.[97]

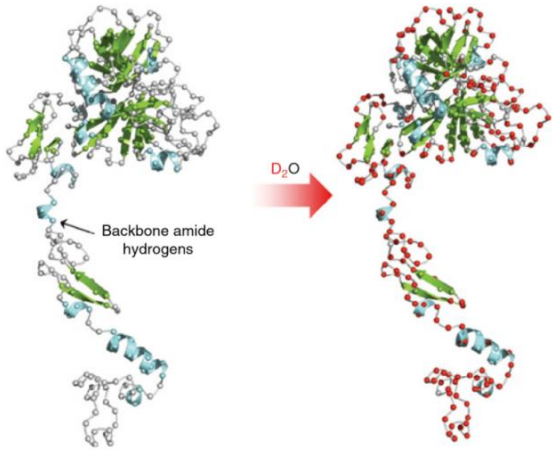

Figure 1.8. Site of hydrogen-deuterium exchange depicted in Factor VIIa. Taken from ref. 97.

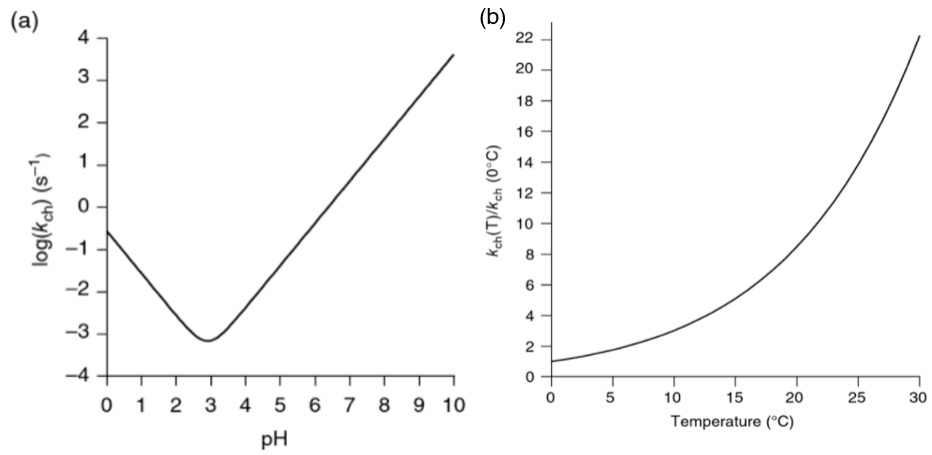

Figure 1.9. The chemical exchange rate, k_{ch}, as a function of (a) pH and (b) temperature (°C). Taken from ref. 97.

Unlike conventional HDX studies performed in solution, this study utilizes HDX in the solid-state. **Figure 1.10** shows schematics of the HDX workflow in solution-state and in the solid-state.[98] Regardless of the phase, the workflow involves D_2O exposure, incubation, reaction quenching, and MS analysis. In solution HDX, a protein is diluted directly into the D_2O solution to initiate exchange, whereas solid-state HDX exposes a lyophilized protein to a D_2O vapor in a desiccator with controlled D_2O activity (i.e., relative humidity, RH in D_2O) and temperature. The RH inside the desiccator is controlled by saturating D_2O solution with various salts.[99] The temperature for incubation may vary from 4 °C to 70 °C. Typically, the upper limit of the incubation temperature is recommended not to exceed the glass transition temperature (T_g) of the product, and the lower limit of the incubation temperature is recommended around 4 °C to allow a detectable rate of exchange. After incubation, the exchange reaction is quenched by flash freezing with liquid nitrogen, after which the samples are stored at -80 °C. Prior to MS analysis, the reaction is further quenched by diluting with low pH buffer to minimize back-exchange. The mass difference between hydrogen (H) and deuterium (D) detected by MS allows measurement of the number of exchanged deuterons, which serves as a measure of the inter- and intra-molecular hydrogen bond network of the protein in the solid sample. The extent of deuterium incorporation has been shown to be correlated with stability on storage for a number of proteins.[100-101] ssHDX can be used to screen protein formulations and select those most likely to be stable. The method offers the advantage that it only takes days to weeks to distinguish stability differences among formulations, rather than the months typically required for stability studies. Furthermore, mass

spectrometric analysis (MS) coupled with ssHDX also provides high resolution information on the protein and its solid environment, and allows simultaneous analysis of various molecular species such as adducts or degradants. To date, ssHDX has shown its applicability in evaluating stability in various therapeutic proteins such as myoglobin,[102-103] a monoclonal antibody,[104] and a therapeutic fragment antigen-binding (Fab) protein.[105] The study presented here extends ssHDX-MS to ADCs and provides knowledge on solid-state stability of ADCs.

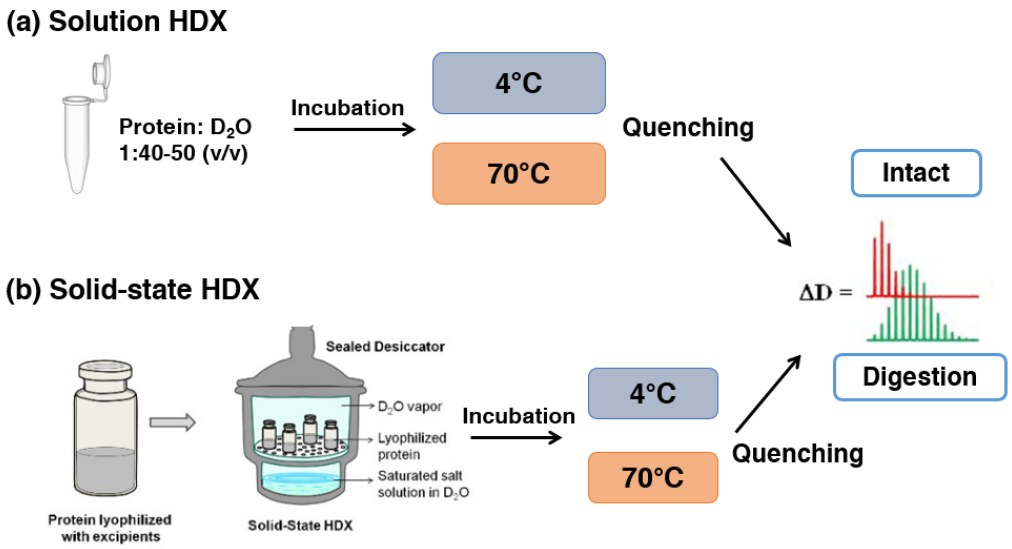

Figure 1.10. Experimental scheme of (a) solution-state and (b) solid-state HDX-MS. Partially taken from ref. 98.

1.5 Specific aims

The overall objective of the studies presented in this dissertation is to provide a deeper understanding of the solid-state stability of ADCs and their linker systems, in order to aid in formulating ADCs with improved stability and reduced off-target toxicity.

Compared to mAbs, conjugation with a linker system affects the ADC in its susceptibility to various degradation pathways.[31,37] In the past, studies have been conducted 1) to develop linkers with improved *in vivo* stability,[29,73] and 2) to understand the deconjugation mechanisms *in vivo*.[4,41,46,49] In contrast, *in vitro* stability has received little attention in the published literature. Although all nine of the U.S. approved ADCs are lyophilized to minimize degradation, there is little published information on solid-state stability of ADCs.[85-89] To evaluate lyophilized solids, pharmaceutical development scientists rely heavily on long-term stability studies to select the best

formulation, which take months to complete. Furthermore, characterization methods that are used orthogonally with accelerated stability studies such as FT-IR, Raman spectroscopy, NIR, DSC, XRPD are often poorly correlated with stability.[98] Thus, stability evaluation of solid-state products is often a bottleneck in their development.

The long-term goal of this study is to characterize lyophilized ADC formulations to improve their *in vitro* stability. The solid-state stability of ADC formulations will be investigated on exposure to varying risk factors. The work will investigate the applicability of ssHDX as a short-term predictor for solid-state stability of ADC formulations, as compared to accelerated stability studies.

The study consists of the following specific aims:

Aim 1: Compare solid-state stability of ADC formulations with commonly used lyoprotectants using ssHDX and accelerated stability studies.

Aim 2: Compare solid-state stability of the parent mAb and ADCs in varying protein concentrations and interfacial stress.

Aim 3: Compare the stability of a model hydrazone linker in solution-state and solid-state at varying pre-lyophilization pH.

Successful completion of these Aims is expected to significantly reduce the time required for formulation development of ADCs. Furthermore, improved understanding of the solid-state stability of ADCs will improve their safety and efficacy, reducing the risks of undesired toxicity on patients and of potential recall of the product.

1.6 References

1. Carter PJ, Lazar GA 2018. Next generation antibody drugs: pursuit of the 'high-hanging fruit'. Nature Reviews Drug Discovery 17(3):197-223.

2. Coats S, Williams M, Kebble B, Dixit R, Tseng L, Yao NS, Tice DA, Soria JC 2019. Antibody-Drug Conjugates: Future Directions in Clinical and Translational Strategies to Improve the Therapeutic Index. Clinical Cancer Research 25(18):5441-5448.

3. Jain N, Smith SW, Ghone S, Tomczuk B 2015. Current ADC Linker Chemistry. Pharmaceutical Research 32(11):3526-3540.

4. Bargh JD, Isidro-Llobet A, Parker JS, Spring DR 2019. Cleavable linkers in antibody-drug conjugates. Chemical Society Reviews 48(16):4361-4374.

5. Kommineni N, Pandi P, Chella N, Domb AJ, Khan W Antibody drug conjugates: Development, characterization, and regulatory considerations. Polymers for Advanced Technologies:17.

6. Beck A, Goetsch L, Dumontet C, Corvaia N 2017. Strategies and challenges for the next generation of antibody drug conjugates. Nature Reviews Drug Discovery 16(5):315-337.

7. Hoffmann RM, Coumbe BGT, Josephs DH, Mele S, Ilieva KM, Cheung A, Tutt AN, Spicer JF, Thurston DE, Crescioli S, Karagiannis SN 2018. Antibody structure and engineering considerations for the design and function of Antibody Drug Conjugates (ADCs). Oncoimmunology 7(3):11.

8. Birrer MJ, Moore KN, Betella I, Bates RC 2019. Antibody-Drug Conjugate-Based Therapeutics: State of the Science. Jnci-Journal of the National Cancer Institute 111(6):538-549.

9. Wagh A, Song HT, Zeng M, Tao L, Das TK 2018. Challenges and new frontiers in analytical characterization of antibody-drug conjugates. Mabs 10(2):222-243.

10. Yao HZ, Jiang F, Lu AP, Zhang G 2016. Methods to Design and Synthesize Antibody-Drug Conjugates (ADCs). International Journal of Molecular Sciences 17(2):16.

11. Neupane R, Bergquist J 2017. Analytical techniques for the characterization of Antibody Drug Conjugates: Challenges and prospects. European Journal of Mass Spectrometry 23(6):417-426.

12. Mou S, Huang Y, Rosenbaum AI 2018. ADME Considerations and Bioanalytical Strategies for Pharmacokinetic Assessments of Antibody-Drug Conjugates. Antibodies 7(4):15.

13. Todoroki K, Yamada T, Mizuno H, Toyo'oka T 2018. Current Mass Spectrometric Tools for the Bioanalyses of Therapeutic Monoclonal Antibodies and Antibody-Drug Conjugates. Analytical Sciences 34(4):397-406.

14. Rabia LA, Desai AA, Jhajj HS, Tessier PM 2018. Understanding and overcoming trade-offs between antibody affinity, specificity, stability and solubility. Biochemical Engineering Journal 137:365-374.

15. Lam XM, Yang JY, Cleland JL 1997. Antioxidants for prevention of methionine oxidation in recombinant monoclonal antibody HER2. Journal of Pharmaceutical Sciences 86(11):1250- 1255.

16. Reissner KJ, Aswad DW 2003. Deamidation and isoaspartate formation in proteins: unwanted alterations or surreptitious signals? Cellular and Molecular Life Sciences 60(7):1281-1295.

17. Wakankar AA, Borchardt RT 2006. Formulation considerations for proteins susceptible to asparagine deamidation and aspartate isomerization. Journal of Pharmaceutical Sciences 95(11):2321-2336.

18. Manning MC, Chou DK, Murphy BM, Payne RW, Katayama DS 2010. Stability of Protein Pharmaceuticals: An Update. Pharmaceutical Research 27(4):544-575.

19. Chaudhuri R, Cheng Y, Middaugh CR, Volkin DB 2014. High-Throughput Biophysical Analysis of Protein Therapeutics to Examine Interrelationships Between Aggregate Formation and Conformational Stability. Aaps Journal 16(1):48-64.

20. Xie HS, Audette C, Hoffee M, Lambert JM, Blattler WA 2004. Pharmacokinetics and biodistribution of the antitumor immunoconjugate, cantuzumab mertansine (huC242-DM1), and its two components in mice. Journal of Pharmacology and Experimental Therapeutics 308(3):1073-1082.

21. Lucas AT, Price LSL, Schorzman AN, Storrie M, Piscitelli JA, Razo J, Zamboni WC 2018. Factors Affecting the Pharmacology of Antibody-Drug Conjugates. Antibodies 7(1):28.

22. Jefferis R 2012. Isotype and glycoform selection for antibody therapeutics. Archives of Biochemistry and Biophysics 526(2):159-166.

23. Tang HC, Liu Y, Yu ZJ, Lin L, Liu WS, Han Q, Wei MJ, Jin Y 2019. The Analysis of Key Factors Related to ADCs Structural Design. Frontiers in Pharmacology 10:11.

24. Rossin R, van Duijnhoven SMJ, ten Hoeve W, Janssen HM, Kleijn LHJ, Hoeben FJM, Versteegen RM, Robillard MS 2016. Triggered Drug Release from an Antibody-Drug Conjugate Using Fast "Click-to-Release" Chemistry in Mice. Bioconjugate Chemistry 27(7):1697-1706.

25. Abdollahpour-Alitappeh M, Lotfinia M, Gharibi T, Mardaneh J, Farhadihosseinabadi B, Larki P, Faghfourian B, Sepehr KS, Abbaszadeh-Goudarzi K, Abbaszadeh-Goudarzi G, Johari B, Zali MR, Bagheri N 2019. Antibody-drug conjugates (ADCs) for cancer therapy: Strategies, challenges, and successes. Journal of Cellular Physiology 234(5):5628-5642.

26. Schmidt MM, Wittrup KD 2009. A modeling analysis of the effects of molecular size and binding affinity on tumor targeting. Molecular Cancer Therapeutics 8(10):2861-2871.

27. McDonagh CF, Turcott E, Westendorf L, Webster JB, Alley SC, Kim K, Andreyka J, Stone I, Hamblett KJ, Francisco JA, Carter P 2006. Engineered antibody-drug conjugates with defined sites and stoichiometries of drug attachment. Protein Engineering Design & Selection 19(7):299-307.

28. Ducry, L. (2013). Antibody-Drug Conjugates (1st ed. 2013. ed., Methods in Molecular Biology, 1045. Ch.11 Engineering THIOMABs for site-specific conjugation of thiol-reactive linkers. 189-203.

29. Yamada K, Ito Y 2019. Recent Chemical Approaches for Site-Specific Conjugation of Native Antibodies: Technologies toward Next-Generation Antibody-Drug Conjugates. Chembiochem 20(21):2729-2737.

30. Buecheler JW, Winzer M, Weber C, Gieseler H 2020. Alteration of Physicochemical Properties for Antibody-Drug Conjugates and Their Impact on Stability. Journal of Pharmaceutical Sciences 109(1):161-168.

31. Duerr C, Friess W 2019. Antibody-drug conjugates- stability and formulation. European Journal of Pharmaceutics and Biopharmaceutics 139:168-176.

32. Lu J, Jiang F, Lu AP, Zhang G 2016. Linkers Having a Crucial Role in Antibody-Drug Conjugates. International Journal of Molecular Sciences 17(4):22.

33. Phillips GDL, Li GM, Dugger DL, Crocker LM, Parsons KL, Mai E, Blattler WA, Lambert JM, Chari RVJ, Lutz RJ, Wong WLT, Jacobson FS, Koeppen H, Schwall RH, Kenkare-Mitra SR, Spencer SD, Sliwkowski MX 2008. Targeting HER2-Positive Breast Cancer with Trastuzumab-DM1, an Antibody-Cytotoxic Drug Conjugate. Cancer Research 68(22):9280-9290.

34. Ducry L, Stump B 2010. Antibody-Drug Conjugates: Linking Cytotoxic Payloads to Monoclonal Antibodies. Bioconjugate Chemistry 21(1):5-13.

35. Blencowe CA, Russell AT, Greco F, Hayes W, Thornthwaite DW 2011. Self-immolative linkers in polymeric delivery systems. Polymer Chemistry 2(4):773-790.

36. Steiner M, Hartmann I, Perrino E, Casi G, Brighton S, Jelesarov I, Bernardes GJL, Neri D 2013. Spacer length shapes drug release and therapeutic efficacy of traceless disulfide-linked ADCs targeting the tumor neovasculature. Chemical Science 4(1):297-302.

37. Wang, J., Shen, W., & Zaro, J. (2015). Antibody-Drug Conjugates The 21st Century Magic Bullets for Cancer (1st ed. 2015. ed., AAPS Advances in the Pharmaceutical Sciences Series, 17). 4.4.6 Linker stability and safety 69-72.

38. Alley SC, Benjamin DR, Jeffrey SC, Okeley NM, Meyer DL, Sanderson RJ, Senter PD 2008. Contribution of linker stability to the activities of anticancer immunoconjugates. Bioconjugate Chemistry 19(3):759-765.

39. Singh SK, Luisi DL, Pak RH 2015. Antibody-Drug Conjugates: Design, Formulation and Physicochemical Stability. Pharmaceutical Research 32(11):3541-3571.

40. Erickson HK, Lambert JM 2012. ADME of Antibody-Maytansinoid Conjugates. AAPS Journal 14(4):799-805.

41. Kalia J, Raines RT 2008. Hydrolytic stability of hydrazones and oximes. Angewandte Chemie-International Edition 47(39):7523-7526.

42. Ducry, L. (2013). Antibody-Drug Conjugates (1st ed. 2013. ed., Methods in Molecular Biology, 1045. Ch.5 Linker Technologies for Antibody-Drug Conjugates 71-100.

43. Waterman KC, Adami RC, Alsante KM, Antipas AS, Arenson DR, Carrier R, Hong JY, Landis MS, Lombardo F, Shah JC, Shalaev E, Smith SW, Wang H 2002. Hydrolysis in pharmaceutical formulations. Pharmaceutical Development and Technology 7(2):113-146.

44. Wang, J., Shen, W., & Zaro, J. (2015). Antibody-Drug Conjugates The 21st Century Magic Bullets for Cancer (1st ed. 2015. ed., AAPS Advances in the Pharmaceutical Sciences Series, 17). Ch.5 Formulation Development for Antibody-Drug Conjugates 79-96.

45. Mohamed HE, Mohamed AA, Al-Ghobashy MA, Fathalla FA, Abbas SS 2018. Stability assessment of antibody-drug conjugate Trastuzumab emtansine in comparison to parent monoclonal antibody using orthogonal testing protocol. Journal of Pharmaceutical and Biomedical Analysis 150:268-277.

46. Chen T, Su D, Gruenhagen J, Gu C, Li Y, Yehl P, Chetwyn NP, Medley CD 2016. Chemical de-conjugation for investigating the stability of small molecule drugs in antibody-drug conjugates. Journal of Pharmaceutical and Biomedical Analysis 117:304-310.

47. Liu HC, Chumsae C, Gaza-Bulseco G, Hurkmans K, Radziejewski CH 2010. Ranking the Susceptibility of Disulfide Bonds in Human IgGs1 Antibodies by Reduction, Differential Alkylation, and LC-MS Analysis. Analytical Chemistry 82(12):5219-5226.

48. Baldwin AD, Kiick KL 2011. Tunable Degradation of Maleimide-Thiol Adducts in Reducing Environments. Bioconjugate Chemistry 22(10):1946-1953.

49. Zheng K, Chen Y, Wang J, Zheng L, Hutchinson M, Persson J, Ji JY 2019. Characterization of Ring-Opening Reaction of Succinimide Linkers in ADCs. Journal of Pharmaceutical Sciences 108(1):133-141.

50. Szijj, PA, Bahou C, Chudasam V 2018 Minireview: Addressing the retro-Michael instability of maleimide bioconjugates. Drug Discovery Today: Technologies 30:27-34.

51. Shen BQ, Xu KY, Liu LN, Raab H, Bhakta S, Kenrick M, Parsons-Reponte KL, Tien J, Yu SF, Mai E, Li DW, Tibbitts J, Baudys J, Saadi OM, Scales SJ, McDonald PJ, Hass PE, Eigenbrot C, Nguyen T, Solis WA, Fuji RN, Flagella KM, Patel D, Spencer SD, Khawlil LA, Ebens A, Wong WL, Vandlen R, Kaur S, Sliwkowski MX, Scheller RH, Polakis P, Junutula JR 2012. Conjugation site modulates the in vivo stability and therapeutic activity of antibody-drug conjugates. Nature Biotechnology 30(2):184-189.

52. Feng YW, Ooishi A, Honda S 2012. Aggregation factor analysis for protein formulation by a systematic approach using FTIR, SEC and design of experiments techniques. Journal of Pharmaceutical and Biomedical Analysis 57:143-152.

53. Beckley NS, Lazzareschi KP, Chih HW, Sharma VK, Flores HL 2013. Investigation into Temperature-Induced Aggregation of an Antibody Drug Conjugate. Bioconjugate Chemistry 24(10):1674-1683.

54. Gandhi AV, Arlotta KJ, Chen HN, Owen SC, Carpenter JF 2018. Biophysical Properties and Heating-Induced Aggregation of Lysine-Conjugated Antibody-Drug Conjugates. Journal of Pharmaceutical Sciences 107(7):1858-1869.

55. Ross PL, Wolfe JL 2016. Physical and Chemical Stability of Antibody Drug Conjugates: Current Status. Journal of Pharmaceutical Sciences 105(2):391-397.

56. Sundaramurthi P, Shalaev E, Suryanarayanan R 2010. "pH Swing" in Frozen Solutions Consequence of Sequential Crystallization of Buffer Components. Journal of Physical Chemistry Letters 1(1):265-268.

57. Reineke K, Mathys A, Knorr D 2011. Shift of pH-Value During Thermal Treatments in Buffer Solutions and Selected Foods. International Journal of Food Properties 14(4):870-881.

58. Koranne S, Thakral S, Suryanarayanan R 2018. Effect of Formulation and Process Parameters on the Disproportionation of Indomethacin Sodium in Buffered Lyophilized Formulations. Pharmaceutical Research 35(1):13.

59. Kerwin BA, Remmele RL 2007. Protect from light: Photodegradation and protein biologics. Journal of Pharmaceutical Sciences 96(6):1468-1479.

60. Sreedhara A, Yin J, Joyce M, Lau K, Wecksler AT, Deperalta G, Yi L, Wang YJ, Kabakoff B, Kishore RSK 2016. Effect of ambient light on IgG1 monoclonal antibodies during drug product processing and development. European Journal of Pharmaceutics and Biopharmaceutics 100:38-46.

61. Kang H, Tolbert TJ, Schoneich C 2019. Photoinduced Tyrosine Side Chain Fragmentation in IgG4-Fc: Mechanisms and Solvent Isotope Effects. Molecular Pharmaceutics 16(1):258-272.

62. Cockrell GM, Wolfe MS, Wolfe JL, Schoneich C 2015. Photoinduced Aggregation of a Model Antibody-Drug Conjugate. Molecular Pharmaceutics 12(6):1784-1797.

63. Davies MJ, Truscott RJW 2001. Photo-oxidation of proteins and its role in cataractogenesis. Journal of Photochemistry and Photobiology B-Biology 63(1-3):114-125.

64. Steinmann D, Mozziconacci O, Bommana R, Stobaugh JF, Wang YJ, Schoneich C 2017. Photodegradation Pathways of Protein Disulfides: Human Growth Hormone. Pharmaceutical Research 34(12):2756-2778.

65. Christie RJ, Fleming R, Bezabeh B, Woods R, Mao S, Harper J, Joseph A, Wang QL, Xu ZQ, Wu H, Gao CS, Dimasi N 2015. Stabilization of cysteine-linked antibody drug conjugates with N-aryl maleimides. Journal of Controlled Release 220:660-670.

66. Adem YT, Schwarz KA, Duenas E, Patapoff TW, Galush WJ, Esue O 2014. Auristatin Antibody Drug Conjugate Physical Instability and the Role of Drug Payload. Bioconjugate Chemistry 25(4):656-664.

67. Frka-Petesic B, Zanchi D, Martin N, Carayon S, Huille S, Tribet C 2016. Aggregation of Antibody Drug Conjugates at Room Temperature: SAXS and Light Scattering Evidence for Colloidal Instability of a Specific Subpopulation. Langmuir 32(19):4848-4861.

68. Hollander I, Kunz A, Hamann PR 2008. Selection of reaction additives used in the preparation of monomeric antibody-calicheamicin conjugates. Bioconjugate Chemistry 19(1):358-361.

69. Kishore RSK, Kiese S, Fischer S, Pappenberger A, Grauschopf U, Mahler HC 2011. The Degradation of Polysorbates 20 and 80 and its Potential Impact on the Stability of Biotherapeutics. Pharmaceutical Research 28(5):1194-1210.

70. Borisov OV, Ji JYA, Wang YJ, Vega F, Ling VT 2011. Toward Understanding Molecular Heterogeneity of Polysorbates by Application of Liquid Chromatography-Mass Spectrometry with Computer-Aided Data Analysis. Analytical Chemistry 83(10):3934-3942.

71. Loganzo F, Sung M, Gerber HP 2016. Mechanisms of Resistance to Antibody-Drug Conjugates. Molecular Cancer Therapeutics 15(12):2825-2834.

72. Leslie EM, Deeley RG, Cole SPC 2005. Multidrug resistance proteins: role of P-glycoprotein, MRP1, MRP2, and BCRP (ABCG2) in tissue defense. Toxicology and Applied Pharmacology 204(3):216-237.

73. Zhao RY, Wilhelm SD, Audette C, Jones G, Leece BA, Lazar AC, Goldmacher VS, Singh R, Kovtun Y, Widdison WC, Lambert JM, Chari RVJ 2011. Synthesis and Evaluation of Hydrophilic Linkers for Antibody-Maytansinoid Conjugates. Journal of Medicinal Chemistry 54(10):3606-3623.

74. Carpenter JF, Pikal MJ, Chang BS, Randolph TW 1997. Rational design of stable lyophilized protein formulations: Some practical advice. Pharmaceutical Research 14(8):969- 975.

75. Wang W, Singh S, Zeng DL, King K, Nema S 2007. Antibody structure, instability, and formulation. Journal of Pharmaceutical Sciences 96(1):1-26.

76. Wang W 2000. Lyophilization and development of solid protein pharmaceuticals. International Journal of Pharmaceutics 203(1-2):1-60.

77. Kasper JC, Winter G, Friess W 2013. Recent advances and further challenges in lyophilization. European Journal of Pharmaceutics and Biopharmaceutics 85(2):162-169.

78. Cicerone MT, Pikal MJ, Qian KK 2015. Stabilization of proteins in solid form. Advanced Drug Delivery Reviews 93:14-24.

79. Prestrelski SJ, Tedeschi N, Arakawa T, Carpenter JF 1993. DEHYDRATION-INDUCED CONFORMATIONAL TRANSITIONS IN PROTEINS AND THEIR INHIBITION BY STABILIZERS. Biophysical Journal 65(2):661-671.

80. Simon N, Sperber C, Voigtlander C, Born J, Gilbert DF, Seyferth S, Lee G, Kappes B, Friedrich O 2020. Improved stability of polyclonal antibodies: A case study with lyophilization-conserved antibodies raised against epitopes from the malaria parasite Plasmodium falciparum. European Journal of Pharmaceutical Sciences 142:12.

81. Arakawa T, Prestrelski SJ, Kenney WC, Carpenter JF 1993. FACTORS AFFECTING SHORT-TERM AND LONG-TERM STABILITIES OF PROTEINS. Advanced Drug Delivery Reviews 10(1):1-28.

82. Minatovicz B, Sun L, Foran C, Chaudhuri B, Tang C, Shameem M 2020. Freeze-concentration of solutes during bulk freezing and its impact on protein stability. Journal of Drug Delivery Science and Technology 58:15.

83. Barbour NP, Paborji M, Alexander TC, Coppola WP, Bogardus JB 1995. STABILIZATION OF CHIMERIC BR96-DOXORUBICIN IMMUNOCONJUGATE. Pharmaceutical Research 12(2):215-222.

84. Duddu SP, DalMonte PR 1997. Effect of glass transition temperature on the stability of lyophilized formulations containing a chimeric therapeutic monoclonal antibody. Pharmaceutical Research 14(5):591-595.

85. Valliere-Douglass JF, Lewis P, Salas-Solano O, Jiang S 2015. Solid-State mAbs and ADCs Subjected to Heat-Stress Stability Conditions can be Covalently Modified with Buffer and Excipient Molecules. Journal of Pharmaceutical Sciences 104(2):652-665.

86. Clavaud M, Roggo Y, Degardin K, Sacre PY, Hubert P, Ziemons E 2016. Moisture content determination in an antibody-drug conjugate freeze-dried medicine by near-infrared spectroscopy: A case study for release testing. Journal of Pharmaceutical and Biomedical Analysis 131:380-390.

87. Jaime J, Page M 2004. Paclitaxel antibody conjugates and trehalose for preserving the immunulogical activity after freeze-drying. Current Medicinal Chemistry 11(4):439-446.

88. Ramos JR, Taniwaki L, Mendonca R, Ribeiro JAS, Scott IU, Cunha AS, Jorge R 2010. Effect of Lyophilization on the in vitro Biological Activity of Bevacizumab. Investigative Ophthalmology & Visual Science 51(13):2.

89. Rowland AJ, Pietersz GA, McKenzie IFC 1993. PRECLINICAL INVESTIGATION OF THE ANTITUMOR EFFECTS OF ANTI-CD19-IDARUBICIN IMMUNOCONJUGATES. Cancer Immunology Immunotherapy 37(3):195-202.

90. Kielkopf CS, Ghosh M, Anand GS, Brown SHJ. HDX-MS reveals orthosteric and allosteric changes in apolipoprotein-D structural dynamics upon binding of progesterone. Protein Sci. 2019;28(2):365–374.

91. Nemirovskiy, O., Giblin, D.E., Gross, M.L. (1999) Electrospray ionization mass spectrometry and hydrogen/deuterium exchange for probing the interaction of calmodulin with calcium. J. Am Soc Mass Spectrom, 10 (8), 711-718.

92. Sowole, M.A., Konermann, L. (2014) Effects of protein-ligand interactions on hydrogen/deuterium exchange kinetics; canonical and noncanonical scenarios. Anal Chem, 86 (13), 6715-6722.

93. Sharma, A.K., Pavlova, S.T., Kim, J., et al. (2012) Bifunctional compounds for controlling metal-mediated aggregation of the AB42 peptide. J Am Chem Soc, 134 (15), 6625-6636.

94. Zhang, Y., Rempel, D.L., Zhang, J., et al. (2013) Pulsed hydrogen-deuterium exchange mass spectrometry probes conformational changes in amyloid beta (AB) peptide aggregation. Proc Natl Acad Sci USA, 110 (36), 14604–14609.

95. Deng B, Lento C, Wilson DJ. Hydrogen deuterium exchange mass spectrometry in biopharmaceutical discovery and development - a review. Anal Chim Acta. 2016; 940:8–20.

96. Kabaria SR, Mangion I, Makarov AA, Pirrone GF. Use of MALDI-MS with solid-state hydrogen deuterium exchange for semi-automated assessment of peptide and protein physical stability in lyophilized solids. Anal Chim Acta. 2019;1054:114–121.

97. Hydrogen Exchange Mass Spectrometry of Proteins: Fundamentals, Methods, and Applications. (2016). Germany: Wiley. Ch.1 Hydrogen Exchange: A sensitive Analytical Window into Protein Conformation and Dynamics 1-15.

98. Moorthy BS, Iyer LK, Topp EM 2015. Mass Spectrometric Approaches to Study Protein Structure and Interactions in Lyophilized Powders. Jove-Journal of Visualized Experiments Cho 16 (98), e52503.

99. Rockland LB 1960. SATURATED SALT SOLUTIONS FOR STATIC CONTROL OF RELATIVE HUMIDITY BETWEEN 5-DEGREES-C AND 40-DEGREES-C. Analytical Chemistry 32(10):1375-1376.

100. Moorthy BS, Schultz SG, Kim SG, Topp EM 2014. Predicting Protein Aggregation during Storage in Lyophilized Solids Using Solid State Amide Hydrogen/Deuterium Exchange with Mass Spectrometric Analysis (ssHDX-MS). Molecular Pharmaceutics 11(6):1869-1879.

101. Moorthy BS, Zarraga IE, Kumar L, Walters BT, Goldbach P, Topp EM, Allmendinger A 2018. Solid-State Hydrogen Deuterium Exchange Mass Spectrometry: Correlation of Deuterium Uptake and Long-Term Stability of Lyophilized Monoclonal Antibody Formulations. Molecular Pharmaceutics 15(1):1-11.

102. Iyer LK, Sacha GA, Moorthy BS, Nail SL, Topp EM 2016. Process and Formulation Effects on Protein Structure in Lyophilized Solids Using Mass Spectrometric Methods. Journal of Pharmaceutical Sciences 105(5):1684-1692.

103. Sophocleous AM, Zhang J, Topp EM 2012. Localized Hydration in Lyophilized Myoglobin by Hydrogen-Deuterium Exchange Mass Spectrometry. 1. Exchange Mapping. Molecular Pharmaceutics 9(4):718-726.

104. Moussa EM, Singh SK, Kimmel M, Nema S, Topp EM 2018. Probing the Conformation of an IgG1 Monoclonal Antibody in Lyophilized Solids Using Solid-State HydrogenDeuterium Exchange with Mass Spectrometric Analysis (ssHDX-MS). Molecular Pharmaceutics 15(2):356-368.

105. Chandrababu KB, Kumar L, Walters B, Chang D, Nayak P, Allmendinger A, Zarraga I, Topp E 2017. Solid-state hydrogen-deuterium exchange mass spectrometry (ssHDX-MS) analysis of therapeutic fragment antigen-binding (Fab) protein formulations. Abstracts of Papers of the American Chemical Society 253:1.

CHAPTER 2. STABILITY OF ADC FORMULATIONS EVALUATED USING SSHDX-MS

2.1 Abstract

Antibody-drug conjugates (ADCs) have been at the forefront in cancer therapy due to their target specificity. All the FDA approved ADCs are developed in lyophilized form to minimize instability associated with the linker that connects the cytotoxic drug and the antibody during shipping and storage. We present here solid-state hydrogen-deuterium exchange with mass spectrometric analysis (ssHDX-MS) as a tool to analyze protein structure and matrix interactions for formulations of an ADC with and without commonly used excipients. We compared results of the ssHDX-MS with accelerated stability results using size-exclusion chromatography and determined that the former technique was able to successfully identify the destabilizing effects of mannitol and polysorbate 80. In comparison, Fourier-transform infrared spectroscopy results were inconclusive. The agreement between ssHDX-MS and stressed stability studies supports the potential of ssHDX-MS as a method of predicting relative stability of different formulations.

2.2 Introduction

ADCs provide both potency and target specificity by conjugating chemotherapeutic drugs to an antibody. An ADC is an antibody, such as IgG, attached to a linker system. The linker system is used to attach one or more individual molecules of a chemotherapeutic agent to the antibody. The chemotherapeutic agent is delivered directly to a cancer cell that expresses an antigen specific to the antibody. In cancer therapy, ADCs have lower side effects and toxicity than conventional anti-cancer agents because of the substantially lower dose of chemotherapeutic agent needed for treatment.[1] Formulation and processing of ADCs follow similar approaches used for other biological molecules. The goal is to improve stability by decreasing the potential for unfolding and aggregation.[2] Furthermore, because the drug portion of an ADC is highly toxic in its free form, it

is crucial to minimize premature cleavage of the linker, which is often hydrolytically labile. This is often achieved through lyophilization of the formulation.[3,4]

Lyophilization has been widely used to stabilize protein drug formulations. Various excipients are used to ensure stability not only during lyophilization but also during storage.[5] Numerous characterization methods have been used to examine the properties of lyophilized protein formulations. Spectroscopic techniques such as Fourier-transform infrared spectroscopy (FT-IR), Raman spectroscopy, or near-infrared spectroscopy (NIR) are used to assess protein structure. Physical properties of the solid are often assessed by measuring moisture content, crystallinity (e.g., using x-ray powder diffraction, XRPD) and glass transition temperature (T_g) (e.g., using differential scanning calorimetry, DSC). While these methods provide information about the physical and chemical properties of the solid, they are often weakly correlated to the stability of the proteins during shelf storage.[6] As a result, the development and regulation of protein drug products relies heavily on accelerated stability studies to assess the performance of candidate formulations and to develop lyophilization cycles, rather than on robust analytical methods that characterize the product and allow rapid prediction of storage stability.[7,8] Nevertheless, accelerated stability studies have their own limitations. Since they can require months to complete, they can slow formulation development. For lyophilized products, the storage temperature for accelerated stability studies cannot exceed the glass transition temperature of the product without compromising the relevance of the results to the intended storage temperature. As a result, there is a limit to how much these studies can be "accelerated" by increased storage temperature. In addition, accelerated stability studies are coupled with various characterization methods such as size-exclusion chromatography (SEC), ion exchange chromatography (iEC), and methods of particle sizing and counting to further measure physical and chemical stability of the candidate formulations. Therefore, accelerated studies are a time consuming and painstaking process during formulation development. Thus, there is a need for new analytical methods that provide a comprehensive characterization of protein conformation and of the reactive environment in lyophilized solids, allowing real time stability to be predicted with some confidence within a reasonable measurement time.[9,10]

Hydrogen-deuterium exchange (HDX) has been used to probe protein conformation and dynamics in solution with high resolution.[11] HDX detects conformational changes and solvent exposure by measuring the number of deuterons exchanged with amide hydrogens on the amide

backbone. In pharmaceutical development, HDX-MS has been used to probe protein structure as well as the interaction of the protein with ligands or other proteins.[12-16] Over the past decade, our group has developed solid-state hydrogen-deuterium exchange with mass spectrometric analysis (ssHDX-MS) as an adaptation of solution HDX for solid samples. In ssHDX-MS, a lyophilized powder containing a protein of interest is exposed to D_2O vapor at controlled temperature and relative humidity. At various times, samples are withdrawn, reconstituted in a quench buffer, and analyzed as in solution HDX. Often, ssHDX detects differences in formulations within days or weeks of D_2O exposure, rather than the months or years that can be required for stability studies. ssHDX has been shown to be sensitive to formulation and process changes, and the extent of deuteration in various formulations has been correlated with storage stability for myoglobin,[17,18] a monoclonal antibody,[19] and various therapeutic proteins.[20,21] The usefulness of HDX has been demonstrated for analysis of ADCs in solution.[22-25] However, to date there have been no reports of ssHDX-MS analysis and stability of an ADC in a lyophilized solid.

In the studies reported here, ssHDX-MS was used together with other biophysical methods to characterize an ADC in lyophilized samples, and ssHDX-MS metrics were related to ADC storage stability under accelerated conditions.

2.3 Materials and methods

2.3.1 Materials

The ADC is hazardous and should be handled carefully. Personal protective equipment (PPE) was used when handling samples of the ADC and bulk sample handling was performed in a laminar flow hood. All ADC containing samples were treated as hazardous waste, and hazardous waste was disposed of separately from non-hazardous waste.

The ADC under development at Baxter BioPharma Solutions (Bloomington IN) was used. L-histidine, USP (Thermo Fisher Scientific, Pittsburgh PA) and 5 N HCl (VWR Chemicals, Radnor PA) were used to prepare the histidine buffer solution. Sucrose (Sigma Aldrich, St. Louis MO), mannitol (Sigma Aldrich, St. Louis MO), trehalose (Pfanstiehl, Waukegan IL), and super-refined polysorbate 80 (Croda, Edison NJ) were used as excipients. Amicon Ultra filters, regenerated cellulose 10k MWCO (Millipore Sigma, Burlington MA), were used for buffer exchange using centrifugal filtration. Syringe filters with 0.2 µM nominal pore size, surfactant-

free cellulose acetate (SFCA, Thermo Fisher Scientific) were used to filter formulations. Lyophilization vials (3 mL) were obtained from Ompi (Padua, Italy) with 16 x 1 x 35 mm dimensions.

2.3.2 Sample preparation

The frozen ADC stock solution was thawed and exchanged into a 50 mM histidine buffer (pH 6.0) using 10,000 MWCO centrifugal filtration (VWR, Radnor PA). The ADC solution was formulated with different excipients (**Table 2.1**) and filtered using vacuum filtration. The filtered formulations were filled using a 1 mL fill volume into 3 mL Ompi vials and stoppers (West Pharma, Exton PA) were partially seated. The filled vials were lyophilized in a LyoStar II freeze-dryer (SP Scientific, Warminster PA). Mannitol containing formulations and non-mannitol containing formulations were freeze-dried separately using different lyophilization cycles. Mannitol containing formulations were frozen at -40 °C with a ramp rate of 1 °C/min for 180 min at atmospheric pressure. They then were annealed at -15 °C with a ramp rate of 0.5 °C/min at atmospheric pressure for 180 min. Primary drying was performed at -15 °C at 50 mTorr until the difference between pirani and capacitance manometer (CM) gauge readings was 5 mTorr or less. Secondary drying was carried out at 40 °C with a ramp rate of 0.5 °C/min for 420 min. Non-mannitol containing formulations were frozen at -40 °C with a ramp rate of 1 °C/min for 220 min at atmospheric pressure. They then were dried at -20 °C with a ramp rate of 0.5 °C/min at 50 mTorr. When the pirani/CM gauge difference reached 5 mTorr or less, the formulations were further dried at 40 °C with a ramp rate of 0.5 °C/min for 360 min. After secondary drying, the shelf temperature was set at 5 °C and remained under vacuum for both mannitol containing formulations and non-mannitol containing formulations until stoppering and storage. Lyophilization in-process data are provided in supplemental information (**Figure A. 1**).

Table 2.1. Composition and physical properties of lyophilized formulations.

Formulation	Components[a]	T_g (°C)[b]	Average Residual Moisture (%)[c]
Excipient-free	ADC alone	93.0	1.82±0.18
Sucrose	ADC+sucrose (1:5 w/w)	84.1	1.35±0.30
Trehalose	ADC+trehalose (1:5 w/w)	91.0	1.44±0.04
Mannitol	ADC+mannitol (1:5 w/w)	75.5	1.64±0.09
PS80	ADC+PS80 (1:0.02%)	92.1	1.32±0.11
Suc+mann	ADC+sucrose+mannitol (1:5:5) (w/w)	57.8	1.00±0.06
Tre+mann	ADC+trehalose+mannitol (1:5:5) (w/w)	58.2	1.07±0.02

[a] ADC concentration: 2 mg/mL.
[b] Thermally modulated differential scanning calorimetry; see text for details.
[c] Karl Fisher coulometry, n = 6 +/- SD; see text for details.

2.3.3 Determination of protein concentration

Protein concentration was measured on an Agilent Cary 60 UV−Vis spectrophotometer (Agilent Technologies, Santa Clara CA) equipped with a C-Technologies variable pathlength system (Bridgewater Township NJ). Slope spectroscopy collects multiple absorbance data points at several pathlengths to create an absorbance versus pathlength plot. Absorbance values in the linear region of the curve are directly proportional to sample protein concentration based upon a previously determined sample extinction coefficient. No sample preparation or dilution was required. Fibrettes and UV disposable vessels were both purchased from C-Technologies (Bridgewater Township NJ).

2.3.4 Karl Fischer coulometry (KF)

The moisture content of the freeze-dried solids was measured by Mettler DL37 Karl Fischer coulometry (Mettler Toledo, Columbus OH). The headspace of the vials was vented through a syringe containing desiccant in the barrel to avoid introduction of ambient humidity. The vials, cakes, and stoppers were then weighed, and the freeze-dried solids were suspended in anhydrous methanol. Triplicate measurements were performed for each vial and the results for two vials were averaged. Vials and stoppers were rinsed with water and acetone and dried overnight.

Vials and stoppers were re-weighed after drying. The percentage residual water content was calculated using **Eq. (2.1)**:

$$\%H_2O = \frac{\left(\%H_2O \text{ soln.}\right)(WV_1 - WV_2 + WD) - (WD)(\%H_2O \text{ MeOH})}{WV_1 - WV_2}$$

Eq. (2.1)

where, WV_1 is the weight of the filled vial and the stopper and WV_2 is the weight of the filled vial, the stopper, and the diluent. The weight of the diluent WD is calculated from WV_1 and WV_2.

2.3.5 X-ray powder diffraction (XRPD)

XRPD experiments were performed on a Bruker D2 Phaser diffractometer (Bruker AXS, Madison WI) set in Bragg-Brentano geometry between 7 and 35° 2θ at a scan increment of 0.02° 2θ every 0.2 s. The sample was rotated at 5 rpm. The equipment contained a powder holder comprising a Plexiglass disc with a sample well in the center. The freeze-dried solid was crushed using a spatula and the powder was placed in the well. The powder was leveled using a microscope slide such that the sample made a uniform layer on the disc.

2.3.6 Size-exclusion chromatography (SEC)

SEC was used to assess changes in ADC mass during storage, which may be due to aggregation, loss of conjugated drug and/or fragmentation. In SEC, separation was performed using an Agilent 1110 or 1200 series HPLC on a TOSOH Bioscience TSKgel SuperSW3000, 4.6 mm x 30 cm, 4 µm (King of Prussia, PA). The mobile phase was 0.1 M phosphate buffer, 0.1 M sodium sulfate, 7.5% isopropyl alcohol at pH 7.2 with a flow rate of 0.2 mL/min. Samples were controlled at 5 °C and the column was maintained at 30 °C throughout the sequence. Detection was performed at 280 nm. System suitability was checked using a comparative standard and a molecular weight standard prior to sample analysis. Standards and samples were reconstituted or diluted with purified water prior to analysis. A variable injection volume (between 10 and 50 µL) was used to ensure that a constant sample load of about 50 µg was used for both standards and samples. The reported value of % high molecular weight species (%HMW) was calculated using **Eq. (2.2)**.

$$\%\text{HMW} = \frac{\text{Area under the curve of HMW peak}}{\text{Total area under the curve of all peaks}} \times 100\% \quad \text{Eq. (2.2)}$$

2.3.7 Differential scanning calorimetry (DSC)

The freeze-dried solids were examined using a Thermo Q2000 series high temperature Differential Scanning Calorimetry (Thermo Fisher Scientific, Waltham MA) for examination of thermal behavior. Samples were prepared in a glove box purged with nitrogen. Powder compacts were prepared from freeze dried solids (5 − 15 mg) using a stainless-steel rod tamped into a brass tube, forming a compact mass. The powder compacts were sealed in aluminum T_{zero} pans, and an empty pan and lid were used as the thermally inert reference. Samples were analyzed by equilibrating at 25 °C, then initiating a modulation of ±1.0 °C every 120 s. The samples were held isothermally for 5 min, then were ramped to 120 °C at a rate of 0.5 °C/min.

2.3.8 Fourier-transform infrared spectroscopy (FT-IR)

FT-IR was used to assess changes in the secondary structure in solid ADC samples. Lyophilized samples stored at 4 °C were compressed into pellets using KBr (Alfa Aesar, Thermo Fisher Scientific, Haverhill MA) and analyzed using the ABB FTLA2000 FT-IR instrument (ABB, Warminster PA). The amide I region was selected for peak fitting. The resulting FT-IR spectra were deconvoluted to assign corresponding secondary structures to each peak.[26-30] A total of 16 peaks were detected consistently throughout the analysis in each formulation.

2.3.9 Accelerated stability study

Vials containing the lyophilized solids were crimped with flip-off seals and stored in stability chambers at 40 °C (75%RH) for up to 12 weeks and at 50 °C (ambient RH) for up to 8 weeks. At each time point (1, 2, 4, 8 and 12 weeks), samples were retrieved from the stability chambers and stored at 2−8 °C prior to SEC analysis.

2.3.10 Solid-state hydrogen-deuterium exchange (ssHDX-MS)

ssHDX-MS was performed on lyophilized ADC samples to assess protein conformation and matrix interactions. The lyophilized ADC formulations were deuterated in a desiccator at 23%

relative humidity (RH) in D_2O at room temperature. The RH was maintained using a saturated solution of potassium acetate. Vials containing lyophilized solids of the ADC formulation were placed inside the desiccator, without the stoppers, to allow H/D exchange to take place. At specific time points, vials were retrieved from the desiccator, flash-frozen using liquid nitrogen, sealed, and stored at 80 °C until MS analysis.

MS analysis was performed at the intact protein level using a quadrupole time-of-flight mass spectrometer (Agilent 6530 QTOF-LC/MS, Santa Clara CA) with a dual Agilent Jet Stream Electrospray Ionization (AJS ESI) source. For gradient elution, 0.1% formic acid in MS grade water was used as solvent A, and 0.1% formic acid in acetonitrile was used as solvent B. Detailed mass spectrometry parameters are provided in supplemental information (**Table A. 1**). Prior to analyzing deuterated samples, an undeuterated excipient-free ADC as received was directly injected into the MS instrument as a control.

Frozen deuterated ADC samples were thawed at room temperature prior to analysis, then reconstituted and further diluted using 0.1% formic acid in MS grade water, pH 2.0. Agilent MassHunter software was used to deconvolute the extracted mass spectra. The number of deuterons incorporated was then calculated by subtracting the mass of undeuterated protein from the deuterated mass. Deuterium incorporation was not corrected for back exchange. Since the extent of back exchange during MS analysis generally is protein-dependent, and since a single protein was used in these studies, a back exchange correction is unlikely to affect the overall rank order of the candidate formulations.

2.3.11 Statistical analysis

GraphPad Prism 7.02 was used to perform statistical analysis. Both one-way and two-way ANOVA tests, accompanied with Tukey test, were used to compare multiple measurements and test for significant differences among the formulations. Adjusted P-values for each comparison were reported at 95% confidence. In ssHDX-MS studies, deuterium incorporation kinetics were fitted using a one-phase exponential association model after comparing multiple fit-models (**Eq. (2.3)**). In **Eq. (2.3)**, D_{max} is the plateau value, k is the rate constant for deuterium exchange, and t is the time in hours.

$$\#\ \text{of Exchanged Deuterons} = D_{max}\left(1 - e^{(-kt)}\right) \quad \text{Eq. (2.3)}$$

2.4 Results and discussion

2.4.1 Physical and chemical properties of ADC formulations

Seven formulations were prepared with the ADC alone, with a single excipient, and using mixtures of an amorphous sugar and a crystallizing sugar (mannitol) (**Table 2.1**). Samples of the formulations were lyophilized and examined using Karl Fischer Coulometry (KF) and high temperature DSC. T_g values were determined in the reversing heat flow thermogram (**Figure A. 2a**), and only T_g values are reported. Crystallization of mannitol in mannitol-containing formulations at temperatures greater than 110 °C was observed in the non-reversing heat flow thermograms (**Figure A. 2b-d**). The lowest midpoint T_g values were approximately 57.8 °C and 58.2 °C for the formulations containing mannitol. All glass transition temperatures were greater than the accelerated stability storage temperature evaluated in this investigation, and all solids are thus expected to be in the glassy state during storage. The average residual moisture content varied from 1.00% to 1.82%; differences in moisture levels greater than 0.75% are considered significant according to the ANOVA result. Formulations with multiple excipients had moisture levels that were significantly different from the excipient-free formulation. Initial appearance of the lyophilized solids was a white dense cake without any cosmetic defect for all formulations, however shrinkage of the cakes was observed after both stressed stability testing and D_2O exposure.

The crystallinity of lyophilized solids containing ADCs was determined using XRPD (**Figure 2.1**). All formulations that did not contain mannitol ("non-mannitol containing") showed a halo pattern consistent with amorphous solids (**Figure 2.1a**). The diffractograms of mannitol-containing formulations indicated partial crystallization of mannitol (**Figure 2.1b**) despite the annealing step during lyophilization. A formulation containing partially crystalline mannitol may promote degradation of the protein followed by continued crystallization and phase separation of mannitol during storage. This may be due to release of associated moisture[31,32] and/or loss of stabilizing interactions between the matrix and the ADC.

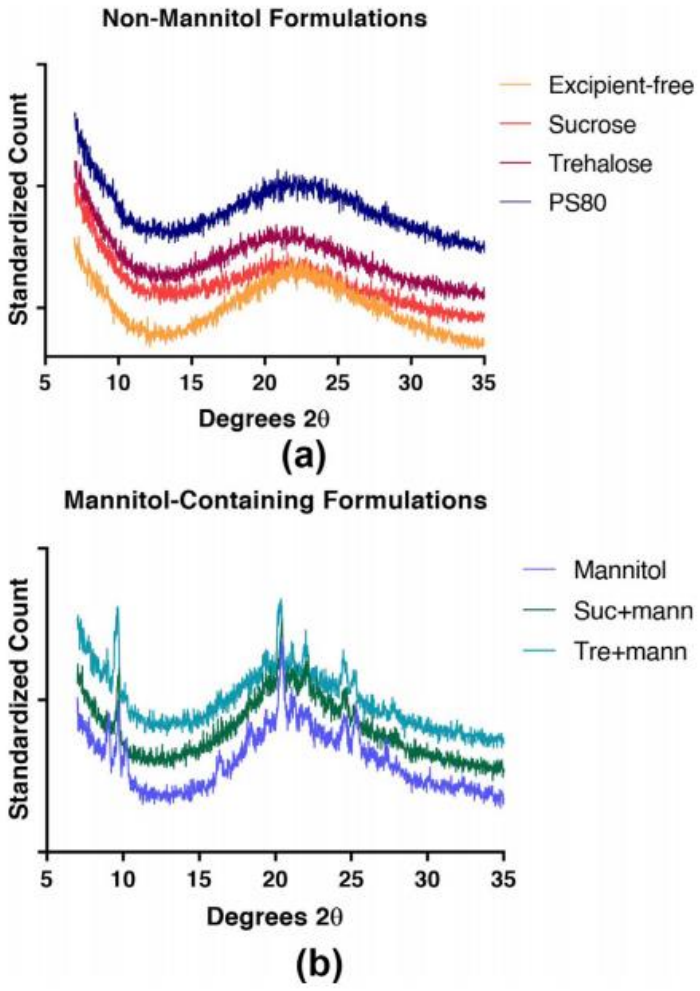

Figure 2.1. X-Ray Powder Diffraction of (a) non-mannitol containing formulations and (b) mannitol containing formulations after lyophilization (t = 0).

As a detection method coupled with HDX, ESI-QTOF mass spectrometry was used to measure the mass of ADC molecules in the formulations. To verify the composition of the ADC samples, pre-treated excipient-free ADC samples were directly injected into the mass spectrometer. ESI-QTOF mass spectrometry detected ADC variants with one conjugated drug molecule (DAR1, 148,364 Da) and four conjugated drug molecules (DAR4, 152,033 Da) as the most abundant species (**Figure 2.2a**). When the extracted mass spectra were deconvoluted using the mass range of fragments, the drug-conjugated light chain (L:T) and drug-conjugated heavy chain-light chain (H:L:2T) were also observed (**Figure 2.2b**). These four species were observed consistently throughout the MS analysis of the deuterated samples. Although other DAR species may be present in the sample, they were not detected with significant abundance during MS analysis for any of

the samples studied here. Moreover, each fragment of ADC detected was detected conjugated with the toxin, indicating that the linker is stable under the experimental conditions, at least in the DAR1 and DAR4 conjugates.

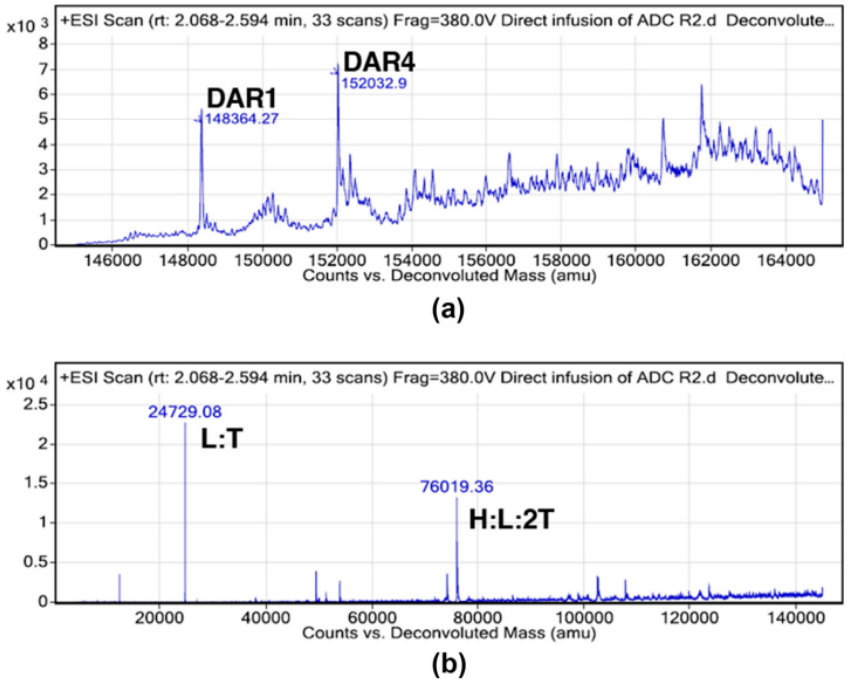

Figure 2.2. Deconvoluted mass spectra of excipient-free ADC as received using the mass range of (a) intact ADC (145kDa-165kDa) and (b) ADC/antibody fragments (4kDa-145kDa). H=heavy chain, L=light chain, T=toxin (drug), L:T = light chain with one conjugated toxin (drug) molecule, H:L:2T = heavy chain plus light chain with two conjugated toxin (drug) molecules, DAR1 = antibody with 1 conjugated toxin (drug) molecule, DAR4 = antibody with 4 conjugated toxin (drug) molecules.

2.4.2 Accelerated stability studies and ssHDX-MS

Figure 2.3 shows the formation of HMW species during ADC storage at 50 °C, as measured by SEC. The high molecular weight percentage was calculated using the peak area measurement on the chromatograms shown in **Figure A. 3**. The mannitol formulation exceeded 5% HMW after 2 weeks of storage and the PS80 formulation exceeded 5% HMW after 4 weeks of storage. Although the PS80 formulation was not significantly different from the other formulations, it showed an increase in aggregation after 4 weeks of storage. The remaining formulations showed little to no HMW content up to 8 weeks of storage. Among the seven formulations, the mannitol and PS80 formulations showed the highest HMW species. Similar results were obtained when the

samples were stored at 40 °C (**Figure A. 4**). Thus, the results of accelerated stability studies suggest that the PS80 and mannitol formulations are the least stable and have the greatest aggregate formation. HMW levels for the other formulations were not significantly different from one another at either condition at the end of the study (**Table A. 2**, **Table A. 3**).

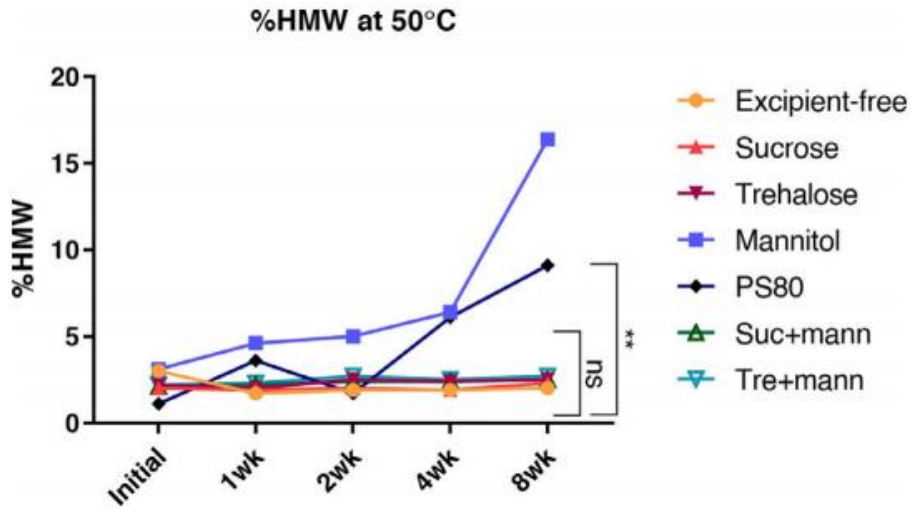

Figure 2.3. Formation of HMWs during storage, as measured by SEC for samples stored at 50 °C. ** = significant different by 2-way ANOVA at tested $p<0.01$. $n=1$.

In ssHDX-MS, greater deuterium incorporation indicates greater exposure of the protein amide groups that may lead to instability. **Figure 2.4a** shows ssHDX-MS kinetics for the seven formulations for DAR4, the most abundant species in the sample. The mannitol formulation showed the greatest deuterium uptake throughout the time course, followed by the PS80 formulation (**Figure 2.4a-b**). This result is in agreement with the SEC data, which indicated the destabilizing effects of mannitol and PS80 among the excipients evaluated. Instability due to mannitol crystallization has been reported previously.[27] Degradation of PS80 leading to oxidation and aggregation of lyophilized biopharmaceuticals has also been reported.[33,34] It is interesting to note that mannitol and PS80 showed destabilizing effects on the ADC that seemed to be stable enough to formulate without any excipients. PS80, in particular, has been known to have a protective effect against instability caused by protein sorption at the ice/freeze concentrate interface during freezing.[35] However, in this study, the accelerated stability data and HDX data both showed destabilization by PS80.

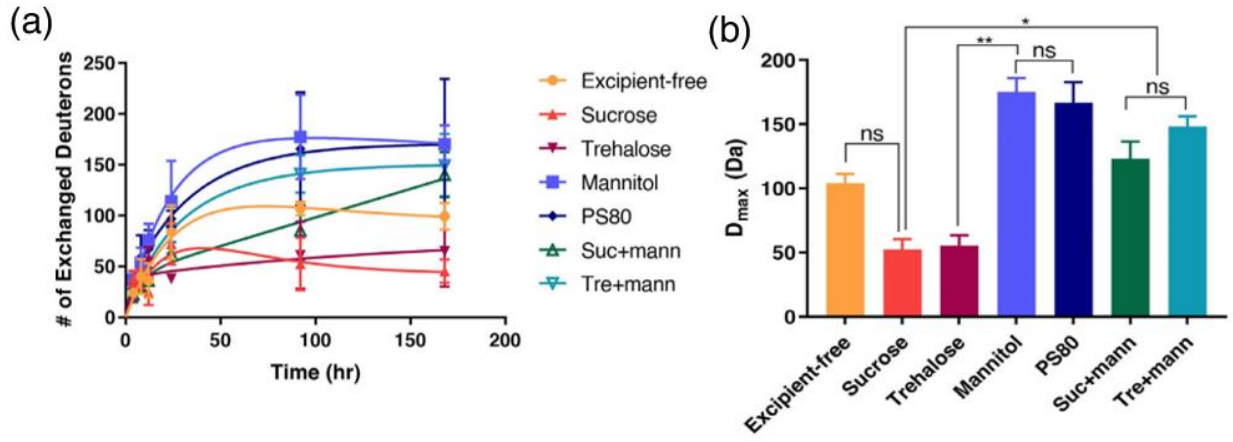

Figure 2.4. Solid-state hydrogen-deuterium exchange (ssHDX-MS) of lyophilized ADC samples after D_2O exposure at 23%RH and room temperature (n = 2±SD) showing (a) deuterium incorporation kinetics among the various formulations and (b) maximum deuterium uptake values (D_{max}) determined by nonlinear regression. Differences among groups in (b) by one-way ANOVA: ns = not significant, ** = significant difference at tested p<0.0021, *=significant difference at p<0.0332.

The formulations containing both mannitol and amorphous sugars also showed high deuterium incorporation, following PS80 and mannitol formulations. Despite partial crystallinity, formulations co-formulated with amorphous sugar showed greater stability than those with mannitol alone, suggesting that the amorphous sugar still provides some stabilizing effect. The formulation containing both trehalose and mannitol showed high deuterium incorporation throughout the entire period of deuterium exposure, whereas the sucrose-mannitol formulation was relatively protected at early times then showed rapid deuterium incorporation after 92 h of D_2O exposure. A decrease in deuteration at later time points was also observed in the excipient-free formulation. These decreases are unexpected and may reflect physical changes in the sample during deuteration (e.g., crystallization of excipient). SEC data for the excipient-free and sucrose formulations did not show high levels of aggregation (**Figure 2.3**), suggesting that ssHDX-MS results are not indicative of stability for these samples, perhaps due to physical changes during deuterium incorporation. Though the overall degrees of deuteration for the other DAR species, namely DAR1 and heavy chain-light chain complex conjugated with two drug molecules (H:L:2T) differed, the rank order of deuteration among the formulations was identical (**Figure A. 5**).

The maximum level of deuterium incorporation (D_{max}, **Eq. (2.3)**) differed among the various formulations (**Figure 2.4b**, **Table A. 4**). ssHDX-MS results were consistent with the results of the stability studies, in that the formulations with the highest deuterium incorporation on ssHDX-MS

(mannitol and PS80, **Figure 2.4b**) also showed the highest HMW levels in accelerated stability studies (**Figure 2.3**). That the ssHDX-MS studies were completed in 168 h (1 week) as opposed to the 8 −12 weeks of the accelerated stability studies suggests that ssHDX-MS can be used to identify the poorest performing ADC formulations more rapidly. Because most formulations showed little or no HMW formation (**Figure 2.3**), however, correlation of deuterium incorporation with HMW formation was not possible. Longer storage of these formulations in accelerated conditions may be required in order to observe appreciable degradation.

2.4.3 Evaluation of structural changes using FT-IR

In addition to the accelerated studies and ssHDX-MS, the lyophilized solids were examined using FT-IR to assess changes in secondary structure (**Figure 2.5**). **Figure 2.5a** shows structural changes in the amide I region, 1610−1700cm^{-1}. Since the intensity was normalized, shifts in overall peak position relative to the excipient-free formulation were considered rather than changes in peak height. The sucrose formulation showed minimal changes in secondary structure when compared to the excipient-free formulation. The trehalose, mannitol, and PS80 formulations showed nearly superimposable peaks in the turn regions (1670−1700 cm^{-1}), yet showed a decrease in band frequencies in the alpha-helix region (1648−1660 cm^{-1}) and beta-sheet regions (1625−1640 cm^{-1}). Moreover, formulations with multiple excipients also showed decreased frequencies in the alpha-helix and beta-sheet regions. Decreases in FT-IR band frequency have been attributed to increases in hydrogen bond (H-bond) strength resulting from decreased electron densities in amide C = O groups.[26] With the exception of the sucrose formulation, the formulations showed increased intermolecular hydrogen bond strength in alpha-helix and beta-sheet structures compared to the excipient-free formulation.

Since the secondary structure of ADC molecules is primarily beta-sheet, **Figure 2.5b** focuses on FT-IR peaks in the beta-sheet region (1625−1640 cm^{-1}). In the beta-sheet region, the band frequencies of the sucrose formulations were shifted to higher wavenumber compared to the excipient-free formulation. With the exception of the sucrose formulation, the remaining formulations showed decreased band frequencies in the peaks corresponding to beta-sheets compared to the excipient-free formulation. The band frequencies of the peaks between 1620 and 1630 cm^{-1} decreased the most in the sucrose-mannitol, and trehalose-mannitol formulations. Trehalose, mannitol, and PS80 showed similar decreases in band frequencies in the beta-sheet

regions. Thus, compared to the excipient-free formulation, only sucrose formulations showed decreased H-bond strength, while the remaining formulations showed increased H-bond strength.

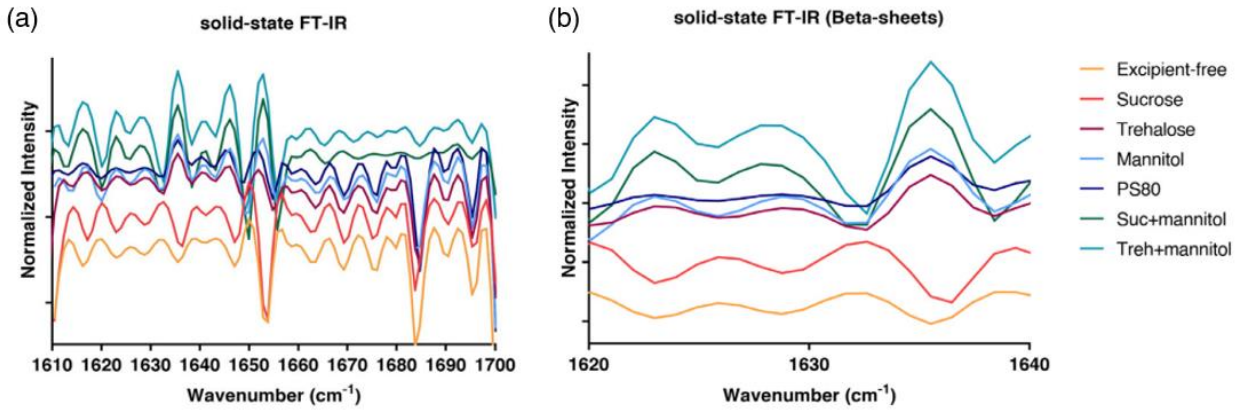

Figure 2.5. Normalized second-derivative FT-IR spectra for lyophilized formulations in (a) amide I region (1610−1700 cm^{-1}) and (b) beta-sheet region (1625−1640 cm^{-1}).

Figure 2.6 shows that the SEC results and FT-IR results are poorly correlated. Moreover, FT-IR did not show clear differences among formulations, and thus it was difficult to rank order the formulations on the basis of FT-IR peak position alone.

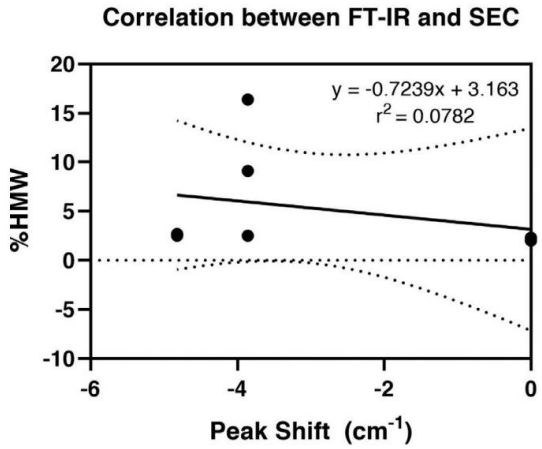

Figure 2.6. Scatter plot of peak shift and %HMW with 95% confidence interval bands and regression line.

2.5 Conclusions

An ADC was lyophilized with various excipients and placed on accelerated stability at 40 °C or 50 °C for up to 12 or 8 weeks, respectively. The samples were analyzed after lyophilization by ssHDX-MS and other physicochemical methods, and the stability samples were analyzed by SEC to determine the extent of protein aggregation. The mannitol and PS80 containing formulations showed the greatest deuterium incorp oration on ssHDX-MS and the highest levels of HMW aggregates, even though the ADC alone does not seem to require a stabilizing excipient. Thus, ssHDX-MS correctly identified the poorest performing ADC formulations in considerably less time than the accelerated stability study. Peak shifts on FT-IR were not predictive of HMW formation in stability studies.

2.6 References

1. Beck A, Goetsch L, Dumontet C, Corvaia N. Strategies and challenges for the next generation of antibody drug conjugates. Nat Rev Drug Discov. 2017;16(5):315–337.

2. Birrer MJ, Moore KN, Betella I, Bates RC. Antibody-drug conjugate-based therapeutics: state of the science. J Natl Cancer Inst. 2019;111(6):538–549.

3. Jain N, Smith SW, Ghone S, Tomczuk B. Current ADC linker chemistry. Pharm Res. 2015;32(11):3526–3540.

4. Singh SK, Luisi DL, Pak RH. Antibody-drug conjugates: design, formulation and physicochemical stability. Pharm Res. 2015;32(11):3541–3571.

5. Baheti A, Kumar L, Bansal AK. Excipients used in lyophilization of small molecules. J Excip Food Chem. 2010:41–54. ISSN 21502668.

6. Moorthy BS, Iyer LK, Topp EM. Mass spectrometric approaches to study protein structure and interactions in lyophilized powders. J Vis Exp. 2015:(98):e52503.

7. Liu JS. Physical characterization of pharmaceutical formulations in frozen and freeze-dried solid states: techniques and applications in freeze-drying development. Pharm Dev Technol. 2006;11(1):3–28.

8. Thiagarajan G, Semple A, James JK, Cheung JK, Shameem M. A comparison of biophysical characterization techniques in predicting monoclonal antibody stability. MAbs. 2016;8(6):1088–1097.

9. Patel H, Sudeendra BR, Balamuralidhara V, Pramod KTM. Comparison of stability testing requirements of ICH with other international regulatory agencies. Pharma Times. 2011;43(9):21–34.

10. Oliva A, Farina JB, Llabres M. An improved methodology for data analysis in accelerated stability studies of peptide drugs: practical considerations. Talanta. 2012; 94:158–166.

11. Wei H, Mo JJ, Tao L, et al. Hydrogen/deuterium exchange mass spectrometry for probing higher order structure of protein therapeutics: methodology and applications. Drug Discov Today. 2014;19(1):95–102.

12. Li YS, Williams TD, Schowen RL, Topp EM. Characterizing protein structure in amorphous solids using hydrogen/deuterium exchange with mass spectrometry. Anal Biochem. 2007;366(1):18–28.

13. Na S, Lee JJ, Joo JWJ, Lee KJ, Paek E. deMix: decoding deuterated distributions from heterogeneous protein states via HDX-MS. Sci Rep. 2019;9:3176.

14. Kielkopf CS, Ghosh M, Anand GS, Brown SHJ. HDX-MS reveals orthosteric and allosteric changes in apolipoprotein-D structural dynamics upon binding of progesterone. Protein Sci. 2019;28(2):365–374.

15. Kabaria SR, Mangion I, Makarov AA, Pirrone GF. Use of MALDI-MS with solid-state hydrogen deuterium exchange for semi-automated assessment of peptide and protein physical stability in lyophilized solids. Anal Chim Acta. 2019;1054:114– 121.

16. Deng B, Lento C, Wilson DJ. Hydrogen deuterium exchange mass spectrometry in biopharmaceutical discovery and development - a review. Anal Chim Acta. 2016; 940:8–20.

17. Iyer LK, Sacha GA, Moorthy BS, Nail SL, Topp EM. Process and formulation effects on protein structure in lyophilized solids using mass spectrometric methods. J Pharm Sci. 2016;105(5):1684–1692.

18. Sophocleous AM, Zhang J, Topp EM. Localized hydration in lyophilized myoglobin by hydrogen-deuterium exchange mass spectrometry. 1. Exchange mapping. Mol Pharm. 2012;9(4):718–726.

19. Moussa EM, Singh SK, Kimmel M, Nema S, Topp EM. Probing the conformation of an IgG1 monoclonal antibody in lyophilized solids using solid-state hydrogen-deuterium exchange with mass spectrometric analysis (ssHDX-MS). Mol Pharm. 2018; 15(2):356–368.

20. Chandrababu KB, Kumar L, Walters B, et al. Solid-state hydrogen-deuterium exchange mass spectrometry (ssHDX-MS) analysis of therapeutic fragment antigen-binding (Fab) protein formulations. Abst Pap Am Chem Soc. 2017;253:1.

21. Li YS, Williams TD, Topp EM. Effects of excipients on protein conformation in lyophilized solids by hydrogen/deuterium exchange mass spectrometry. Pharm Res. 2008;25(2):259–267.

22. Huang RYC, O'Neil SR, Lipovsek D, Chen GD. Conformational assessment of adnectin and adnectin-drug conjugate by hydrogen/deuterium exchange mass spectrometry. J Am Soc Mass Spectrom. 2018;29(7):1524–1531.

23. Pan LY, Salas-Solano O, Valliere-Douglass JF. Conformation and dynamics of interchain cysteine-linked antibody-drug conjugates as revealed by hydrogen/deuterium exchange mass spectrometry. Anal Chem. 2014;86(5):2657–2664.

24. Pan LY, Salas-Solano O, Valliere-Douglass JF. Antibody structural integrity of site-specific antibody-drug conjugates investigated by hydrogen/deuterium exchange mass spectrometry. Anal Chem. 2015;87(11):5669–5676.

25. Valliere-Douglass JF, Hengel SM, Pan LY. Approaches to interchain cysteine-linked ADC characterization by mass spectrometry. Mol Pharm. 2015;12(6): 1774–1783.

26. Jackson M, Mantsch HH. The use and misuse of FTIR spectroscopy in the determination of protein-structure. Crit Rev Biochem Mol Biol. 1995;30(2):95–120.

27. Surewicz WK, Mantsch HH. New insight into protein secondary structure from resolution-enhanced infrared-spectra. Biochim Biophys Acta. 1988;952(2):115–130.

28. Kauppinen JK, Moffatt DJ, Mantsch HH, Cameron DG. Fourier self-deconvolution - a method for resolving intrinsically overlapped bands. Appl Spectrosc. 1981;35 (3):271–276.

29. Byler DM, Susi H. Examination of the secondary structure of proteins by deconvolved ftir spectra. Biopolymers. 1986;25(3):469–487.

30. Luo SQ, Huang CYF, McClelland JF, Graves DJ. A study of protein secondary structure by fourier-transform infrared photoacoustic-spectroscopy and its application for recombinant proteins. Anal Biochem. 1994;216(1):67–76.

31. Kim AI, Akers MJ, Nail SL. The physical state of mannitol after freeze-drying: effects of mannitol concentration, freezing rate, and a noncrystallizing cosolute. J Pharm Sci. 1998;87(8):931–935.

32. Lim JY, Lim DG, Kim KH, Park SK, Jeong SH. Effects of annealing on the physical properties of therapeutic proteins during freeze drying process. Int J Biol Macromol. 2018;107:730–740.

33. Jones MT, Mahler HC, Yadav S, et al. Considerations for the use of polysorbates in biopharmaceuticals. Pharm Res. 2018;35(8):8.

34. Agarkhed M, O'Dell C, Hsieh MC, Zhang JM, Goldstein J, Srivastava A. Effect of polysorbate 80 concentration on thermal and photostability of a monoclonal antibody. AAPS PharmSciTech. 2013;14(1):1–9.

35. Chang BS, Kendrick BS, Carpenter JF. Surface-induced denaturation of proteins during freezing and its inhibition by surfactants. J Pharm Sci. 1996;85(12):1325–1330.

CHAPTER 3. STABILITY COMPARISON BETWEEN PARENT ANTIBODY AND ADC UNDER INTERFACIAL STRESS

3.1 Abstract

Lyophilization, which is used in all currently marketed ADCs, may induce instability during freezing via unfolding of proteins at the ice/freeze-concentrate interface. In this study, the level of aggregation in parent mAb and ADC formulations after lyophilization was compared. Both mAb and ADCs were formulated at protein concentrations from 1 to 10 mg/mL, in the absence/presence of PS80. During storage at 50 °C, ADC formulations showed lower levels of aggregates than low-concentration mAb formulations. Regardless of concentration, both mAb and ADC formulations showed higher aggregate content in the presence of PS80. ssHDX-MS detected significant differences in the extent of maximum deuterium uptake in mAb and ADC formulations, although differences among formulations were not detected for either mAb or ADC.

3.2 Introduction

Currently, all nine of the U.S. FDA approved antibody-drug conjugates (ADCs) are marketed in lyophilized form. Regardless of the linker types, lyophilization is used to ensure the *in vitro* stability of ADC formulations. Yet, the lyophilization process *per se* may induce instability. Freezing, in particular, may cause low temperature stress, increased ionic strength, phase separation, and change in pH followed by selective solute crystallization.[1] The cause of instability is thought to be more than a thermal destabilization effect.[2] According to Franks *et al*., freezing drastically increases the solute concentration, which leads to further chemical degradation reactions.[3] Furthermore, freezing creates an ice/freeze-concentrate interface, which can result in surface-induced partial unfolding of the proteins.[1,4] *Chang et al*. found a good correlation between the freeze-induced denaturation and surface-induced denaturation.[4]

In pharmaceutical development, surfactants are often included as excipients in protein formulation, in an attempt to reduce surface-induced instability. Polysorbate 80 (PS80), also known as Tween 80, is a common surfactant used for alleviating interfacial stress. Due to its relatively low critical micelle concentration (CMC), a PS80 concentration as low as 0.005% to 0.01% has shown a protective effect against freezing denaturation.[5-6] PS80 is thought to exert its

effects at the ice/freeze-concentrate interface, and not in the interstitial space distant from the surface of ice crystals.[1] Kendrick *et al.* studied the effect of PS80 on freeze denaturation using various proteins: tumor necrosis factor binding protein (TNFbp), interleukin-1 receptor antagonist (IL-1ra), basic fibroblast growth factor (bFGF), malate dehydrogenase (MDH), aldolase, and phosphofructokinase (PFK).[6] Chang *et al*. conducted a similar study using ciliary neurotropic factor (CNTF), lactate dehydrogenase (LDH), glutamate dehydrogenase (GDH), PFK, 1L-1ra, and TNFbp.[4]

Unlike natural proteins or the parent monoclonal antibodies (mAb), ADCs have been modified to exhibit hydrophobic payloads and linkers on the protein surface.[7-8] Due to conjugation, the physicochemical properties of ADCs have been altered compared to the parent mAbs.[9] This change in properties increases the susceptibility of ADCs against various stresses such as pH,[10-13] temperature,[14-16] light,[17-20] and excipients.[21-25] In the studies reported here, the *in vitro* stability of ADCs was compared to that of the parent mAb after lyophilization. The primary instability was aggregation and was measured in both the ADC and mAb using size-exclusion chromatography (SEC). PS80 was used as an excipient to vary the interfacial stress at the ice/freeze-concentrate interface. The effect of protein concentration on the stability was also investigated.

3.3 Materials and methods

3.3.1 Materials

The antibody-drug conjugate (ADC) is hazardous and must be handled carefully. Personal protective equipment (PPE) was used when handling samples of the ADC and bulk sample handling was performed in a laminar flow hood. All ADC containing samples were treated as hazardous waste and were disposed of separately from non-hazardous waste.

The parent monoclonal antibody and ADC were provided by Baxter BioPharma Solutions (Bloomington IN). L-histidine, USP (J.T. Baker, Phillipsburg, NJ) and 1 N HCl (VWR Chemicals, Radnor PA) were used to prepare the histidine buffer solution. Polysorbate 80 (J.T. Baker) was used as an excipient. Amicon Ultra filters, regenerated cellulose 10k MWCO (Millipore Sigma, Burlington MA), were used for buffer exchange using centrifugal filtration. Syringe filters with 0.2 µM nominal pore size, surfactant-free cellulose acetate (SFCA, Thermo Fisher Scientific,

Waltham MA) were used to filter the formulations. Lyophilization vials (3 mL; 16 x 1 x 35 mm) were obtained from Ompi (Padua, Italy).

3.3.2 Sample preparation

The frozen parent mAb and ADC were thawed and exchanged into a 50 mM histidine buffer (pH 6.0) using 10,000 MWCO centrifugal filtration (VWR, Radnor PA). The mAb and ADC were formulated separately in various concentrations (**Table 3.1**). To eliminate confounding excipient effects, cryoprotectants such as amorphous sugars or bulking agents were excluded from the formulation; formulations included only buffer salts and PS80 as excipients. An Agilent Cary 60 UV−Vis spectrophotometer (Agilent Technologies, Santa Clara CA) equipped with a C-Technologies variable pathlength system (Bridgewater Township NJ) was used to measure protein concentrations in the stock solutions. A 1% (w/v) PS80 stock solution was prepared in a 50 mM histidine buffer (pH 6.0) to further dilute the PS80-containing formulations. The formulated solutions were filtered using syringe filters (Thermo Scientific, Waltham MA) and filled using a 0.25 mL fill volume into 3 mL Ompi vials and stoppers (West Pharma, Exton PA) and partially seated. The filled vials were lyophilized in a LyoStar III freeze-dryer (SP Scientific, Warminster PA). Both the mAb and ADC formulations were frozen at -40 °C with a ramp rate of 1 °C/min for 3 h at atmospheric pressure. The temperature was then ramped to -20 °C at 0.5 °C/min and 50 mTorr for primary drying. The end point of primary drying was determined using the difference in pirani and capacitance manometer (CM) gauge readings; primary drying was judged to be complete when the difference was 5 mTorr or less. The formulations were further dried at 40 °C with a ramp rate of 0.5 °C/min for 6 h. After secondary drying, the shelf temperature was set at 5 °C and samples remained under vacuum until stoppering and storage. Lyophilization in-process data are provided in supplemental information (**Figure B. 1**).

Table 3.1. Composition of the formulations.

Formulation	Protein concentration (mAb or ADC)	PS80 (w/v%)
A	10 mg/mL	-
B		0.02%
C	5 mg/mL	-
D		0.02%
E	2.5 mg/mL	-
F		0.02%
G	1 mg/mL	-
H		0.02%

3.3.3 Accelerated stability study

Vials containing the lyophilized solids were crimped with flip-off seals and stored in stability chambers at 50 °C (ambient RH) for up to 12 weeks. At each time point, samples were retrieved from the stability chambers and stored at 2−8 °C prior to analysis.

3.3.4 Size exclusion chromatography (SEC)

Size exclusion chromatography was used to measure the percent high molecular weight (HMW) species in the solids after accelerated stability storage. For separation, an Agilent 1110 or 1200 series HPLC on a TOSOH Bioscience TSKgel SuperSW3000, 4.6 mm x 30 cm, 4 µm (King of Prussia, PA) was used. 0.1 M phosphate buffer, 0.1 M sodium sulfate, 7.5% isopropyl alcohol at pH 7.2 were used as a mobile phase with a flow rate of 0.2 mL/min. Additional details regarding the SEC method were reported previously.[26]

3.3.5 Solid-state hydrogen-deuterium exchange (ssHDX-MS)

The lyophilized solids in unstoppered vials were deuterated in a desiccator at 23% relative humidity (RH) in D_2O at room temperature. The RH was controlled by saturating the D_2O solution with potassium acetate. At each time point, vials were retrieved from the desiccator, flash-frozen using liquid nitrogen, sealed, and stored at -80 °C until MS analysis. ssHDX-MS analysis was conducted as described previously.[26] MS analysis was performed using a quadrupole time-of-flight mass spectrometer (Agilent 6530 QTOF -LC/MS, Santa Clara CA) with a dual Agilent Jet Stream Electrospray Ionization (AJS ESI) source was used.

3.3.6 Statistical analysis

GraphPad Prism 9.1.1 was used to perform statistical analysis. Both one-way and two-way ANOVA tests, accompanied with Tukey test, were used to compare multiple measurements and test for significant differences among the formulations. Adjusted P-values for each comparison were reported at 95% confidence. In ssHDX-MS studies, deuterium incorporation kinetics were fitted using a one-phase exponential association model after comparing and evaluating other models (**Eq. (3.1)**). In **Eq. (3.1)**, D_{max} is the plateau value, *k* is the rate constant for deuterium exchange, and t is the time in hours.

$$\#\ \text{of Exchanged Deuterons} = D_{max}\left(1 - e^{(-kt)}\right) \quad \text{Eq. (3.1)}$$

3.4 Results and discussion

3.4.1 Accelerated stability difference between parent mAb and ADC

Accelerated stability studies were conducted using a conventional method to monitor *in vitro* stability of drug products. High molecular weight (HMW) species in the lyophilized solids after storage under accelerated conditions were measured using size-exclusion chromatography (SEC) (**Figure 3.1**).

As shown in **Figure 3.1a**, low-concentration mAb formulations, ranging from 1 mg/mL to 2.5 mg/mL, exceeded an aggregation level of 20% by 4 weeks of storage. The 5 mg/mL mAb formulation in the absence of PS80 remained under 5% HMW up to 18 weeks of storage, whereas that in the presence of PS80 began to form aggregated species after 4 weeks of storage. In contrast to mAb formulations, ADC formulations showed less than 6% HMW throughout the 12-week storage period (**Figure 3.1b)**. According to ANOVA, regardless of the presence of PS80, HMW levels in the 5 mg/mL ADC formulation were statistically different from those in the 1 mg/mL formulation containing PS80. A higher level of statistical difference was found between formulations at 2.5 mg/mL without PS80 and at 1 mg/mL containing PS80 (**Figure 3.1b**, **Table B. 2**). The high level of aggregated species at the initial time points for the 1 mg/mL ADC formulation in the absence of PS80 was also observed in a repeated stability study, suggesting that reversible

aggregation may occur in the early time course, though measurement errors cannot be ruled out (data not shown).

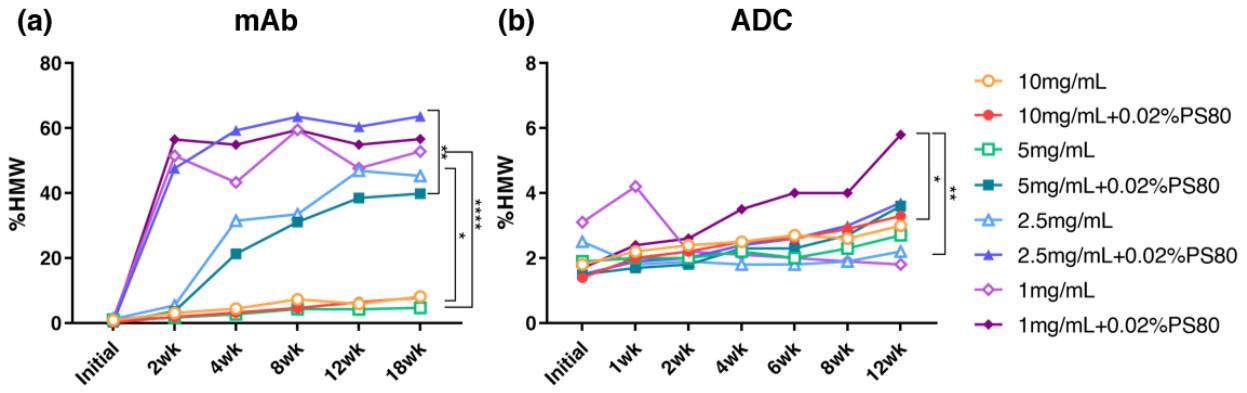

Figure 3.1. Aggregated species in (a) mAb up to 18 weeks of storage and (b) ADC up to 12 weeks of storage at 50°C measured by SEC. ****= significantly different at p<0.0001, ** = significantly different at p<0.0021, * = significantly different at p<0.0332.

Interestingly, conjugation to payloads and linkers greatly enhanced the *in vitro* stability of the mAb, particularly at low concentrations. ADC conjugation is generally thought to perturb the native structure of mAbs, increasing aggregation propensity.[27] Thus, that the stability of the ADC formulations was better than that of the corresponding mAb formulations was unexpected. Prior to storage, mAb formulations showed 0.66% ± 0.52% HMWs on average (n = 8; **Figure 3.1a**) and ADC formulations showed 1.93% HMWs ± 0.59% on average (n = 8; **Figure 3.1b**). The initial levels of aggregates in the mAb and ADC formulations were significantly different (p = 0.0004, t-test). Despite higher initial aggregate content, ADC formulations formed aggregates at a distinctly slower rate than low-concentration mAb formulations.

Both mAb and ADC formulations showed higher levels of aggregates in the presence of PS80. An adverse effect of PS80 on ADC formulations has been reported previously, though the structure of the ADC in the present study differs from that in the previous report.[26] The presence of peroxide in PS80 may attribute to the instability in PS80-containing formulations.[28] In general, aggregation in mAb formulations was more sensitive to decreases in concentration than to the presence of surfactant (**Figure 3.1a**, **Table B. 1**). Conversely, ADC formulations were less sensitive to either a decrease in concentration or the presence of surfactant than the mAb formulations (**Figure 3.1b**, **Table B. 2**).

3.4.2 Solid characterization using ssHDX-MS

In a previous study, the extent of deuterium incorporation measured in ssHDX-MS was correlated with the stability of ADC formulations containing various excipients.[26] Here, the ADC formulations did not contain any cryoprotectants to allow instability driven by the lyophilization process *per se* to be evaluated. **Figure 3.2a-b** shows ssHDX-MS kinetics after D_2O exposure for the mAb and ADC formulations of **Figure 3.1**. While SEC analysis showing effects of formulation on aggregation for both mAb and ADC formulations, neither mAb nor ADC showed significant differences among formulations on ssHDX-MS. In the past studies, ssHDX-MS showed good correlation with long-term stability studies when formulated with sugars, which incorporate protein-matrix hydrogen bonding.[26,29-30] **Figure 3.2c** compares the maximum deuterium uptake in mAb and ADC formulations. In the ADC formulations, drug-to-antibody ratios (DAR) of 1, 4, and 5 were detected consistently throughout the MS analysis. The different DAR species did not show significant differences in deuterium incorporation, whereas mAb and ADCs did show significant differences (**Figure 3.2c**). This may be due to the conjugation process, by which the native structure of mAb is partially disrupted to expose the sites of conjugation. Therefore, the backbone amide groups of ADCs may be less protected from exchange than in the mAbs.

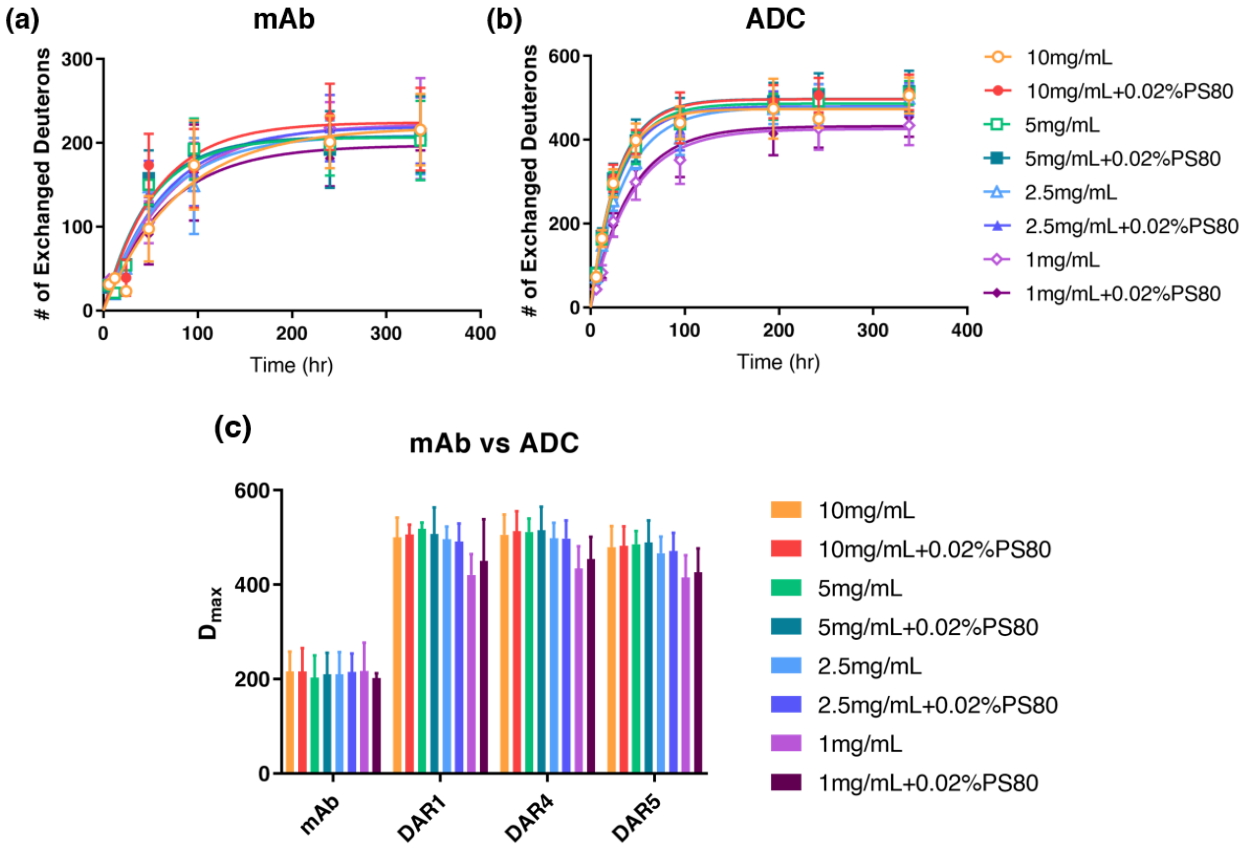

Figure 3.2. ssHDX-MS kinetics of (a) mAb and (b) DAR4 species after D_2O exposure at 23%RH at room temperature (*n*=2±SD); and (c) maximum deuterium uptake determined by nonlinear regression.

3.5 Conclusions

Accelerated stability studies on mAb formulations and ADC formulations with varying concentrations in the absence/presence of PS80 were conducted to monitor instability driven by the lyophilization process. Regardless of the concentration, PS80 had an adverse effect on the *in vitro* stability of both mAb formulations and ADC formulations. At low concentrations, ADC formulations showed less aggregate formation than mAb formulations, suggesting the *in vitro* stability enhancement by conjugation to payloads and linkers. ssHDX-MS also detected a significant difference of maximum deuterium uptake level between mAb formulations and ADC formulations. With different physicochemical properties, the parent mAb and ADCs showed different propensities for aggregation.

3.6 References

1. Schwegman JJ, Carpenter JF, Nail SL 2009. Evidence of Partial Unfolding of Proteins at the Ice/Freeze-Concentrate Interface by Infrared Microscopy. Journal of Pharmaceutical Sciences 98(9):3239-3246.

2. Strambini GB, Gabellieri E 1996. Proteins in frozen solutions: Evidence of ice-induced partial unfolding. Biophysical Journal 70(2):971-976.

3. Franks F 1990. Freeze-drying: from empiricism to predictability. Cryo-Letters 11(2):93-110.

4. Chang BS, Kendrick BS, Carpenter JF 1996. Surface-induced denaturation of proteins during freezing and its inhibition by surfactants. Journal of Pharmaceutical Sciences 85(12):1325-1330.

5. Nema S, Avis KE 1993. Freeze-thaw studies of a model protein, lactate dehydrogenase, in the presence of cryoprotectants. Journal of Parenteral Science and Technology 47(2):76-83.

6. Kendrick B, Chang B, Carpenter JF 1995. Detergent stabilization of proteins against surface and freezing denaturation. Pharmaceutical Research (New York) 12(9 SUPPL.):S85-S85.

7. Jain N, Smith SW, Ghone S, Tomczuk B 2015. Current ADC Linker Chemistry. Pharmaceutical Research 32(11):3526-3540.

8. Hoffmann RM, Coumbe BGT, Josephs DH, Mele S, Ilieva KM, Cheung A, Tutt AN, Spicer JF, Thurston DE, Crescioli S, Karagiannis SN 2018. Antibody structure and engineering considerations for the design and function of Antibody Drug Conjugates (ADCs). Oncoimmunology 7(3):11.

9. Buecheler JW, Winzer M, Weber C, Gieseler H 2020. Alteration of Physicochemical Properties for Antibody-Drug Conjugates and Their Impact on Stability. Journal of Pharmaceutical Sciences 109(1):161-168.

10. Ducry, L. (2013). Antibody-Drug Conjugates (1st ed. 2013. ed., Methods in Molecular Biology, 1045. Ch.5 Linker Technologies for Antibody-Drug Conjugates 71-100.

11. Waterman KC, Adami RC, Alsante KM, Antipas AS, Arenson DR, Carrier R, Hong JY, Landis MS, Lombardo F, Shah JC, Shalaev E, Smith SW, Wang H 2002. Hydrolysis in pharmaceutical formulations. Pharmaceutical Development and Technology 7(2):113-146.

12. Mohamed HE, Mohamed AA, Al-Ghobashy MA, Fathalla FA, Abbas SS 2018. Stability assessment of antibody-drug conjugate Trastuzumab emtansine in comparison to parent monoclonal antibody using orthogonal testing protocol. Journal of Pharmaceutical and Biomedical Analysis 150:268-277.

13. Chen T, Su D, Gruenhagen J, Gu C, Li Y, Yehl P, Chetwyn NP, Medley CD 2016. Chemical de-conjugation for investigating the stability of small molecule drugs in antibody-drug conjugates. Journal of Pharmaceutical and Biomedical Analysis 117:304-310.

14. Feng YW, Ooishi A, Honda S 2012. Aggregation factor analysis for protein formulation by a systematic approach using FTIR, SEC and design of experiments techniques. Journal of Pharmaceutical and Biomedical Analysis 57:143-152.

15. Beckley NS, Lazzareschi KP, Chih HW, Sharma VK, Flores HL 2013. Investigation into Temperature-Induced Aggregation of an Antibody Drug Conjugate. Bioconjugate Chemistry 24(10):1674-1683.

16. Gandhi AV, Arlotta KJ, Chen HN, Owen SC, Carpenter JF 2018. Biophysical Properties and Heating-Induced Aggregation of Lysine-Conjugated Antibody-Drug Conjugates. Journal of Pharmaceutical Sciences 107(7):1858-1869.

17. Kerwin BA, Remmele RL 2007. Protect from light: Photodegradation and protein biologics. Journal of Pharmaceutical Sciences 96(6):1468-1479.

18. Cockrell GM, Wolfe MS, Wolfe JL, Schoneich C 2015. Photoinduced Aggregation of a Model Antibody-Drug Conjugate. Molecular Pharmaceutics 12(6):1784-1797.

19. Davies MJ, Truscott RJW 2001. Photo-oxidation of proteins and its role in cataractogenesis. Journal of Photochemistry and Photobiology B-Biology 63(1-3):114-125.

20. Steinmann D, Mozziconacci O, Bommana R, Stobaugh JF, Wang YJ, Schoneich C 2017. Photodegradation Pathways of Protein Disulfides: Human Growth Hormone. Pharmaceutical Research 34(12):2756-2778.

21. Christie RJ, Fleming R, Bezabeh B, Woods R, Mao S, Harper J, Joseph A, Wang QL, Xu ZQ, Wu H, Gao CS, Dimasi N 2015. Stabilization of cysteine-linked antibody drug conjugates with N-aryl maleimides. Journal of Controlled Release 220:660-670.

22. Adem YT, Schwarz KA, Duenas E, Patapoff TW, Galush WJ, Esue O 2014. Auristatin Antibody Drug Conjugate Physical Instability and the Role of Drug Payload. Bioconjugate Chemistry 25(4):656-664.

23. Frka-Petesic B, Zanchi D, Martin N, Carayon S, Huille S, Tribet C 2016. Aggregation of Antibody Drug Conjugates at Room Temperature: SAXS and Light Scattering Evidence for Colloidal Instability of a Specific Subpopulation. Langmuir 32(19):4848-4861.

24. Hollander I, Kunz A, Hamann PR 2008. Selection of reaction additives used in the preparation of monomeric antibody-calicheamicin conjugates. Bioconjugate Chemistry 19(1):358-361.

25. Ross PL, Wolfe JL 2016. Physical and Chemical Stability of Antibody Drug Conjugates: Current Status. Journal of Pharmaceutical Sciences 105(2):391-397.

26. Cho E, Mayhugh BM, Srinivasan JM, Sacha GA, Nail SL, Topp EM 2021. Stability of antibody drug conjugate formulations evaluated using solid-state hydrogen-deuterium exchange mass spectrometry. Journal of pharmaceutical sciences 110(6):2379-2385.

27. Yao HZ, Jiang F, Lu AP, Zhang G 2016. Methods to Design and Synthesize Antibody-Drug Conjugates (ADCs). International Journal of Molecular Sciences 17(2):16.

28. Kishore RSK, Kiese S, Fischer S, Pappenberger A, Grauschopf U, Mahler HC 2011. The Degradation of Polysorbates 20 and 80 and its Potential Impact on the Stability of Biotherapeutics. Pharmaceutical Research 28(5):1194-1210.

29. Moorthy BS, Schultz SG, Kim SG, Topp EM 2014. Predicting Protein Aggregation during Storage in Lyophilized Solids Using Solid State Amide Hydrogen/Deuterium Exchange with Mass Spectrometric Analysis (ssHDX-MS). Molecular Pharmaceutics 11(6):1869-1879.

30. Moorthy BS, Zarraga IE, Kumar L, Walters BT, Goldbach P, Topp EM, Allmendinger A 2018. Solid-State Hydrogen Deuterium Exchange Mass Spectrometry: Correlation of Deuterium Uptake and Long-Term Stability of Lyophilized Monoclonal Antibody Formulations. Molecular Pharmaceutics 15(1):1-11.

CHAPTER 4. LINKER STABILITY COMPARISON BETWEEN SOLUTION-STATE AND SOLID-STATE HYDRAZONE COMPOUND

4.1 Abstract

Hydrazone linkers in antibody-drug conjugates (ADCs) may undergo *in vitro* cleavage during shelf storage. Since maintaining the stability of the linker is crucial to assuring the safety and efficacy of ADCs, understanding the conditions that promote *in vitro* cleavage of the hydrazone linker is also critical. In this study, the chemical degradation of hydrazone linkers in solution and lyophilized solid samples at various pre-lyophilization pH was compared using three model compounds that resemble the linker hydrazone moiety. Nevertheless, poor aqueous solubility and rapid degradation at room temperature were the challenges with these model compounds.

4.2 Introduction

In recent decades, growing technology has enabled the synthesis of antibody-drug conjugates (ADCs) with various linker types. ADC linkers are often categorized into two main types: cleavable and non-cleavable. Cleavable linkers include enzyme-labile and pH-labile linkers, which are sensitive to proteases or pH at the target site. Non-cleavable linkers are designed to undergo lysosomal degradation at the target site to release the payload from the parent antibody.[1-2] Cleavable linkers and non-cleavable linkers can be used in combination to achieve the desired plasma stability and release profile at the target site.[1,3-4] There are ongoing efforts to develop new types of linkers to lower pre-mature release of the payload and overcome current analytical and formulation challenges associated with ADCs.[2,5]

Since ADC payloads are highly toxic in their free form, the *in vitro* and *in vivo* stability of linkers is crucial in assuring the safety and efficacy of ADCs. Thus, linker stability has been studied extensively in the past to understand the susceptibility of the linkers to degradation under various conditions, and various *in vivo* deconjugation/degradation mechanisms of different linker types have been reported.[2-3,6-9] However, there have been few studies on the *in vitro* stability of ADC linkers under conditions relevant for the shipping and storage of the drug product.[10-16]

There are several challenges associated with studying the *in vitro* stability of linkers using the intact ADC. First, the deconjugated payload species is extremely toxic and may endanger the researcher when it is produced during the experiments. The non-selective conjugation process during manufacturing yields a mixture of ADCs with various drug-to-antibody ratio (DAR) species conjugated at random sites.[17-18] Thus, the heterogeneous nature of ADC batches complicates analysis. Deconjugation from the parent antibody drastically decreases the aqueous solubility of the payload. As a result, the deconjugated species may not be detected, or may clog analytical instruments such as mass spectrometers and chromatography columns.

In this study, instead of using an intact ADC, model compounds that resemble the hydrazone-based linker and the drug moiety were selected to minimize the challenges stated above. A hydrazone-based linker has been utilized in the ADC products Mylotarg® and Besponsa® as a pH-labile linker, which deconjugates at pH 5 and is stable at physiological pH.[2,19] Unlike other cleavable linkers, pH-labile linkers are at risk of *in vitro* cleavage due to their deconjugation mechanism,[8] and require greater care in formulation than other linker types. Barbour *et al*. studied the solid-state stability of a hydrazone-based ADC (BR96- doxorubicin) at a pre-lyophilization pH of 7.5 using various excipients.[10] They reported that an optimal pH and temperature could not assure long-term stability of a solution-state hydrazone-based ADC, whereas lyophilization in the presence of sugars improved long-term stability. Yet, the susceptibility of hydrazone linkers to degradation at varying pH conditions during lyophilization[20] is still not known. In this study, a pre-lyophilization pH ranging from 5 to 9 in various types of buffers was used to compare linker stability in solution-state and in the solid-state for hydrazone model compounds.

4.3 Materials and methods

4.3.1 Materials

Methyl 2-[(E)-phenylmethylidene]-1-hydrazinecarboxylate (MolPort, Beacon NY); 2,3-piperidinedione 3-((4-methyl-2-nitrophenyl) hydrazone) (Sigma Aldrich, St. Louis MO); and 2,3-butanedione mono (phenyl hydrazone) (Sigma Aldrich) were tested as hydrazone model compounds. Benzaldehyde (Sigma Aldrich) and phenylhydrazine (Enamine, Monmouth Jct. NJ) were used as analysis standards of expected degradant species.

Potassium phosphate monobasic (Sigma Aldrich) and potassium phosphate dibasic (Sigma Aldrich) were used to prepare 50 mM potassium phosphate buffer with pH 6 and 7. Trizma® base (Sigma Aldrich) and Trizma® hydrochloride (Sigma Aldrich) were used to prepare 50 mM tris buffer with pH 9. Sodium citrate dihydrate (Sigma Aldrich) and citric acid (Sigma Aldrich) were used to prepare 50 mM citrate buffer with pH 5 and 6. Sucrose (Sigma Aldrich) with purity greater than 99.5% was used as a cryoprotectant during lyophilization. 1 N hydrochloric acid (Fisher Scientific, Hampton NH) was used to adjust pH of the buffers. Nylon membrane disc filters (PALL Life Sciences, Port Washington NY) with 0.2 µM nominal pore size and 47 mm diameter were used to filter buffer solutions. Syringe filters (Millipore, Tullagreen Ireland), low protein binding durapore (PVDF), with 0.22 µM nominal pore size and 33 mm diameter were used to filter final formulations. 2 mL-lyophilization vials (DWK life sciences, Rockwood TN) with stoppers (DWK Life Sciences) were used to store both solution-state and solid-state formulations.

4.3.2 Solubility Testing

A 3-5 mg sample of the model compound was weighed on a weighing boat using a balance (Mettler Toledo, Model# AE240, Columbus OH). The weighed compounds were dissolved in USP grade ethanol (KOPTEC, King of Prussia PA) (1% v/v of the final volume). The dissolved solution was further diluted into various concentrations using each buffer: 50mM citrate buffer (pH 5, 6), 50 mM potassium phosphate buffer (pH 6, 7), and 50 mM tris buffer (pH 9). The diluted solutions were manually agitated to promote dissolution of the model compounds. After agitation, the presence of solid contents in the solution was observed visually to monitor complete dissolution of the model compounds.

4.3.3 UV standard curve

Standard curves for both the model compounds and degradant standards were determined using a UV-Vis (Agilent 89090A, Santa Clara CA) coupled spectrophotometer (Agilent 8453). The spectra were obtained from 200 nm to 400 nm, regardless of compound. For each UV analysis, 200 µL of analyte solution was filled into a 10 mm pathlength cuvette (Starna cells, Atascadero CA).

4.3.4 Sample Preparation

Each hydrazone model compound was dissolved in ethanol (1% v/v of the final volume). The dissolved solutions were further diluted with each of the five formulation buffers to achieve a final concentration of 0.15 mg/mL. The formulation buffers contained 1:10 (w/w) sucrose as a cryoprotectant for lyophilization. Sucrose containing formulation buffers were also used to prepare solution-state samples to maintain the same composition as solid-state samples. Each final formulation was filtered using a PVDF syringe filter and filled into 2 mL-lyophilization vials using a 0.5 mL fill volume. Half of the prepared samples were stored in the solution-state at 4 °C prior to stability studies, and the rest of the samples were lyophilized in a LyoStar III freeze-dryer (SP Scientific, Warminster PA) using the conservative cycle described in **Table 4.1**.

Table 4.1. Lyophilization cycle used for solid-state sample preparation

Stage	Set Temp (°C)	Pressure (mTorr)	Ramp Rate (°C/min)	Duration (min)
Freezing	-40	atm.pressure	1	180
Primary Drying	-20	50	0.5	Pirani/CM diff=10mT
Secondary Drying	40	50	0.5	240
Stoppering	5	50	N/A	N/A

4.3.5 Preliminary stability study

Solution-state model compounds 1 and 3 were prepared at a concentration of 0.1 mg/mL in various buffers without sucrose. The vials were stoppered and sealed using parafilm (Bemis, Neenah WI). The vials were stored at room temperature and in a 50 °C oven (Fisher Scientific), protected from light. At each time point, the samples were analyzed using UV spectrophotometry immediately after retrieval.

4.3.6 Accelerated stability study

Both solid-state and solution-state samples were sealed using parafilm over the stoppers to prevent evaporation. The sealed vials were placed in a cryo box and then stored at room temperature and in a 50 °C oven, protected from light. At each time point, the samples were retrieved from the stored cryo box and flash-frozen using liquid nitrogen. The quenched samples were stored at -80 °C prior to analysis.

4.3.7 Aldehyde colorimetric assay

An aldehyde colorimetric assay kit (Sigma Aldrich) was used to measure the amount of benzaldehyde present in the samples after stability storage. Prior to analysis, the samples stored at -80 °C were thawed and treated with the reagents on a 96 well-plate (BD Falcon, Franklin Lakes NJ). During the incubation, the 96 well-plate was protected from light. After incubation, absorbance was measured at wavelength between 620 nm and 660 nm using a Synergy 4 plate reader (BioTek, Winooski, VT).

4.4 Results and discussion

4.4.1 Selection of hydrazone model compounds

Figure 4.1 shows the structures of hydrazone-based linkers utilized in ADCs. ADCs use a hydrazone linker in a combination with other non-cleavable linkers. In **Figure 4.1a**, hydrazone is coupled with a maleimidomethyl cyclohexane-1-carboxylate (MCC) linker, and **Figure 4.1b** shows a hydrazone linker coupled with a maleimidocaproyl (MC) linker. In both ADCs, the hydrazone linker is stabilized by the adjacent carbonyl group by electron delocalization (**Figure 4.1**, **Figure 4.2**).[21]

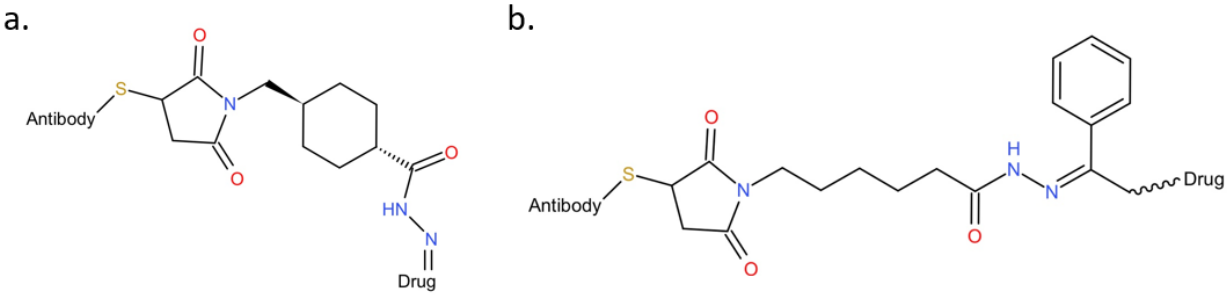

Figure 4.1. Structures of hydrazone linkers in the (a) milatuzumab-doxorubicin[1] and (b) MMAE conjugated mAb.[19]

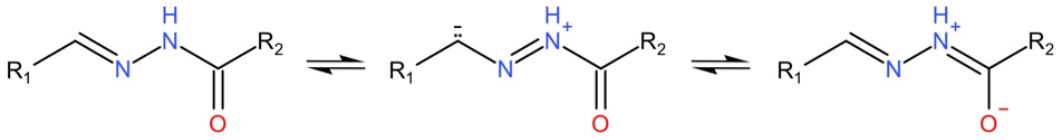

Figure 4.2. Resonance structures of hydrazones with neighboring carbonyl group. Adapted from ref. 21

In selecting model compounds for this study, several criteria were taken into consideration. First, the hydrazone should have an adjacent carbonyl group to resemble the linker chemistry in ADCs. In addition, the compound should contain an aromatic ring-structure to enable UV analysis. Lastly, the Log P of the compound should not exceed 3.0 to minimize challenges associated with aqueous solubility. According to the criteria stated above, three model compounds were selected (**Figure 4.3**). Since the non-cleavable linker moiety is highly hydrophobic, model compounds that represent only the hydrazone linker moiety were selected. For convenience, each model compound is denoted by number hereinafter (i.e., model compound 1).

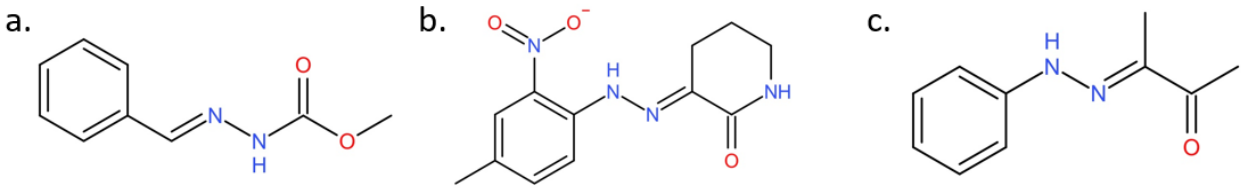

Figure 4.3. Structures of hydrazone model compounds. **a.** methyl 2-[(E)-phenylmethylidene]- 1-hydrazinecarboxylate; **b.** 2,3-piperidinedione 3-((4-methyl-2-nitrophenyl) hydrazone); **c.** 2,3- butanedione mono (phenyl hydrazone)

Since the model compounds were selected from commercially available products, they do not fully represent the linker chemistry in ADCs. Model compound 1 contains an ester group instead of a carbonyl alone, which may undergo ester hydrolysis. Model compound 2 contains a carbonyl group on the opposite side of the intended position, and not directly adjacent to the hydrazone. In addition, a nitro group on the benzene may influence electron delocalization. Model compound 3 contains a carbonyl group, not directly adjacent to the hydrazone, attached to the opposite side of the hydrazone moiety. Thus, each model compound has slightly different electron delocalization environment compared to that of ADCs.

4.4.2 Determination of aqueous solubility and detectability

The model compounds were hydrophobic, having log P values of 1.7, 2.4, and 2.0, respectively. Therefore, ethanol was used as a co-solvent to increase the aqueous solubility of the model compounds and ensure dissolution. The volume of ethanol was limited to 1% (v/v) to avoid complications during lyophilization. Based on the log P values of the model compounds, the desired solubility was set to 0.1 mg/mL with 1% ethanol (v/v). When aqueous solubility was tested, model compound 2 failed to meet the desired solubility, and thus was excluded from the study. Model compound 3 in 50 mM potassium phosphate buffer at pH 7 also did not meet the desired solubility, yet a 0.02 mg/mL was deemed an acceptable solubility for analysis.

Table 4.2. Aqueous solubility testing results of hydrazone model compounds with 1% (v/v) ethanol.

	Model Compound 1	Model Compound 2	Model Compound 3
Citrate pH 5	0.1 mg/mL	Failed	0.1 mg/mL
Citrate pH 6	0.1 mg/mL	Failed	0.1 mg/mL
Potassium Phosphate pH 6	0.1 mg/mL	Failed	0.1 mg/mL
Potassium Phosphate pH 7	0.1 mg/mL	Failed	0.02 mg/mL
TRIS pH 9	0.1 mg/mL	Failed	0.1 mg/mL

The model compounds that passed solubility testing were then formulated in various buffers, and their detectability was tested using a UV spectrophotometer. For the UV analysis, predicted degradation products that contain benzene in their structures were purchased and used to generate standard curves of the cleaved products (**Figure 4.4**). However, the ester hydrolysis degradation product with the ring structure was not commercially available. **Figure 4.5** shows UV spectra of the parent model compounds and the corresponding degradation products scanned in a range of 250-400 nm. Both model compound 1 and model compound 3 had overlapping bands with their degradation products, especially model compound 1. Compared to model compound 1, UV analysis of the model compound 3 may be less complicated because the absorbances at λ_{max}

(345 nm) of model compound 3 are merely overlapping with a band of the degradation product, phenylhydrazine. Although model compound 1 has overlapping bands, generation of ratio spectra of the model compound and the degradation product may enable concentration measurement in a binary mixture.[22]

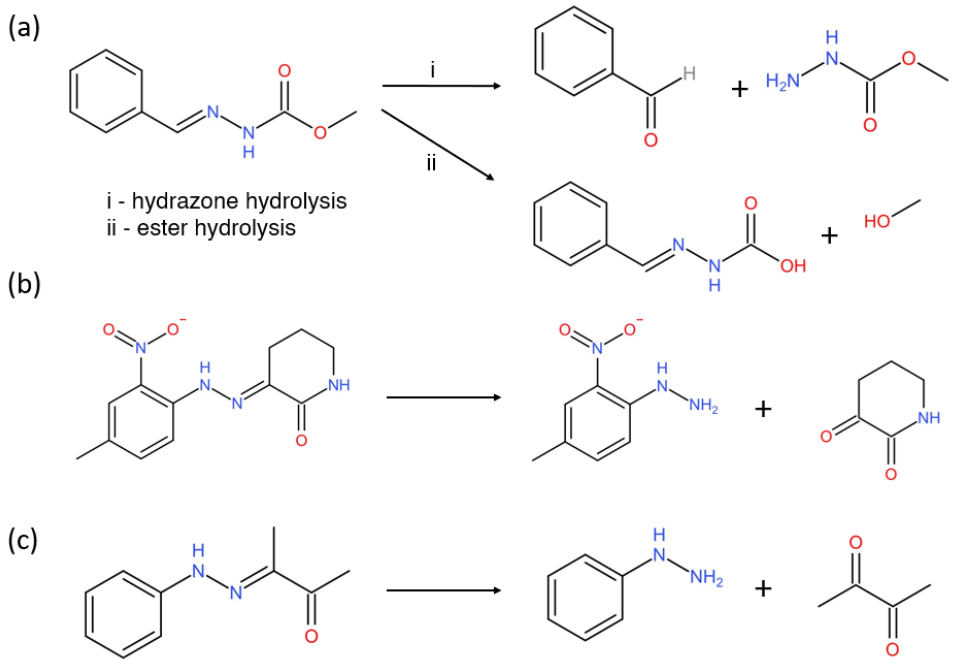

Figure 4.4. Predicted degradation products of (a) the model compound 1, (b) 2, and (c) 3.

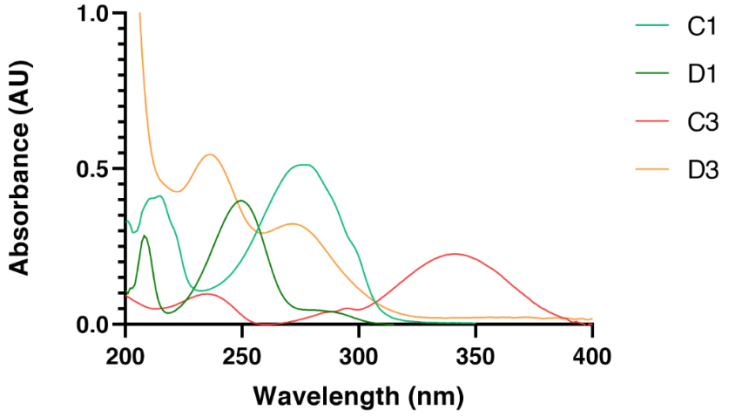

Figure 4.5. UV spectra of the model compounds and predicted degradation products.
C1: the model compound 1, D1: benzaldehyde, C3: the model compound 3, and D3: phenylhydrazine.

Although the UV spectra were acquired in the range of 200-400 nm, the λ_{max} of each compound was used to determine linearity of the standard curves in various buffers (**Figure 4.6**). The linearity of the standard curves generated using the model compound 1 were good, having r^2 values greater than 0.97 (**Table C. 1**). Similarly, the standard curves generated using a benzaldehyde, which is a predicted degradation of model compound 1, had a good linearity regardless of buffer type (**Table C. 2**). Yet, benzaldehyde was more sensitive to changes in buffer type than the parent molecule during UV analysis. Regardless of buffer type, model compound 3 showed an inconsistency in absorbance readings during UV analysis, and thus failed to generate acceptable standard curves (data not shown).

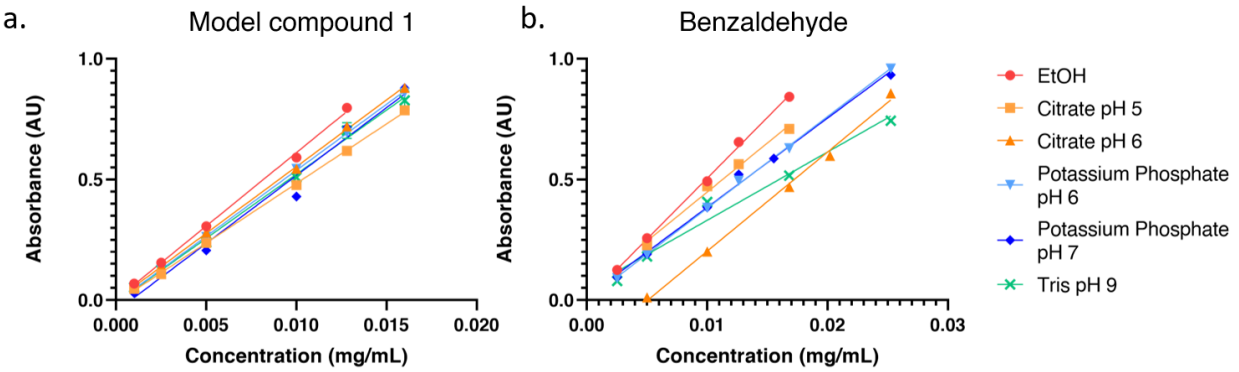

Figure 4.6. UV standard curve of a) the model compound 1 at 280 nm and b) benzaldehyde at 245 nm in various buffers and pH. (n = 2±SD)

4.4.3 Identification of degradation products

To identify degradation products, the model compounds were formulated in 50 mM citrate buffer with pH 5, which is a deconjugation pH of the hydrazone linker, and stored in solution-state at RT and 50 °C for a week (**Figure 4.7**). Model compound 1 showed a decrease in the parent molecule peak after 40 h at 50 °C, and the spectra were superimposed for formulations stored at RT and 50 °C for a week. Thus, a storage period of 1 week was considered sufficient to observe degradation of model compound 1 in solution under these conditions. To visualize the amount of degraded parent molecule after 1 wk of storage, an equimolar spectrum of the benzaldehyde standard was plotted in green (**Figure 4.7a**). Yet, increased absorbance at a λ_{max} of benzaldehyde (245 nm) in the 1 wk samples was not clearly observed at RT and 50 °C. As shown in **Figure 4.4**, model compound 1 has two potential degradation pathways: hydrazone and ester hydrolysis. Using

UV analysis, the degradation products of the model compound 1 could not be clearly identified. Model compound 3 showed higher absorbance when stored at 50 °C compared to RT, suggesting incomplete dissolution of the model compound 3 at RT (**Figure 4.7b**). The inconsistent absorbance readings observed during UV analysis may also be attributed to incomplete dissolution of model compound 3 at RT. Therefore, model compound 3 was excluded from the study.

To elucidate the degradation pathways that the model compound 1 undergoes, an aldehyde colorimetric assay was performed on a solution-state formulation in 50 mM citrate buffer pH 5 stored at 50 °C for 2 weeks (data not shown). The assay did not detect any aldehyde from either the benzaldehyde control or the solution-state formulation after 2 wk storage. Negative readings on the benzaldehyde control may indicate a limitation of the assay rather than absence of benzaldehyde in the solution-state formulation.

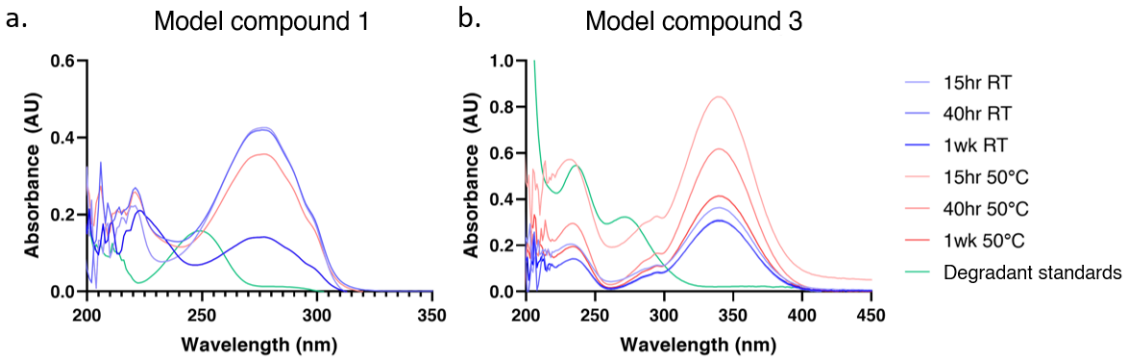

Figure 4.7. UV spectra of a) the model compound 1 and b) the model compound 3 after stability storage at RT and 50°C.

4.4.4 Comparison of solution-state and solid-state stability of the model compound

To compare the solution-state and solid-state stability of model compound 1, formulations were stored at RT and 50 °C for up to 47 days. The samples were then analyzed using UV spectrophotometry, and the percent loss of the parent molecule was calculated using the standard curves obtained at 280 nm (**Figure 4.6**, **Figure C. 2**).

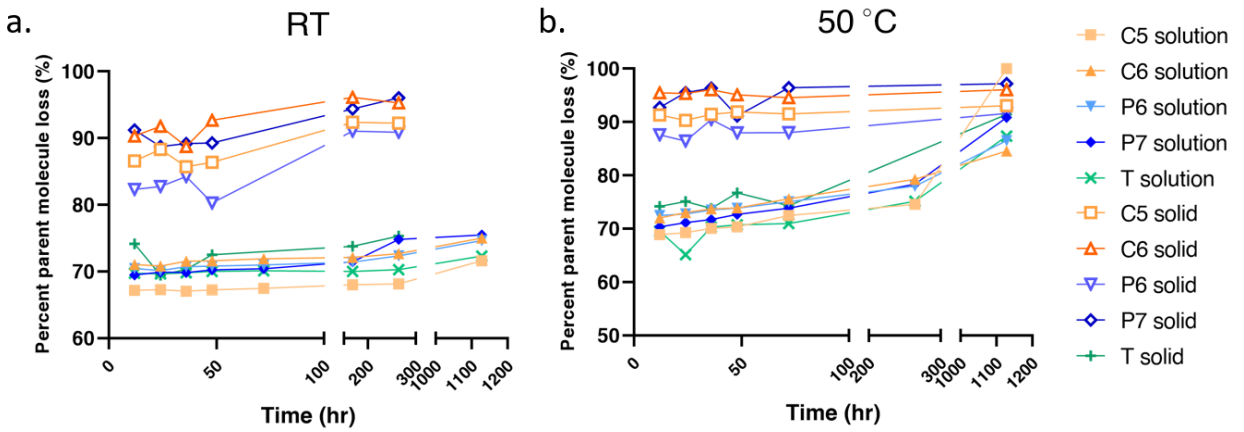

Figure 4.8. Stability kinetics of the model compound 1 in solution-state and solid-state stored at a) RT and b) 50 °C.

As shown in **Figure 4.8**, the rank order of the stability is similar at RT and 50 °C. At both temperatures, the solid-state formulations showed higher percent loss of the parent molecule than solution-state formulations. However, regardless of phases and buffer types, the initial percent loss was greater than 60%. Pre-storage degradation was observed in both solid-state and solution-state formulation in Tris buffer with parent molecule loss of 71.20% and 60.06%, respectively (data not shown). According to Barbour *et al*., the lyophilization process causes minimal hydrolysis of the hydrazone, but the rate of hydrazone linker cleavage for solution-state BR96-DOX was greater at room temperature than at 2-8 °C or -15 °C.[10] The initial degradation shown in **Figure 4.8** may also be attributed to the rapid degradation at RT, considering that the duration of sample preparation was 4-5 hours. The greater instability shown in the solid-state formulation may also be due to longer exposure to RT while transferring the samples to a different facility. Based on the duration of exposure at RT, model compound 1 had a faster degradation rate than BR96-DOX investigated by Barbour *et al*.[10] Due to the issues stated above, comparison between the solution-state and the solid-state model compound 1 using **Figure 4.8** may not be valid.

4.5 Conclusions

To study the stability of pH-labile hydrazone linker in model compounds, various approaches were made in this study. Due to the hydrophobic nature of the linker, solubility was one of most significant challenges encountered; two model compounds were excluded due to this issue. Only model compound 1 overcame the solubility issue by using ethanol as a co-solvent.

However, compound 1 contains both hydrazone and ester groups in its structure, and thus has two potential degradation pathways. In this study, elucidation of the degradation pathways could not be performed due to limitations in time and instruments. In future studies, high performance liquid chromatography (HPLC) or mass spectrometry may be used to clearly identify the degradation products. Synthesis of a model compound that represents the linker chemistry of the hydrazone linker in ADC may better depict resonances formed by electron delocalization.

The stability study results showed rapid degradation of solution-state model compound 1 at room temperature, hindering a robust comparison between the solution-state and the solid-state model compound formulations. In the future, discontinuous sample preparation with smaller batch sizes may prevent extensive pre-storage degradation.

4.6 References

1. Jain N, Smith SW, Ghone S, Tomczuk B 2015. Current ADC Linker Chemistry. Pharmaceutical Research 32(11):3526-3540.

2. Bargh JD, Isidro-Llobet A, Parker JS, Spring DR 2019. Cleavable linkers in antibody-drug conjugates. Chemical Society Reviews 48(16):4361-4374.

3. Beck A, Goetsch L, Dumontet C, Corvaia N 2017. Strategies and challenges for the next generation of antibody drug conjugates. Nature Reviews Drug Discovery 16(5):315-337.

4. Phillips GDL, Li GM, Dugger DL, Crocker LM, Parsons KL, Mai E, Blattler WA, Lambert JM, Chari RVJ, Lutz RJ, Wong WLT, Jacobson FS, Koeppen H, Schwall RH, Kenkare-Mitra SR, Spencer SD, Sliwkowski MX 2008. Targeting HER2-Positive Breast Cancer with Trastuzumab-DM1, an Antibody-Cytotoxic Drug Conjugate. Cancer Research 68(22):9280- 9290.

5. Yao HZ, Jiang F, Lu AP, Zhang G 2016. Methods to Design and Synthesize Antibody-Drug Conjugates (ADCs). International Journal of Molecular Sciences 17(2):16.

6. Carter PJ, Lazar GA 2018. Next generation antibody drugs: pursuit of the 'high-hanging fruit'. Nature Reviews Drug Discovery 17(3):197-223.

7. Kommineni N, Pandi P, Chella N, Domb AJ, Khan W Antibody drug conjugates: Development, characterization, and regulatory considerations. Polymers for Advanced Technologies:17.

8. Hoffmann RM, Coumbe BGT, Josephs DH, Mele S, Ilieva KM, Cheung A, Tutt AN, Spicer JF, Thurston DE, Crescioli S, Karagiannis SN 2018. Antibody structure and engineering considerations for the design and function of Antibody Drug Conjugates (ADCs). Oncoimmunology 7(3):11.

9. Birrer MJ, Moore KN, Betella I, Bates RC 2019. Antibody-Drug Conjugate-Based Therapeutics: State of the Science. Jnci-Journal of the National Cancer Institute 111(6):538- 549.

10. Barbour NP, Paborji M, Alexander TC, Coppola WP, Bogardus JB 1995. STABILIZATION OF CHIMERIC BR96-DOXORUBICIN IMMUNOCONJUGATE. Pharmaceutical Research 12(2):215-222.

11. Duddu SP, DalMonte PR 1997. Effect of glass transition temperature on the stability of lyophilized formulations containing a chimeric therapeutic monoclonal antibody. Pharmaceutical Research 14(5):591-595.

12. Valliere-Douglass JF, Lewis P, Salas-Solano O, Jiang S 2015. Solid-State mAbs and ADCs Subjected to Heat-Stress Stability Conditions can be Covalently Modified with Buffer and Excipient Molecules. Journal of Pharmaceutical Sciences 104(2):652-665.

13. Clavaud M, Roggo Y, Degardin K, Sacre PY, Hubert P, Ziemons E 2016. Moisture content determination in an antibody-drug conjugate freeze-dried medicine by near-infrared spectroscopy: A case study for release testing. Journal of Pharmaceutical and Biomedical Analysis 131:380-390.

14. Jaime J, Page M 2004. Paclitaxel antibody conjugates and trehalose for preserving the immunulogical activity after freeze-drying. Current Medicinal Chemistry 11(4):439-446.

15. Ramos JR, Taniwaki L, Mendonca R, Ribeiro JAS, Scott IU, Cunha AS, Jorge R 2010. Effect of Lyophilization on the in vitro Biological Activity of Bevacizumab. Investigative Ophthalmology & Visual Science 51(13):2.

16. Rowland AJ, Pietersz GA, McKenzie IFC 1993. PRECLINICAL INVESTIGATION OF THE ANTITUMOR EFFECTS OF ANTI-CD19-IDARUBICIN IMMUNOCONJUGATES. Cancer Immunology Immunotherapy 37(3):195-202.

17. Singh SK, Luisi DL, Pak RH 2015. Antibody-Drug Conjugates: Design, Formulation and Physicochemical Stability. Pharmaceutical Research 32(11):3541-3571.

18. Neupane R, Bergquist J 2017. Analytical techniques for the characterization of Antibody Drug Conjugates: Challenges and prospects. European Journal of Mass Spectrometry 23(6):417-426.

19. Doronina SO, Toki BE, Torgov MY, Mendelsohn BA, Cerveny CG, Chace DF, DeBlanc RL, Gearing RP, Bovee TD, Siegall CB, Francisco JA, Wahl AF, Meyer DL, Senter PD 2003. Development of potent monoclonal antibody auristatin conjugates for cancer therapy. Nature Biotechnology 21(7):778-784.

20. Sundaramurthi P, Shalaev E, Suryanarayanan R 2010. "pH Swing" in Frozen Solutions - Consequence of Sequential Crystallization of Buffer Components. Journal of Physical Chemistry Letters 1(1):265-268.

21. Kalia J, Raines RT 2008. Hydrolytic stability of hydrazones and oximes. Angewandte Chemie-International Edition 47(39):7523-7526.

22. Belal TS, Daabees HG, Abdel-Khalek MM, Mahrous MS, Khamis MM 2013. New simple spectrophotometric method for determination of the binary mixtures (atorvastatin calcium and ezetimibe; candesartan cilexetil and hydrochlorothiazide) in tablets. Journal of Pharmaceutical Analysis 3(2):118-126.

CHAPTER 5. CONCLUSIONS

Due to the complexity and toxicity of antibody-drug conjugates (ADCs), stability is more critical than for the parent monoclonal antibody (mAb). Introduction of a linker system leads to changes in physicochemical properties of ADC molecules relative to the parent mAb, hence increasing the risks of instability induced by various factors such as pH, temperature, and interaction with excipients.[1] Although all the currently marketed ADCs are manufactured in a lyophilized form, the solid-state stability of ADCs, especially during shelf storage, is not fully understood. Therefore, this dissertation has incorporated novel approaches to address the knowledge gap on solid-state stability of ADCs.

The first two studies presented in Chapters 2-3 introduced solid-state hydrogen/deuterium exchange coupled with mass spectrometry (ssHDX-MS) as a short-term predictor of solid-state stability in ADC formulations. The study showed the capability of ssHDX-MS to analyze complex molecules such as ADCs; previously, mAb was the largest molecule analyzed using this method. In both chapters, the ssHDX-MS results were compared to the percent aggregates formed in accelerated stability studies. In Chapter 2, ssHDX-MS was used to analyze matrix interactions between the ADCs and commonly used excipients: sucrose, trehalose, mannitol, and polysorbate 80 (PS80). In Chapter 3, conformational changes of ADCs after lyophilization were monitored using ssHDX-MS. In this study, PS80 and buffer salts were the only excipients included in the formulations. The results from these chapters showed better correlation between the ssHDX-MS and the accelerated stability studies in the presence of sugars. That suggests that excipients with protein-matrix H-bonding capability increase the predictability of ssHDX-MS when analyzing solid-state ADCs. Moreover, the two studies showed the capability of ssHDX-MS to simultaneously analyze ADCs with different drug-to-antibody ratio (DAR) without purification. Unlike the accelerated stability studies, ssHDX-MS may detect conformational changes in few weeks. Understanding the correlation between ssHDX-MS and long-term stability studies may accelerate the development of solid-state ADC products.

In Chapter 4, the *in vitro* stability of a pH-labile hydrazone linker was investigated using three model compounds. Selection of model compounds from commercially available products was difficult due to structural differences from the hydrazone linker in ADCs. The difference in neighboring organic groups led to a slightly different electron delocalization, which may not

represent the actual hydrazone linker. In addition, the hydrophobic nature of the linker with poor aqueous solubility complicated both formulation and analysis throughout the study. Although one of the model compounds overcame the solubility issue by formulating with ethanol, the model compound had a high rate of degradation at room temperature. As a result, an extensive amount of the parent molecule was degraded even before accelerated stability storage. Despite the challenges, ongoing efforts to understand the solid-state linker stability of ADCs are crucial to avoid *in vitro* cleavage of the linkers. In future studies, other pH-labile linkers such as carbonate linker could be studied using an approach similar to that presented in this study.[2]

As the use of lyophilization increases for biologics, knowledge of the solid-state chemistry of these complex molecules will also be in greater demand. With the growing ADC market, various types of linkers are already under development and will be utilized in the future.[2] Thus, analytical methods will have to adapt rapidly to enable stability evaluation of ADCs with novel linkers. Since the ADCs used in this dissertation was limited to one type of linker, different types of ADCs may be used to investigate the capability of the ssHDX-MS for predicting stability. In the future studies, it will be interesting to employ ssHDX-MS to study molecules with even greater complexity such as freeze-dried vaccines.[3-4]

5.1 Reference

1. Buecheler JW, Winzer M, Weber C, Gieseler H 2020. Alteration of Physicochemical Properties for Antibody-Drug Conjugates and Their Impact on Stability. Journal of Pharmaceutical Sciences 109(1):161-168.

2. Bargh JD, Isidro-Llobet A, Parker JS, Spring DR 2019. Cleavable linkers in antibody-drug conjugates. Chemical Society Reviews 48(16):4361-4374.

3. Abd El Fadeel MR, El-Dakhly AT, Allam AM, Farag TK, El-kholy AAM 2020. Preparation and efficacy of freeze-dried inactivated vaccine against bovine viral diarrhea virus genotypes 1 and 2, bovine herpes virus type 1.1, bovine parainfluenza-3 virus, and bovine respiratory syncytial virus. Clinical and Experimental Vaccine Research 9(2):119-125.

4. Chen Y, Liao QB, Chen TY, Zhang YC, Yuan WE, Xu JQ, Zhang XY Freeze-Drying Formulations Increased the Adenovirus and Poxvirus Vaccine Storage Times and Antigen Stabilities. Virologica Sinica:8.

APPENDIX A. CHAPTER 2 SUPPLEMENTARY INFORMATION

Table A. 1. Mass spectrometry parameters

Source	Dual AJS ESI		
Gas Temp	350°C	**Vcap**	5500V
Drying Gas	8L/min	**Nozzle Voltage**	1000V
Nebulizer	35psig	**Fragmentor**	380V
Sheath Gas Temp	400°C	**Skimmer**	65V
Sheath Gas Flow	11L/min	**RF Vpp**	750V
Mass Range	3200-20000m/z	**Acquisition Mode**	Positive, Extended Mass Range

Table A. 2. Tukey multiple comparison analysis results for accelerated studies at 40°C after 12 weeks of storage. α=0.05; number of families=6; number of comparisons per family=21.

12wks at 40°C	Mean Diff.	95% CI of Diff.	Significant?	Summary	Adjusted P Value
Excipient-free vs. Sucrose	-0.3	-22.25 to 21.65	No	ns	>0.9999
Excipient-free vs. Trehalose	-0.2	-22.15 to 21.75	No	ns	>0.9999
Excipient-free vs. Mannitol	-14.4	-36.35 to 7.552	No	ns	0.3946
Excipient-free vs. PS80	-27.4	-49.35 to -5.448	Yes	**	0.0073
Excipient-free vs. Suc+mann	-0.6	-22.55 to 21.35	No	ns	>0.9999
Excipient-free vs. Tre+mann	-0.9	-22.85 to 21.05	No	ns	>0.9999
Sucrose vs. Trehalose	0.1	-21.85 to 22.05	No	ns	>0.9999
Sucrose vs. Mannitol	-14.1	-36.05 to 7.852	No	ns	0.4193
Sucrose vs. PS80	-27.1	-49.05 to -5.148	Yes	**	0.0082
Sucrose vs. Suc+mann	-0.3	-22.25 to 21.65	No	ns	>0.9999
Sucrose vs. Tre+mann	-0.6	-22.55 to 21.35	No	ns	>0.9999
Trehalose vs. Mannitol	-14.2	-36.15 to 7.752	No	ns	0.411
Trehalose vs. PS80	-27.2	-49.15 to -5.248	Yes	**	0.0079
Trehalose vs. Suc+mann	-0.4	-22.35 to 21.55	No	ns	>0.9999
Trehalose vs. Tre+mann	-0.7	-22.65 to 21.25	No	ns	>0.9999
Mannitol vs. PS80	-13	-34.95 to 8.952	No	ns	0.5147
Mannitol vs. Suc+mann	13.8	-8.152 to 35.75	No	ns	0.4446
Mannitol vs. Tre+mann	13.5	-8.452 to 35.45	No	ns	0.4705
PS80 vs. Suc+mann	26.8	4.848 to 48.75	Yes	**	0.0092
PS80 vs. Tre+mann	26.5	4.548 to 48.45	Yes	*	0.0102
Suc+mann vs. Tre+mann	-0.3	-22.25 to 21.65	No	ns	>0.9999

Table A. 3. Tukey multiple comparison analysis results for accelerated studies at 50°C after 8 weeks of storage. α=0.05; number of families=5; number of comparisons per family=21.

8wks at 50°C	Mean Diff.	95% CI of Diff.	Significant?	Summary	Adjusted P Value
Excipient-free vs. Sucrose	-0.3	-10.24 to 9.642	No	ns	>0.9999
Excipient-free vs. Trehalose	-0.5	-10.44 to 9.442	No	ns	>0.9999
Excipient-free vs. Mannitol	-14.4	-24.34 to -4.458	Yes	**	0.0017
Excipient-free vs. PS80	-7.1	-17.04 to 2.842	No	ns	0.2873
Excipient-free vs. Suc+mann	-0.5	-10.44 to 9.442	No	ns	>0.9999
Excipient-free vs. Tre+mann	-0.7	-10.64 to 9.242	No	ns	>0.9999
Sucrose vs. Trehalose	-0.2	-10.14 to 9.742	No	ns	>0.9999
Sucrose vs. Mannitol	-14.1	-24.04 to -4.158	Yes	**	0.0022
Sucrose vs. PS80	-6.8	-16.74 to 3.142	No	ns	0.3337
Sucrose vs. Suc+mann	-0.2	-10.14 to 9.742	No	ns	>0.9999
Sucrose vs. Tre+mann	-0.4	-10.34 to 9.542	No	ns	>0.9999
Trehalose vs. Mannitol	-13.9	-23.84 to -3.958	Yes	**	0.0025
Trehalose vs. PS80	-6.6	-16.54 to 3.342	No	ns	0.3669
Trehalose vs. Suc+mann	0	-9.942 to 9.942	No	ns	>0.9999
Trehalose vs. Tre+mann	-0.2	-10.14 to 9.742	No	ns	>0.9999
Mannitol vs. PS80	7.3	-2.642 to 17.24	No	ns	0.2588
Mannitol vs. Suc+mann	13.9	3.958 to 23.84	Yes	**	0.0025
Mannitol vs. Tre+mann	13.7	3.758 to 23.64	Yes	**	0.003
PS80 vs. Suc+mann	6.6	-3.342 to 16.54	No	ns	0.3669
PS80 vs. Tre+mann	6.4	-3.542 to 16.34	No	ns	0.402
Suc+mann vs. Tre+mann	-0.2	-10.14 to 9.742	No	ns	>0.9999

Table A. 4. Tukey multiple comparison analysis results for D_{max} values derived from HDX studies. α=0.05; number of families=1; number of comparisons per family=21.

	Mean Diff.	95.% CI of Diff.	Significant?	Summary	Adjusted P Value
Excipient-free vs. Sucrose	51.57	-8.795 to 111.9	No	ns	0.0993
Excipient-free vs. Trehalose	48.43	-11.94 to 108.8	No	ns	0.1272
Excipient-free vs. Mannitol	-71.2	-131.6 to -10.83	Yes	*	0.0223
Excipient-free vs. PS80	-62.8	-123.2 to -2.435	Yes	*	0.0415
Excipient-free vs. Suc+mann	-19.3	-79.67 to 41.07	No	ns	0.8475
Excipient-free vs. Tre+mann	-44	-104.4 to 16.37	No	ns	0.1802
Sucrose vs. Trehalose	-3.14	-63.51 to 57.23	No	ns	>0.9999
Sucrose vs. Mannitol	-122.8	-183.1 to -62.4	Yes	***	0.001
Sucrose vs. PS80	-114.4	-174.7 to -54	Yes	**	0.0015
Sucrose vs. Suc+mann	-70.87	-131.2 to -10.5	Yes	*	0.0228
Sucrose vs. Tre+mann	-95.57	-155.9 to -35.2	Yes	**	0.0044
Trehalose vs. Mannitol	-119.6	-180 to -59.26	Yes	**	0.0011
Trehalose vs. PS80	-111.2	-171.6 to -50.86	Yes	**	0.0018
Trehalose vs. Suc+mann	-67.73	-128.1 to -7.365	Yes	*	0.0287
Trehalose vs. Tre+mann	-92.43	-152.8 to -32.06	Yes	**	0.0053
Mannitol vs. PS80	8.4	-51.97 to 68.77	No	ns	0.9966
Mannitol vs. Suc+mann	51.9	-8.465 to 112.3	No	ns	0.0967
Mannitol vs. Tre+mann	27.2	-33.17 to 87.57	No	ns	0.5916
PS80 vs. Suc+mann	43.5	-16.87 to 103.9	No	ns	0.1874
PS80 vs. Tre+mann	18.8	-41.57 to 79.17	No	ns	0.861
Suc+mann vs. Tre+mann	-24.7	-85.07 to 35.67	No	ns	0.6768

(a)

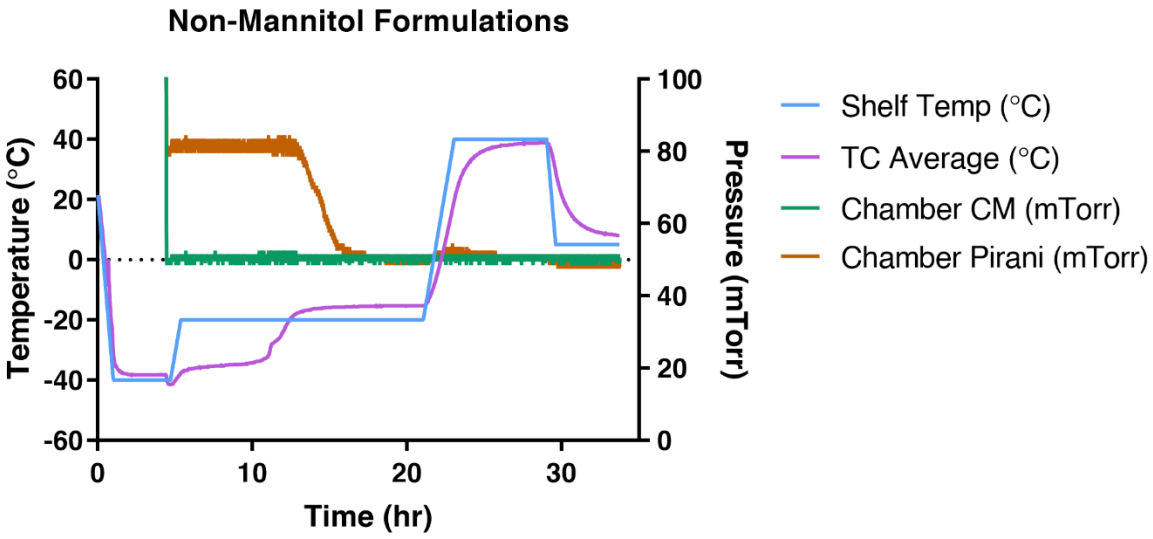

(b)

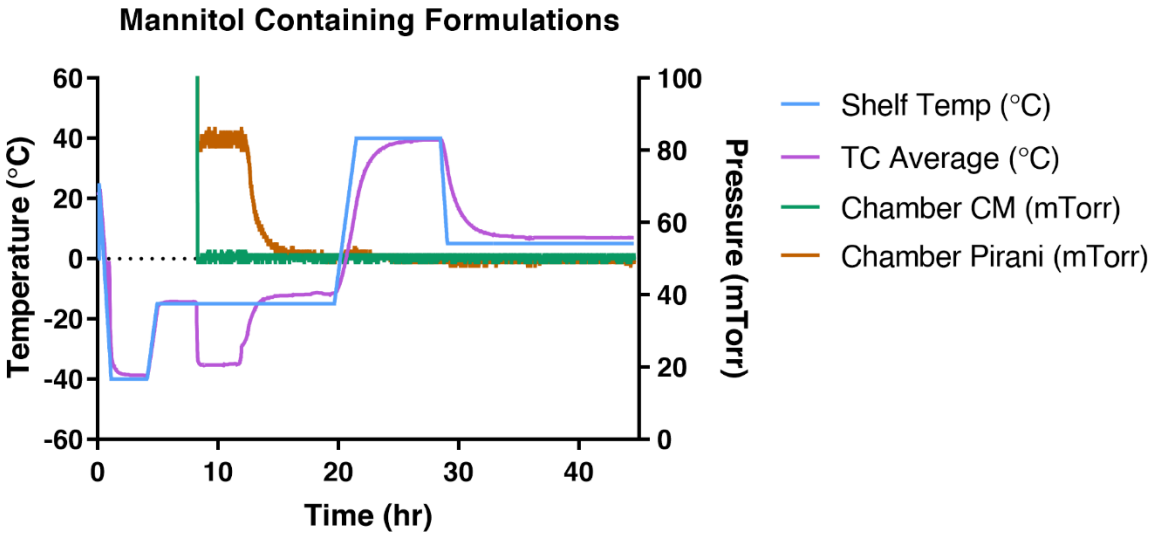

Figure A. 1. Lyophilization process data of (a) non-mannitol formulations and (b) mannitol containing formulations.

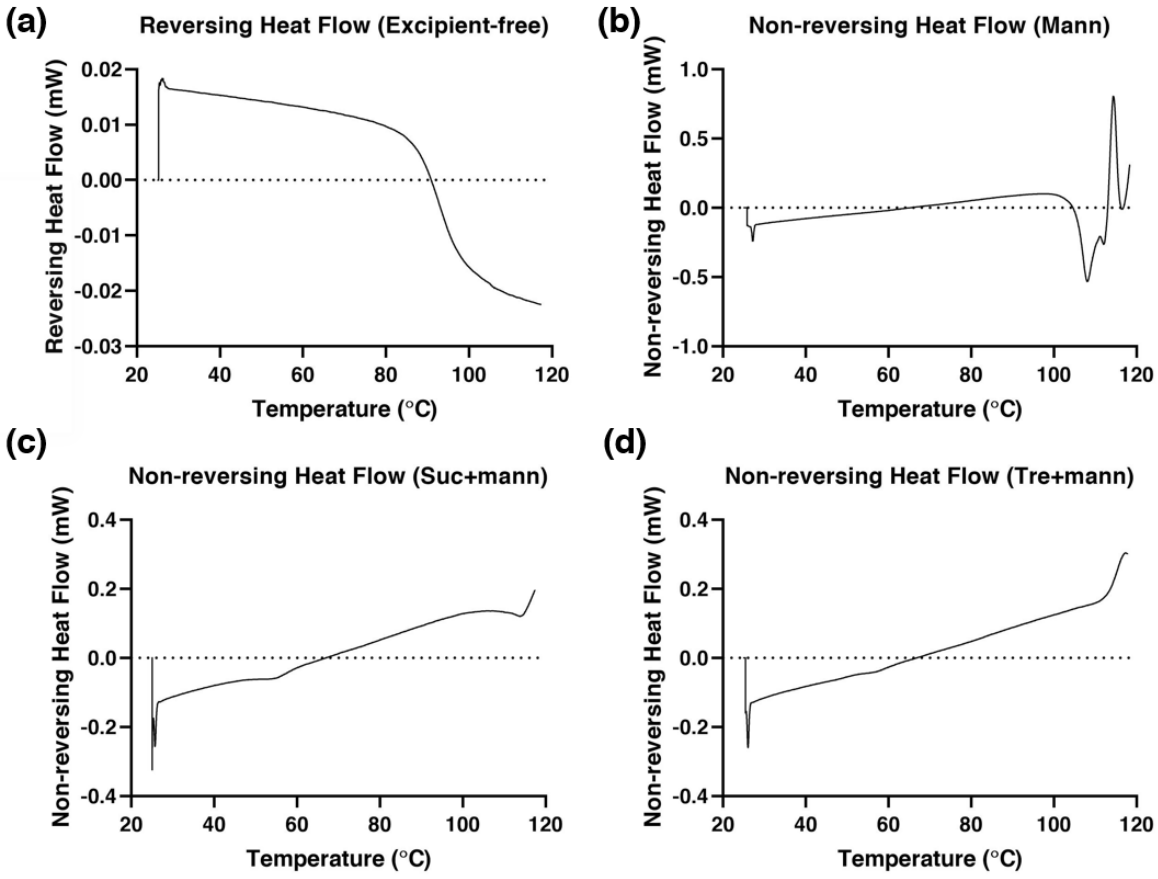

Figure A. 2. Differential Scanning Calorimetry (a) Reversing heat flow thermogram of excipient-free formulation; and non-reversing heat flow thermogram of (b) mannitol, (c) sucrose-mannitol, and (d) trehalose-mannitol formulations.

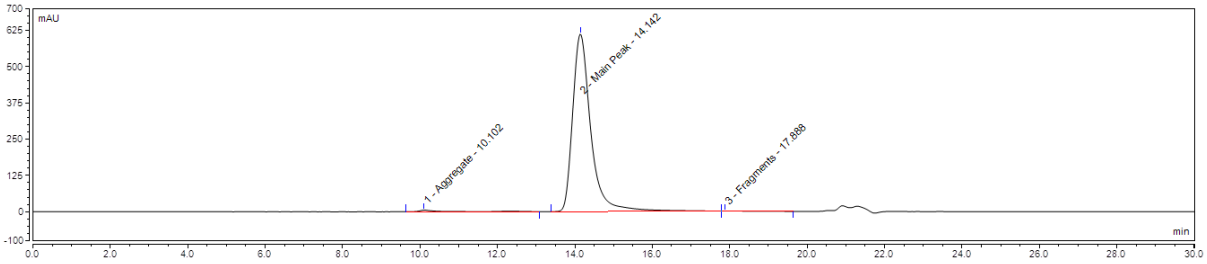

Figure A. 3. Size Exclusion Chromatogram of trehalose formulation at t=0, presented as a representative chromatogram.

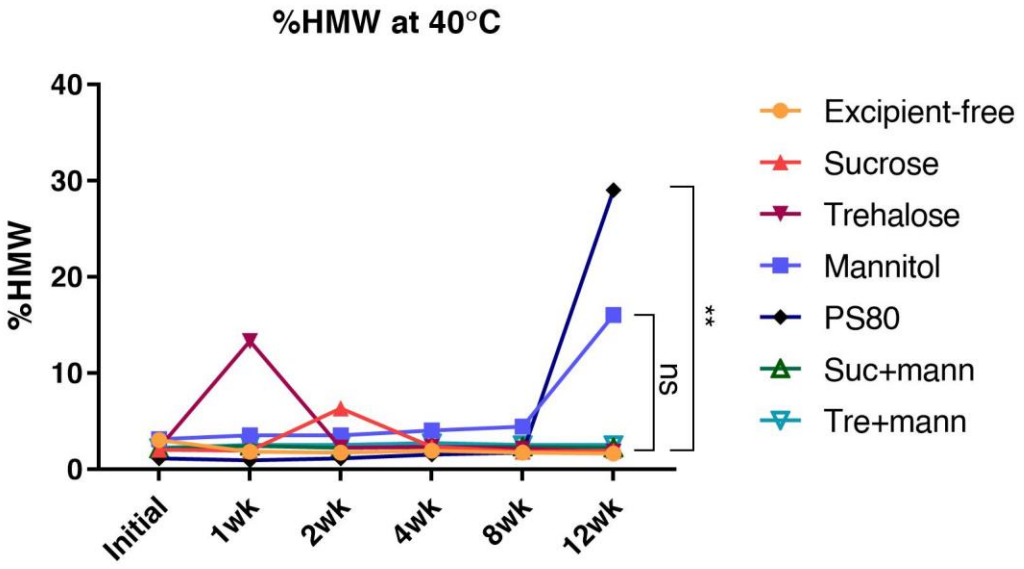

Figure A. 4. Formation of HMWs during storage, as measured by SEC for samples stored at 40°C. ** = significant different by 2-way ANOVA p <0.01. n=1.

(a)

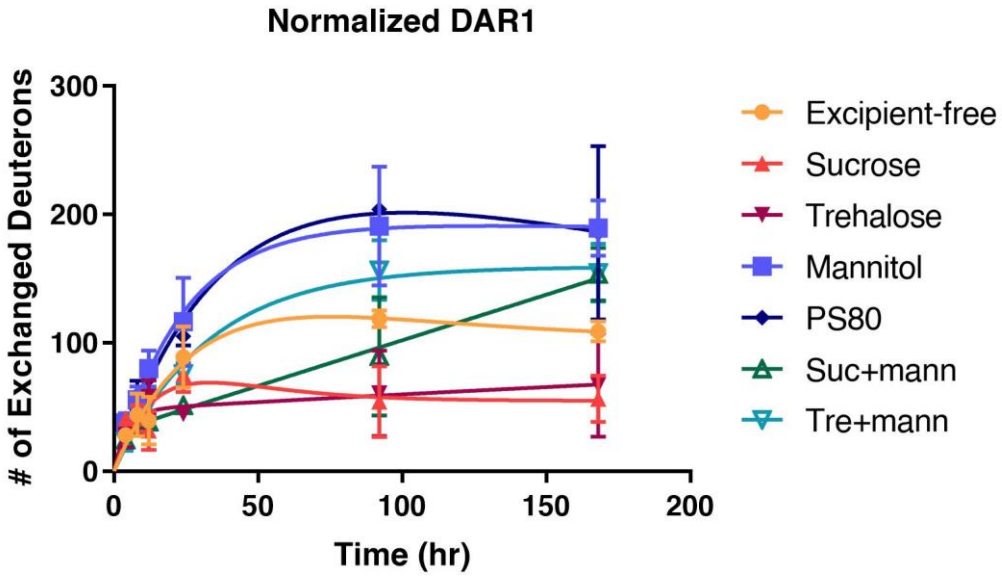

(b)

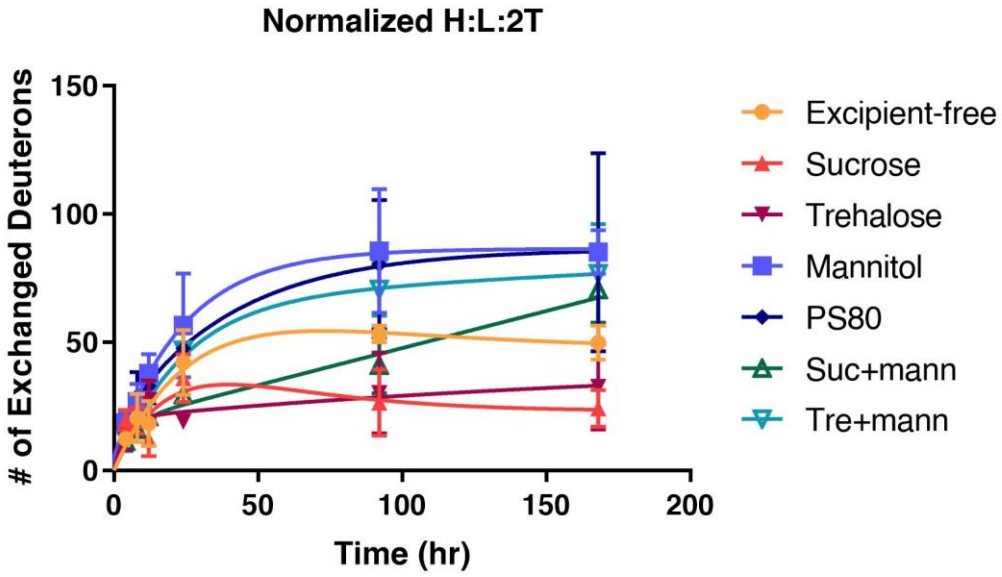

Figure A. 5. Kinetics of hydrogen-deuterium exchange (HDX) after D_2O exposure at 23%RH at room temperature (n=2±SD) calculated using the masses of (a) DAR1 and (b) heavy chain-light chain containing two toxins.

APPENDIX B. CHAPTER 3 SUPPLEMENTARY INFORMATION

(a)

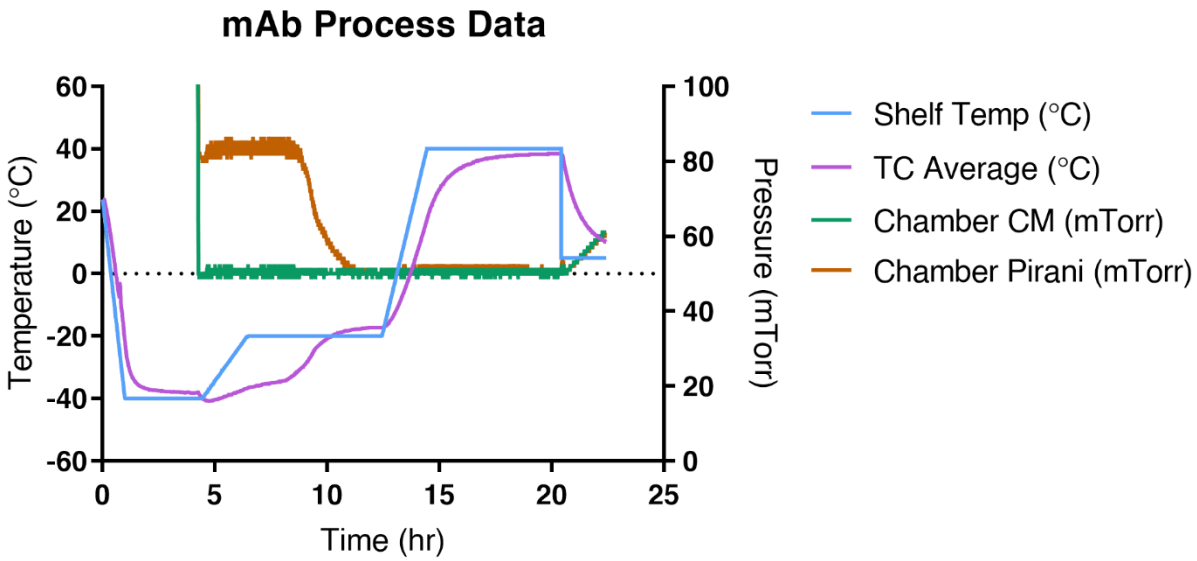

(b)

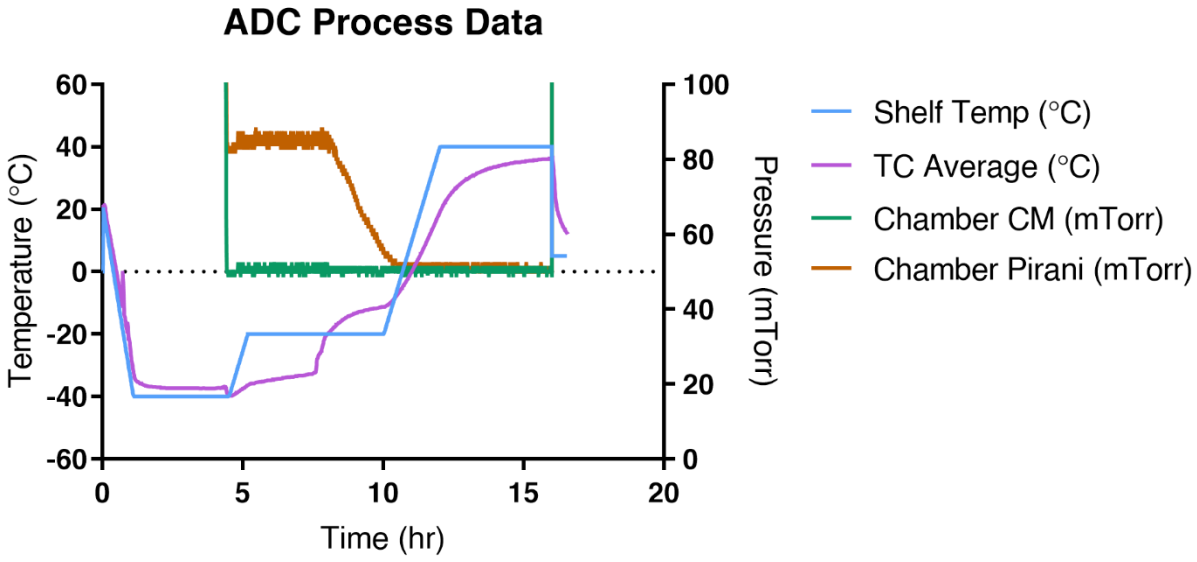

Figure B. 1. Lyophilization process data of (a) parent mAb and (b) ADC.

Table B. 1. Tukey multiple comparison analysis results for mAb accelerated studies at 50°C after 18 weeks of storage. α=0.05; number of families=1; number of comparisons per family=28.

10 mg/mL								ns
5 mg/mL								*
2.5 mg/mL	*	*						**
1 mg/mL	****	****						****
10 mg/mL+PS80			*	****				
5 mg/mL+PS80								
2.5 mg/mL+PS80	****	****	*		****	**		
1 mg/mL+PS80	****	****			****	*		
	10 mg/mL	5 mg/mL	2.5 mg/mL	1 mg/mL	10 mg/mL+PS80	5 mg/mL+PS80	2.5 mg/mL+PS80	1 mg/mL+PS80

Table B. 2. Tukey multiple comparison analysis results for ADC accelerated studies at 50°C after 12 weeks of storage. α=0.05; number of families=1; number of comparisons per family=28.

10 mg/mL								ns
5 mg/mL								*
2.5 mg/mL								**
1 mg/mL								
10 mg/mL+PS80								
5 mg/mL+PS80								
2.5 mg/mL+PS80								
1 mg/mL+PS80		*				*	**	
	10 mg/mL	5 mg/mL	2.5 mg/mL	1 mg/mL	10 mg/mL+PS80	5 mg/mL+PS80	2.5 mg/mL+PS80	1 mg/mL+PS80

APPENDIX C. CHAPTER 4 SUPPLEMENTARY INFORMATION

Table C. 1. Simple linear regression data of the UV standard curves measured using the model compound 1 in various buffers and pH obtained at 280 nm.

	EtOH	Citrate pH 5	Citrate pH 6	Potassium Phosphate pH 6	Potassium Phosphate pH 7	Tris pH 9
Slope	60.86	49.34	55.26	54.72	56.27	53.16
Y-intercept	0.00	-0.01	0.00	-0.01	-0.05	-0.01
R squared	0.998	0.999	0.999	0.999	0.979	0.994

Table C. 2. Simple linear regression data of the UV standard curves measured using a benzaldehyde in various buffers and pH obtained at 245 nm.

	EtOH	Citrate pH 5	Citrate pH 6	Potassium Phosphate pH 6	Potassium Phosphate pH 7	Tris pH 9
Slope	50.41	40.64	41.09	38.01	37.00	28.30
Y-intercept	0.00	0.04	-0.21	0.00	0.01	0.05
R squared	0.998	0.990	0.996	0.999	0.996	0.972

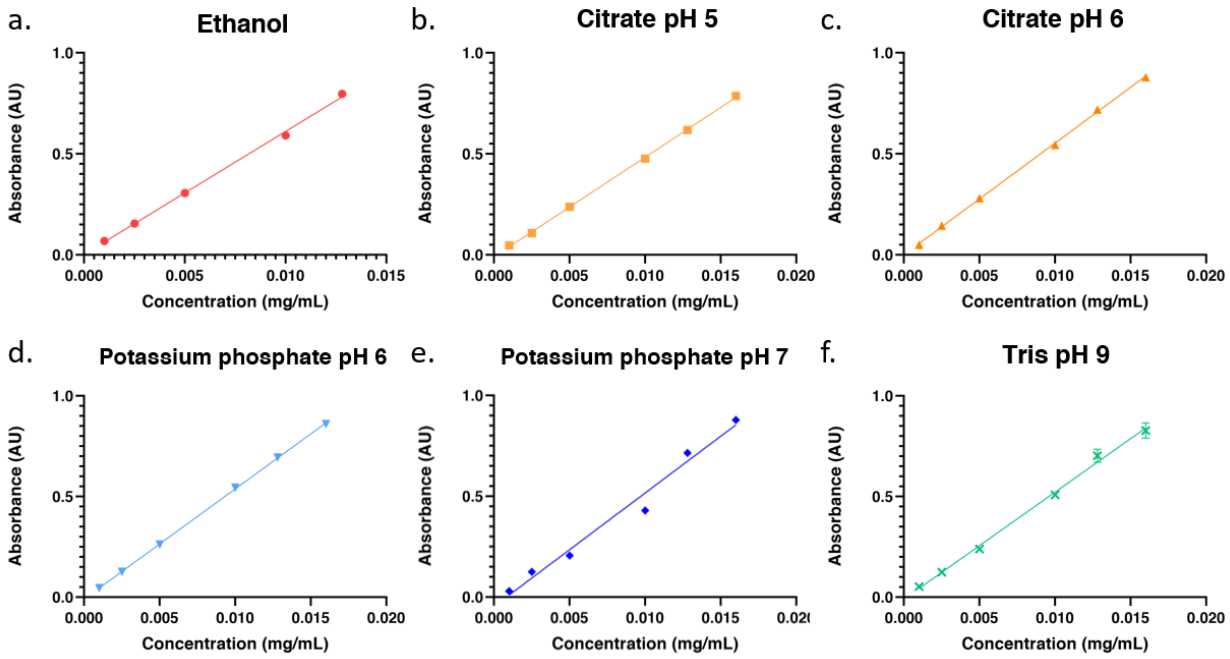

Figure C. 1. UV standard curves of the hydrazone model compound 1 formulated in a. ethanol, b. 50 mM citrate buffer pH 5, c. 50 mM citrate buffer pH 6, d. 50 mM potassium phosphate pH 6, e. 50 mM potassium phosphate pH 7, and 50 mM tris buffer pH 9, obtained at 280 nm. (n=2)

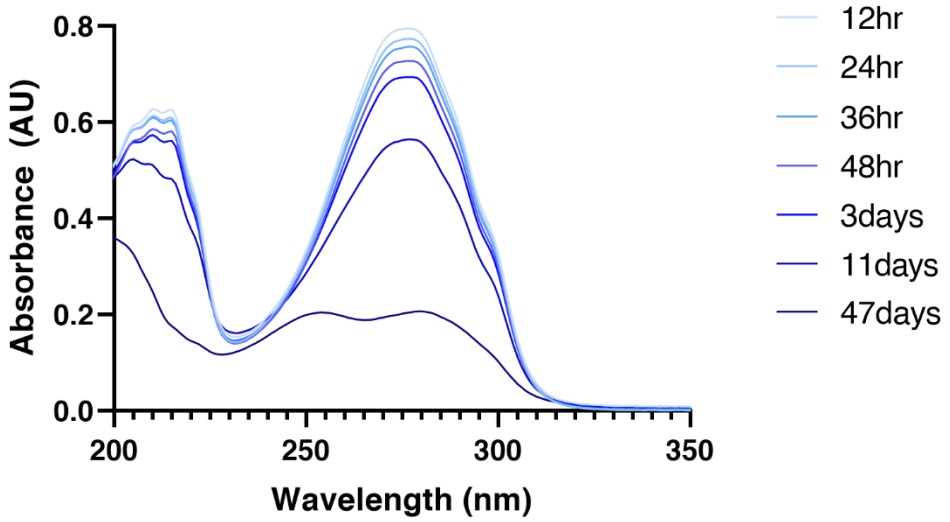

Figure C. 2. UV spectra of solution-state model compound 1 in 50mM potassium phosphate buffer with pH 7 stored at 50 °C.